Biology of mouse mucosal-associated invariant T cells

Yue Cui

Université Paris Descartes

Ecole doctorale Gc2iD

Laboratoire Immunologie/ INSERM U932

Biologie des cellules MAIT chez la souris

(Biology of mouse mucosal-associated invariant T cells)

Yue Cui

Thèse de doctorat d'Immunologie

Dirigée par Docteur Olivier Lantz

Présentée et soutenue publiquement le 27 Octobre 2015

Devant un jury composé de :

Professeur Paul Klenerman	Rapporteur
Professeur Nicolas Glaichenhaus	Rapporteur
Docteur Kamel Benlagha	Examinateur
Docteur Emmanuel Treiner	Examinateur

Résumé (en français)

Les cellules T invariantes associées aux muqueuse (MAIT) sont des lymphocytes innés caractérisés par l'expression d'un récepteur des cellules T semi-invariant (iTCR) et restreints par la molécule du complexe majeur d'histocompatibilité de classe Ib, MR1. Chez l'homme, les cellules MAIT sont abondantes dans le sang (1 à 10%), l'intestin (3 à 5%) et le foie (20 à 40%) et réagissent contre des métabolites microbiens. En raison de leur rareté dans les souris de laboratoire classiques, les études sur les cellules MAIT murines ont été principalement effectuées sur des souris transgéniques (Tg) pour des TCR MAIT. Cependant, ces cellules MAIT Tg ne récapitulent pas de manière adéquate le phénotype des cellules MAIT humaines. Ici, nous décrivons une souche de souris congénique que nous avons générée qui possède des cellules MAIT qui ressemblent aux cellules MAIT humaines. Nous utilisons cet outil pour étudier les caractéristiques des cellules MAIT murines.

L'étude de souches de souris consanguines d'origine sauvage montre que la souche CAST/Ei présente une fréquence des cellules MAIT nettement supérieur à celle retrouvée dans la souche C57BL/6. Un seul locus est impliqué et a été localisé dans la région TCRα. Ceci a permis la génération d'une souche "MAIT" congénique, qui ont été en outre croisé à une souris Tg pour un rapporteur GFP du facteur transcriptionnel RORγt sur la base de données antérieurs montrant que les MAITs humaines expriment ce facteur. Grâce à cet outil, nous montrons que les MAITs murines sont $CD4^{-}CD8^{-/lo}$, ont un phénotype mémoire effecteurs ($CD44^{+}$) et coexpriment PLZF et RORγt. Ces MAITs murines sont orientées vers une localisation tissulaire ($CCR6^{+}CCR7^{-}$) et résident préférentiellement dans les tissus non lymphoïdes périphériques, y compris les poumons, le foie et la peau. Après stimulation du TCR, les MAITs produisent des cytokines $T_H1/2/17$ et sont aussi activées par de antigènes bactériens (par exemple semi-purifié fraction bactérienne ou 5-OP-RU) d'une manière dépendant de MR1. Les MAITs ont une forte expression de récepteurs de cytokines (IL-7R, IL-18Rα, IL-12Rβ) et peuvent ainsi répondre à des cytokines innées. Lors d'une infection expérimentale des voies urinaires, les MAITs migrent vers la vessie et ont une activité protectrice anti-bactérienne.

Au total, nos résultats démontrent que les cellules MAIT murines ressemblent étroitement à leurs homologues humains. Ce nouveau modèle murin sera un outil puissant pour faire avancer notre compréhension de la biologie des cellules MAIT en situation normale et pathologique.

Abstract

Mucosal-associated invariant T cells (MAIT) are innate lymphocytes that express a semi-invariant T cell receptor (iTCR) and are restricted by the major histocompatibility complex (MHC) related molecule, MR1. In human, MAIT cells are abundant in the blood (1-10%), gut (3-5%), and liver (20-40%). They react against microbial-derived riboflavin metabolites that are common in bacteria and yeast. Due to the paucity of MAIT cells in classical inbred laboratory mice, studies on mouse MAIT cells were mostly performed in TCR-transgenic (Tg) mice. However, these Tg MAIT cells do not adequately recapitulate the phenotype of human MAIT cells. Herein, we present a recently generated congenic mouse strain harboring MAIT cells that closely resemble human MAIT cells and use this tool to study the characteristics of natural mouse MAIT cell.

An analysis of wild-derived inbred mouse strains revealed that CAST/Ei strain has increased frequency of MAIT cells than C57BL/6 mice. This was linked to a locus on the TCRα region. Introduction of such locus into C57BL/6 mice generated a "MAIT" congenic strain, which were further crossed to Rorc(γt)-Gfp^{TG} reporter strain based on previous findings of RORγt expression on human MAIT cells. Using this tool, we show that natural mouse MAIT cells are CD4^{-}CD8$^{-/lo}$, display an effector memory phenotype (CD44^{+}), and coexpress the transcription factors PLZF and RORγt. They exhibit tissue-homing properties (CCR6^{+}CCR7^{-}) and preferentially reside in peripheral non-lymphoid tissues, including lung, liver, and skin. Upon TCR ligation, MAIT cells produce T_H1/2/17 type cytokines and react to bacterial-derived antigens (i.e. semi-purified bacterial fraction or 5-OP-RU) in an MR1-dependent manner. They have high expression of cytokine receptors (IL-7R, IL-18Rα, IL-12Rβ) and may respond to the corresponding innate cytokines. During experimental urinary tract infection, MAIT cells migrate to the bladder and display a protective anti-bacterial activity.

Altogether, our results demonstrate that mouse MAIT cells resemble their human counterparts more closely than previously recognized and therefore this new mouse model will be a powerful tool for advancing our understanding of MAIT cell biology in health and disease.

Keywords: MAIT cell, wild-derived inbred mice, RORγt

Contents

Abbreviations

APC	Antigen presenting cell
B6	C57BL/6
CAST	CAST/Ei
CMV	Cytomegalovirus
DAG	Diacylglycerol
DHA	Dihydroxyacetone
DN	Double negative ($CD4^-$ $CD8^-$)
Glyx	Glyoxal
GSL	Glycosphingolipid
HCV	Hepatitis C virus
HIV	Human immunodeficiency virus
IBD	Inflammatory bowel disease
iGb3	Isoglobotrihexosylceramide
ILC	Innate lymphoid cell
iNKT	Invariant natural killer T cell
iTCR	Invariant TCR
LFA-1	Lymphocyte function-associated antigen-1
mAb	Monoclonal antibody
MAIT	Mucosal associated invariant T cell
MeG	Methylglyoxal
MHC	Major histocompatibility complex
MLN	Mesenteric lymph node
PIM4	Phosphatidylinositol tetramannoside
PLZF	Promyelocytic leukaemia zinc finger
PMA	Phorbol 12-myristate 13-acetate
RA	Rheumatoid arthritis
rRL-6-CH_2OH	Reduced 6-hydroxymethyl-8-D-ribityllumazine
RL-6-Me-7-OH	7-hydroxy-6-methyl-8-D-ribityllumazine
RL-6,7-diMe	6,7-dimethyl-8-D-ribityllumazine
ROR	Retinoic acid receptor-related orphan receptor
SLE	Systemic lupus erythematosus
SNP	Single nucleotide polymorphism
SPF	Specific pathogen-free
TB	Tuberculosis
TCR	T cell receptor
T_{FH}	T follicular helper cell
Tg	Transgenic
T_H	T helper cell
TLR	Toll-like receptor

5-A-RU	5-Amino-6-D-ribitylaminouracil
5-OE-RU	5-(2-oxoethylideneamino)-6-D-ribitylaminouracil
5-OP-RU	5-(2-oxopropylideneamino)-6-D-ribitylaminouracil
6-FP	6-formylpterin
α-GalCer	α-galactosylceramide
β-GalCer	β-galactosylceramide
β-GlcCer	β-glucosylceramide

Introduction

Immune responses can generally be classified into two groups: innate and adaptive immunity. As its name suggests, innate immunity consists of cells and proteins that are always present and rapidly respond in sites where infections or cellular stress originate. The main components of innate immunity are physical epithelial barrier (e.g., skin, mucosa), phagocytes (e.g., macrophages, dendritic cells), and plasma proteins (e.g., complement). However, the diversity of antigens recognized by innate immune components is limited and nonspecific. Adaptive immune components, on the other hand, recognize almost infinite diversity of antigens. Although a naïve lymphocyte carries receptors with a single specificity, the specificity of each lymphocyte is unique resulting in diverse repertoires of these populations. This is dependent on the rearrangement of their antigen receptors. When naïve lymphocytes encounter their antigens, they undergo clonal expansion, differentiation and then migrate to the affected tissues, where they exert antigen-specific effector functions and provide long-term memory. However, not all immune cells behave according to the schema. Over the last two decades, the discovery of innate lymphoid cells (ILC) and innate-like T and B cells, such as γδ T cells and B1 cells, has blurred the boundary between innate and adaptive immunity[1].

A crucial feature of adaptive immune response is the release of a complex diversity of cytokines by T cells. Upon antigen recognition, T helper cells (T_H) differentiate into different subsets, namely, T_H1, T_H2, T_H17, T_{REG}, T_H9, and T follicular helper (T_{FH}) cells[2]. These functional subsets thereby regulate immune responses through their distinct cytokine secretion patterns. Interestingly, the recently appreciated ILCs can produce many T_H cell-type cytokines and mirror the expression of T_H lineage-specific transcription factors, despite a lack of antigen-specific T cell receptors[3].

Unlike classical lymphocytes, which recognize a large range of antigens, innate-like lymphocytes express restricted antigen receptors that are semi-invariant or germline encoded and often self-reactive. Functionally, they appear to produce effector components more rapidly than convectional naïve lymphocytes[1]. Their

restricted repertoire and rapid effector functions follow the scheme of innate rather than adaptive immunity.

Innate-like T cells require T cell receptor (TCR) for development but then alter their TCR responsiveness to accommodate their innate mode of activation[4]. Among TCRαβ T cells, two populations with semi-invariant TCR, known as invariant natural killer T (iNKT) cells and mucosal associated invariant T (MAIT) cells, were discovered in the early 1990s[5–8]. These two innate-like populations have distinct properties compared with mainstream T cells. As their names imply, these T cell populations have restricted TCRα usage paired with limited repertoire of TCRβ chains, suggesting a limited antigen recognition pattern. Unlike conventional T cells, which recognize peptide bound to polymorphic major histocompatibility complex (MHC) class I or II molecules, they recognize their cognate antigens presented by non-polymorphic, nonclassical and evolutionarily conserved MHC class I like molecules: glycolipid antigen bound to CD1d for NKT cells and vitamin B2 precursor metabolite bound to MR1 for MAIT cells[9–15]. Functionally, in response to antigen or cytokine stimulation, they produce copious amount of cytokines more rapidly than conventional naïve T cells[16–19]. In addition, they are mostly localized in mucosal tissues, where pathogens are first encountered.

Despite their abundance in human and evolutionary conservation among species, the importance of MAIT cells have just recently been appreciated due to the finding of their anti-microbial function[20,21]. Over the past few years, MAIT cells have been implicated in a number of infectious and autoimmune diseases, however, their exact roles remain elusive, in part due to their scarcity in mice, which hampers *in vivo* studies and therefore the understanding of MAIT cell biology. This thesis will focus on the description of a recently established mouse model in which MAIT cells are naturally increased. This model herein allowed extensive phenotypic and functional analyses of mouse MAIT cells. An experimental urinary tract infection model was used to validate *in vivo* anti-bacterial function of these cells.

Invariant TCRαβ T cells

Invariant αβ T cells were originally described in 1993 as TCR αβ T cell subsets expressing invariant TCRα rearrangement in DN T cell compartment, including Vα24-Jα18 and Vα7.2-Jα33 (formerly Vα24-JαQ and Vα7.2-Jα(IGRJα14)), now

known as iNKT and MAIT cells[5]. Porcelli et al. suggested that these cells recognize a limited spectrum of antigens in the context of non-polymorphic antigen-presenting molecules, which were later found to be CD1d and MR1 respectively. iNKT and MAIT cells share many distinct and important properties compared with conventional T cells (Table 1). Interestingly, it seems likely that the frequencies of these two populations are inversely associated in both human and mice – for example, MAIT cells represent up to 40% of human liver T cells whereas iNKT cells account for merely 1% of such population[18,22] – suggesting that iNKT and MAIT cells may have redundant functions. Given that iNKT cells have been studied more extensively than MAIT cells, we will firstly elaborate on some important properties of iNKT cells.

Table 1. Characteristics of iNKT and MAIT cells compared to conventional T cells[23–25]

Characteristic	iNKT	MAIT	Conventional T
TCRα chain	hVα24-Jα18 mVα14-Jα18	hVα7.2-Jα33/12/20 mVα19-Jα33	Diverse
Associated Vβ	hVβ11 mVβ8.2/7/2	hVβ2/13.2 mVβ6/8	Diverse
Restricting molecule	CD1d Non-polymorphic	MR1 Non-polymorphic	MHC-I or II Highly polymorphic
Ligand	Glycolipids, phospholipids	Vitamin B2 precursor metabolites	Peptides
Selecting cells	DP thymocytes	DP thymocytes	Thymic epithelium
PLZF expression	Yes	Yes	No
Coreceptor	CD4, DN, CD8αα	CD8αα, CD8αβ^{int}, DN	CD4 or CD8
Frequency (% of CD3)	0.0001-1% in blood, 1% in liver (human) 1-3% in spleen, ≤50% in liver (mouse)	1-10% in blood, 20-40% in liver, 3-5% in gut (human) ~0.1% in LP (mouse)	~60% (CD4$^+$), ~30% (CD8$^+$) in blood (human) and spleen (mouse)
Tissue distribution	Liver, thymus, spleen, lung, BM, LN, and fatty tissue	Liver, gut, lung, and blood	Blood, lymphoid tissues
Peripheral phenotype	Memory	Memory	Naïve prior to antigen exposure
Functional phenotype	T_H1/2/17	T_H1/17	Diverse

h, human; **m**, mouse; **DP**, double positive (CD4$^+$CD8$^+$); **DN**, double negative (CD4$^-$CD8$^-$); **int**, intermediate; **LP**, lamina propria; **BM**, bone marrow; **LN**, lymph node; **MHC**, major histocompatibility complex.

iNKT cells

Functional Subsets of iNKT Cells

iNKT cells have been classified into three functional subsets, NKT1, NKT2 and NKT17[26,27] (Figure 1), evident in their resemblance of T_H1, T_H2, T_H17 cells, in terms of cytokine secretion pattern (i.e., IFN-γ, IL-4 and IL-17) and the expression of lineage-specific transcription factor (i.e., T-bet, GATA-3 and RORγt). Consistent with their T-bet expression, NKT1 cells are capable of producing T_H1 type cytokine IFN-γ, but also secrete low level of T_H2 type cytokine IL-4. NKT2 cells, on the other hand, are GATA3^{hi} cells and mainly produce IL-4 and IL-13. Like T_H17 cells, NKT3 cells produce IL-17 and express higher levels of RORγt[27]. In addition to these lineage-specific transcription factors and cytokines, NKT1, NKT2, and NKT17 cells can also be distinguished as PLZF^{lo}, PLZF^{hi} and PLZF^{int} cells according to the expression level of transcription factor promyelocytic leukaemia zinc finger (PLZF)[26]. PLZF is a master regulator of NKT linage and is induced immediately after positive selection. In the absence of PLZF, NKT cells fail to acquire effector-memory phenotype and exhibit a defective secretion of IL-4 and IFN-γ[28].

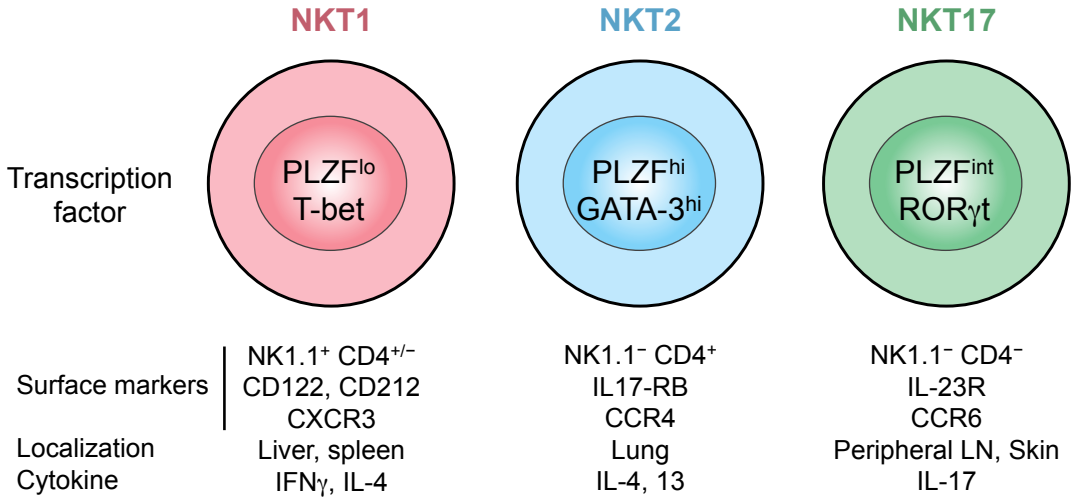

Figure 1. Functional subsets of iNKT cells. Characteristics of iNKT subsets, NKT1, NKT2, and NKT17, identified by intracellular expression of transcription factors, expression of surface markers, prominent tissue localization, and cytokine production.

In line with the identification of iNKT functional subsets, distinctive features of these cells have also been revealed[23,26,27] (Figure 1). NKT1 cells express NK lineage receptors, including NK1.1, Ly49, NKG2D, CD94, and DX5, whereas NKT2 and NKT17 lack expression of these markers[26]. Other surface makers expressed by NKT1 cells are also absent in NKT2 and NKT17 cells, for example, CD122 (IL-2Rβ), CD212 (IL-12Rβ2), and CXCR3. In contrast, NKT2 cells highly express IL-17RB, the receptor for IL-25, while NKT17 cell express IL-23R and CCR6[23,27,29]. The tissue localization of these subsets also varies, with NKT1 cells predominant in liver and spleen, NKT2 cells in lung and NKT17 cells in peripheral LN and skin[26,30].

iNKT Cell Activation

iNKT cells recognize both exogenous and endogenous antigens presented by CD1d molecules[23]. Three distinct pathways mediated by microbial antigens, endogenous glycolipid antigens, or innate cytokines have been described for iNKT activation (Figure 2), [17,23,31,32].

1. Microbial antigen mediated

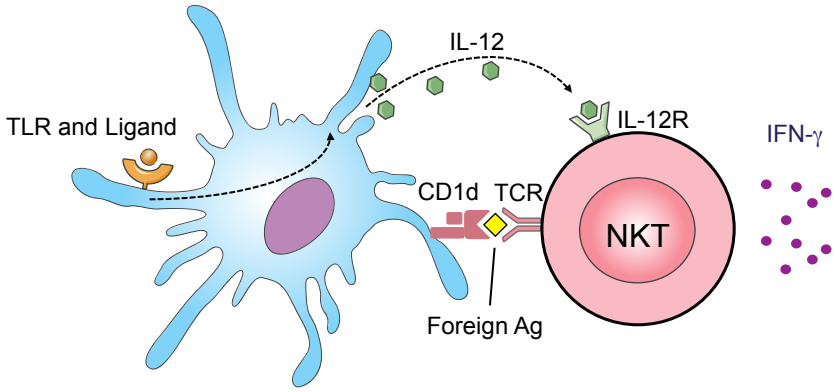

2. Endogenous antigen mediated

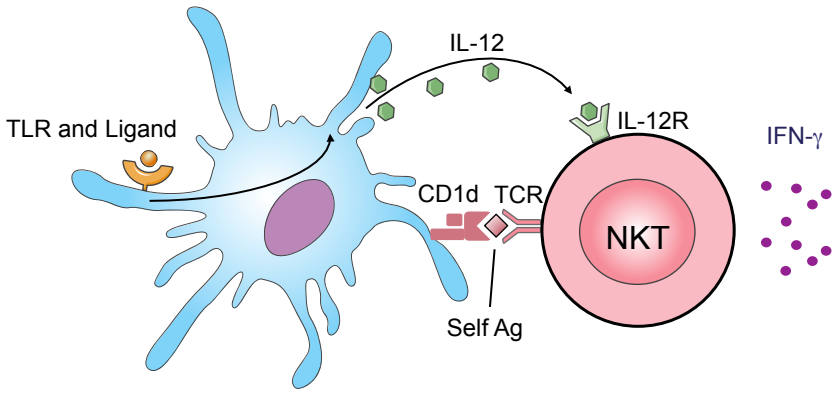

3. Innate cytokine mediated

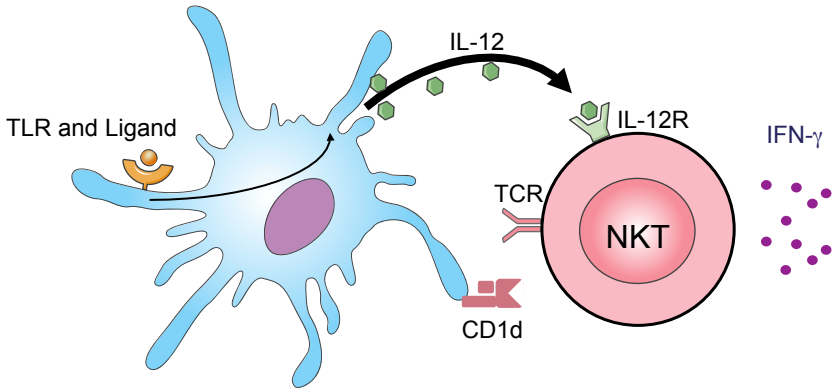

Figure 2. Activation pathways of iNKT cells. iNKT cells activation pathway **(1)** through foreign antigen recognition in which cytokines from APCs are less dependent, **(2)** by endogenous lipid antigens presented by APC, usually required for cytokines from innate cells, **(3)** or mediated solely by cytokines, irrespective of the expression of lipid antigens or TCR. Figures were generated using images from Servier Medical Art (www.servier.com), licensed under the Creative Commons Attribution 3.0 Unported License (http://creativecommons.org/license/by/3.0/).

Alpha-galactosylceramide (α-GalCer) was the first described antigen for iNKT cells which originated initially from marine sponge[33]. Subsequently, a series of naturally occurring microbial antigens were discovered, such as glycosphingolipids (GSL) from *Sphingomonas* spp.[34–36], glycosylated diacylglycerols (Glc-DAG) found in *Borrelia burgdorferi*[37] and *Streptococcus pneumoniae*[38], phosphatidylinositol tetramannoside (PIM4) derived from *Mycobacterium bovis* BCG[39], and cholesterol-glycoside from *Helicobacter pylori*[40]. These microbial antigens can activate iNKT cells in a TCR-dependent manner during infection.

In addition to direct recognition of exogenous antigens, iNKT cell can be activated indirectly by innate cytokines (e.g., IL-12) produced by antigen presenting cell (APC) upon toll-like receptor (TLR) activation, together with a weak TCR signal generated from ligation of endogenous lipid antigens[17]. Such pathway allows iNKT cells to respond to those pathogens that lack CD1d-restricted lipid antigens but express TLR ligands, such as virus and *Salmonella typhimurium*[36,41]. Currently known self-lipid antigens include β-galactosylceramide (β-GalCer), β-glucosylceramide (β-GlcCer), isoglobotrihexosyl-ceramide (iGb3), disialoganglioside, and self-phospholipid antigens as well as recently identified α-linked glycosylceramides[42,43].

Moreover, growing evidences suggest that iNKT cells can be activated by innate cytokines, regardless of TCR engagement[32,44–46]. Recently, using Nur77^{gfp} reporter mice, which have been used to identify cells with experience of antigen receptor but

not inflammatory signaling, Holzapfel and colleagues demonstrated that iNKT cells produced IFN-γ but did not upregulate GFP in response to cytomegalovirus (CMV), *Salmonella typhimurium* or TLR stimulation, therefore they underwent TCR-independent activation[32]. This finding agrees with another study in which iNKT cells stimulated with TLR agonists induced IFN-γ production, irrespective of the presence of TCR on mature iNKT cells[47].

MAIT cells

MAIT cells were originally identified by their invariant TCR (iTCR) usage Vα7.2-Jα33[5] (Vα19-Jα33 in mice) and firstly described in 1990s[7]. However, strong interest on MAIT cells has been recently aroused due to the finding of their anti-microbial function[20,21]. The following sections will explore what is currently known about MAIT cells.

MAIT Cell Phenotype

As its name suggests, MAIT cells are mainly located in mucosal tissues, such as gut, liver and lung[18] (Table 1). In human, they comprise 1-10% of blood T cells, 20-40% of liver T cells and 3-5% of intestinal T cells. Additionally, MAIT specific iTCR transcripts Vα7.2-Jα33/12 were also observed in kidney, tonsil, LN, prostate, and ovary[48].

Memory Phenotype and Tissue Tropism

Human MAIT cells are identified as Vα7.2 $CD161^{hi}$ T cells and are predominantly $CD8^+$ or double negative (DN)[18,49]. A very minor subset of $CD4^+$ MAIT cells has also been recognized by MR1 tetramers[50]. Human MAIT cells from adult peripheral blood have an effector memory phenotype ($CD45RO^+$, $CD62L^-$, $CD95^+$) and exhibit tissue-homing properties ($CCR2^+$, $CCR5^+$, $CCR6^+$, $CXCR6^+$, $CCR9^+$, $CCR7^-$)[18,51]. Whereas in cord blood, they express a naïve phenotype ($CD45RA^+$, $CD62L^+$) and bear the chemokine receptor CCR6[49,51–53]. A recent study suggests that MAIT cells from second trimester fetal tissues display various phenotypes[54]. In fetal thymus, spleen and mesenteric lymph node (MLN), MAIT cells express a naïve phenotype ($CD45RO^{lo}$) while those from fetal liver, lung, and intestine seem to be memory-type cells ($CD45RO^{hi}$, $CD62L^{lo}$, $CD25^{hi}$). Notably, the majority of $CD161^{hi}$ cells in fetal

tissues are Vα7.2^{-} whereas those from adult are mostly Vα7.2^{+} (<95%)[18,54,55]. In cord blood, CD161^{hi}CD8^{+} cells are already programmed to a MAIT-like phenotype and they are mostly Vα7.2^{-}(~80%)[53]. After birth, Vα7.2^{+} MAIT cells expand and dominate the CD161^{hi} population[52,55]. Whether similar developmental events occur in the fetal tissues remains to be addressed. However, unlike cord blood in which CD161^{hi} population comprises a minority of CD8 T cells, fetal tissues harbor a vast majority of CD161^{hi} population, raising the possibility that a classical MHC-restricted T cell may express CD161 along with Vα7.2. Without further confirmation of MR1 restriction by Vα7.2^{+}CD161^{hi} population from fetal tissues (e.g. MR1-tetramer staining, TCR repertoire analysis, MR1 blocking assay), the phenotype of fetal MAIT cells is not conclusive.

Surface Molecules CD161, CD26 and Cytokine Receptors

In addition to their invariant TCR and mucosal localization, MAIT cells can also be identified by additional surface molecules and transcription factors.

Together with Vα7.2, high expression of CD161 identifies all MAIT cells from periphery blood and jejunum[50]. Although the usage of CD161 antibody to define MAIT cells from tissues has been questioned, it is currently one of the most reliable and commercially available reagent to study MAIT cells in human. CD161, also known as NKR-P1A or KLRB1, is a C-type lectin receptor expressed by the majority (>90%) of NK cells and a large proportion (~24%) of peripheral T cells, including both αβ and γδ T cells[56]. CD161 expression has been associated with a memory phenotype and IL-17 secretion potential of circulating T cells[57]. On NK cells, ligation of CD161 results in an inhibition of cytotoxicity[56]. Regarding MAIT cells, opposing effects of CD161 ligation were reported[55,58]. Le Bourhis et al. showed that triggering of CD161 on MAIT cells inhibited their cytokine secretion but had no effect on cytotoxicity, whereas Fergusson and colleagues found an increased production of IFN-γ and TNF-α upon CD161 simulation.

CD161 remains unchanged during overnight activation but its downregulation has been observed along with proliferation in response to *E.coli*[59]. Ligation of CD161 by its ligand or anti-CD161 also induces its transient downregulation[55]. Therefore, it may be unreliable to identify activated MAIT cells by merely using CD161. Additional markers and MR1-tetramers are definitely required to solve this problem. Recently, CD26, a dipeptidase that can cleave and inactivate a number of chemokines, has been

suggested to accurately identify human bacteria-reactive MAIT cells[60]. On unstimulated MAIT cells, CD26 are coexpressed with CD161. In response to bacteria, both molecules are downregulated[60]. However, downregulation of CD26 is less pronounced compared with CD161, thus providing an alternative to identify MAIT cells with a higher sensitivity.

In addition, IL-18Rα also unequivocally identifies MAIT cells[20]. MAIT cells express the highest levels of IL-18Rα among all human T lymphocytes[51]. Expression of IL-18Rα by MAIT cells was also reported in cord blood, fetal liver, and mucosal tissues while only a small proportion of MAIT from fetal thymus, spleen, and MLN express this receptor, suggesting that MAIT cells may undergo a stepwise maturation[18,53,54]. Other cytokine receptors, such as IL-12Rβ, IL-23R and IL-7Rα, are also expressed by MAIT cells[18,51,55,61,62]. In contrast with IL-18Rα, IL-7Rα is universally expressed by fetal MAIT cells from either lymphoid organs or mucosal tissues[54]. Accordingly, the expression of cytokine receptors by MAIT cells in steady state suggests the potential reactivity of MAIT cells to cytokine stimulation.

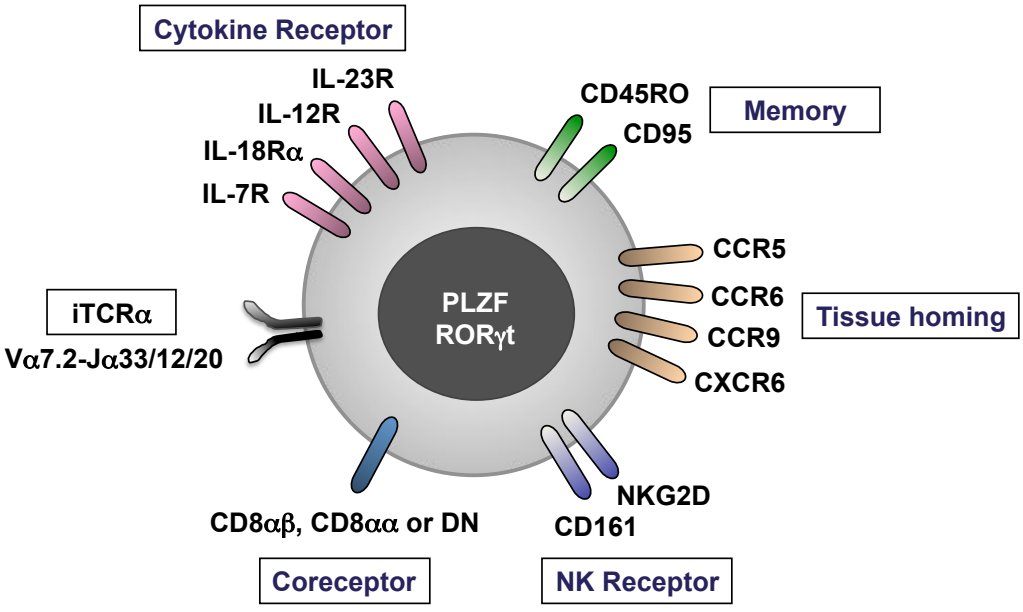

Figure 3. Phenotype of MAIT cell from peripheral blood. In addition to its iTCR, human MAIT cells express a variety of surface receptors, including CD8α and β coreceptor, NK receptors, tissue-homing chemokine receptors, cytokine receptors, as well as memory markers. They also express transcription factors PLZF and RORγt.

Transcription Factors PLZF and RORγt

Expression of transcription factors PLZF and RORγt have been described in human MAIT cells. PLZF, also known as ZBTB16, is expressed by NKT cells, MAIT cells and a subset of γδ T cells (Vγ1-Vδ7.3)[26]. PLZF has been known to orchestrate acquisition of an innate-like effector program of NKT cells, including their effector-memory phenotype and the ability to secrete IL-4 and IFN-γ at a single cell level[28,63]. Although NKT and MAIT cells share similar developmental program (i.e., thymic selection by DP thymocytes in the context of non-classical MHC-I molecules), their developmental pathways are distinct[64]. NKT cells expand and acquire an effector-memory phenotype in the thymus, whereas MAIT cells remain naïve in both adult and fetal thymus[49,52,54]. In line with their naïve phenotype, low levels of PLZF were observed in fetal thymus[54], suggesting PLZF may play a role in the development of MAIT cells. A recent study on mouse MAIT cells underlines the importance of PLZF for MAIT development[65]. Rahimpour et al. showed that MAIT cells were almost absent in thymus, spleen, and lymph nodes from PLZF knockout mice. In addition to its role on NKT and MAIT development, PLZF was also reported as an essential inducer of homing and adhesion properties of NKT cells[66]. Whether PLZF regulates MAIT cells in the same manner remains to be elucidated.

RORγt is the other important transcription factor expressed by MAIT cells. RORγt was initially described as a key transcription factor of T_H17 cells[67], known to direct the differentiation program of these cells and to induce genes encoding IL-17[67]. Over the last few years, RORγt expressions by ILC, NKT cells, and γδ T cells were also reported[68–70]. Among $CD8^+$ T cells, MAIT cells account for the majority of RORγt expressing cells[18,51,55]. Study on mouse MAIT cells using MR1 tetramer revealed two functional subsets of MAIT cells governed by the expression of transcription factor T-bet or RORγt, consistent with their IFN-γ or IL-17 producing capacity[65]. Upregulation of T-bet was also observed in human MAIT cells stimulated with PFA-fixed *E. coli*[59].

MAIT Cell Activation

One of the most important findings in the field of MAIT research is the anti-microbial activity of MAIT cells against a broad range of bacteria and yeast[20,21], which includes *E. coli, Pseudomonas aeroginosa, Klebsiella pneumonia, Lactobacillus acidophilus, Staphylococcus aureus, Staphylococcus epidermidis, Mycobacterium abscessus, Mycobacterium tuberculosis, Salmonella typhimurium, Saccharomyces cerevisiae, Candida glabrata, and Candida albicans*[20,21]. In contrast, *Enterococcus faecalis, Streptococcus group A, and Listeria monocytogenes* are not able to activate MAIT cells in an MR1-dependent manner[20,21]. MAIT reactivity to a wide range of microbes suggests the presence of common antigen(s) in these microbes[14,20,21].

MAIT Ligands and its TCR

MAIT TCR is restricted to non-polymorphic MHC-I like molecule, MR1, that is highly conserved in mammals and displays high levels of cross-reactivity[71,72]. MR1 transcripts and protein are ubiquitously expressed in all cell types and tissues, however their surface expression levels are exceedingly low[72].

Similar to other MHC-I and MHC-I like molecules, refolding of MR1 requires antigens to stabilize its structure. Interesting observation of MR1 refolded in cell culture medium RPMI 1640 led to the discovery of MAIT ligand – vitamin B metabolites[14]. However, the initial finding of folic acid (vitamin B9) metabolite 6-formylpterin (6-FP), which stabilized MR1, was not able to activate MAIT cells[14]. The following work on refolding MR1 with the culture supernatant of *Samonella typhimurium* (previously described bacteria strain which activates MAIT cells[21,73]) revealed the stimulatory ligands with a mass to charge ratio (*m/z*) of 329.11, that are riboflavin (vitamin B2) derivatives: reduced 6-hydroxymethyl-8-D-ribityllumazine (rRL-6-CH_2OH) ($C_{12}H_{18}N_4O_7$), 7-hydroxy-6-methyl-8-D-ribityllumazine (RL-6-Me-7-OH) ($C_{12}H_{16}N_4O_7$) and its precursor, 6,7-dimethyl-8-D-ribityllumazine (RL-6,7-diMe) ($C_{13}H_{16}N_4O_6$)[14]. Notably, the distribution of riboflavin biosynthesis pathway is consistent with the selective activation ability of previously described bacterial strains[20,21].

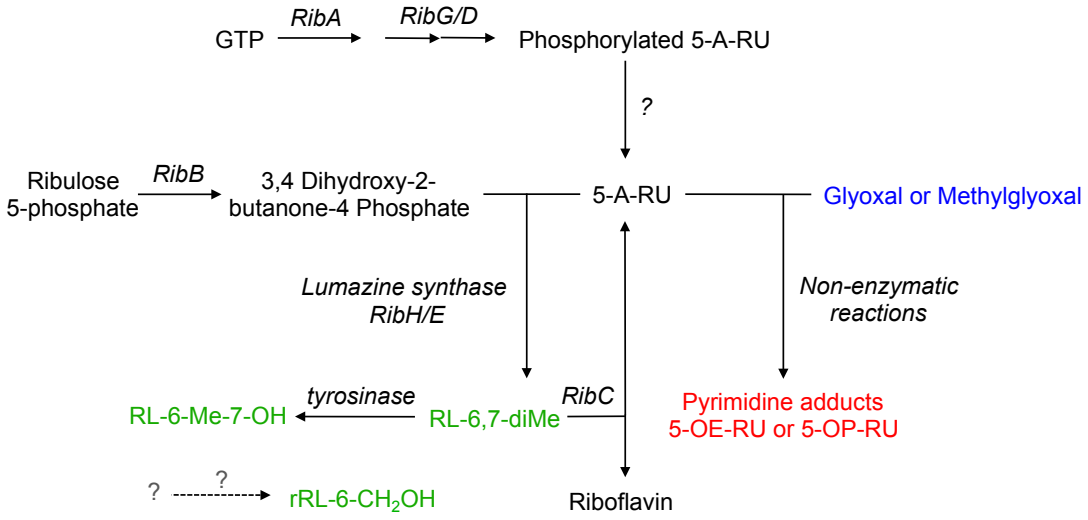

Figure 4. Riboflavin biosynthesis pathway and formation of MAIT antigens. Riboflavin biosynthesis has been described in both Gram-positive and Gram-negative bacteria. Microbial synthesis from GTP and ribulose-5-phosphate occurs through seven enzymatic steps (*Rib*). The intermediate compound 5-A-RU is the precursor of MAIT cell antigen. It gives rise to lumazine derivatives (green) or pyrimidine adducts (red, MAIT antigens). Dismutation of lumazine derivatives yields riboflavin and 5-A-RU. The latter is then recycled in the pathway. *Note: The riboflavin synthetic enzymes vary according to bacteria species. The enzymes from Lactococcus lactis*[15] *(RibA, B, C, G, H) and E.coli* [74] *(RibA, B, C, D, E) are shown.*

To further identify the origin of MAIT ligand, culture supernatant from *Lactococcus lactis* with individual mutation in the four genes of riboflavin operon (RibGBAH) were tested for activation of Jukat. MAIT cells[15]. The study showed that MAIT activation required genes encoding enzymes that synthesize riboflavin (RibA and RibG) and revealed an important intermediate compound 5-Amino-6-D-ribitylaminouracil (5-A-RU) which is the precursor of chemically unstable MAIT antigens 5-(2-oxoethylideneamino)-6-D-ribitylaminouracil (5-OE-RU) and 5-(2-oxopropylideneamino)-6-D-ribitylaminouracil (5-OP-RU)[15]. These transitory antigens are formed via non-enzymatic reaction of 5-A-RU with glyoxal (Glyx) or methylglyoxal (MeG) –byproducts of other metabolic pathways – and are stabilized by MR1. Mass spectra detected a single *m/z* 329.11 species in MR1 refolded with 5-A-RU and MeG (to form 5-OP-RU) suggesting the initially identified antigen was 5-OP-RU[14,15]. Consistently, the *m/z* 315.09 species (corresponding to 5-OE-RU) were also identified in MR1 eluate from *E.coli* and *S. typhimurium*[15]. The importance of riboflavin metabolites for MAIT activation was also reported in mice[74]. Soudais et al. showed that in addition to Glyx and MeG, dihydroxyacetone (DHA), a metabolic

intermediate from glycolysis pathway, can also form MAIT antigens through non-enzymatic reaction with 5-A-RU. Since DHA is unlikely to condensate with 5-A-RU under physiological conditions, this effect may result from the conversion of DHA to MeG. In the same work, stimulatory capacity of 5-OP-RU on murine MAIT cells was confirmed by MAIT activation following intraperitoneal injection of this compound into Vα19-Tg mice.

MAIT cells are characterized by their canonical invariant TCRα Vα7.2-Jα33 (TRAV1-2–TRAJ33), which pairs with an array of TCRβ chains dominated by Vβ2/13 (TRBV20/6)[5,7,48,50,73]. Functionally, invariant TCRα chains mediate interaction with MR1, in which two residues centrally located on opposing sides of antigen-binding cleft of MR1 are essential for MAIT activation, whereas TCRβ usage fine-tunes MR1-TCR recognition, therefore MAIT responses in an antigen-dependent manner[73,75].

Recently, by using MR1 tetramer, additional Jα usages Jα20/12 (TRAJ20/12) were identified in human MAIT cells[50]. Vα7.2-Jα12 subset was also revealed in another study using deep sequencing[48]. Lepore et al. showed Vα7.2-Jα12 T cells represent a significant fraction of circulating MAIT cells. These cells react to riboflavin-synthesizing bacteria, exert cytotoxicity against intracellular bacteria, and are able to secrete $T_H1/2$ cytokines. In some donors or tissues, such as colon, they outnumber canonical Vα7.2-Jα33 MAIT cells[48]. In addition, Gold et al. evaluated MAIT TCR repertoire against different microbes (Mycobacterium smegmatis, *Salmonella typhimurium, and Candida albicans*) and found heterogeneity of TCR usage, especially for TCRβ chains[76]. This study raises the possibility that MAIT cells may expand in response to specific pathogen. Indeed, this observation requires further confirmation as MAIT cells were defined as CD8 T cells that express TRAV1-2 (Vα7.2) and secrete TNF in response to bacterial stimulation, without using MAIT specific markers such as CD161 or IL-18Rα. Hence, a proportion of conventional T cell expressing the same TCR may be included in the analyses. In agreement with the above study, Eckle et al. demonstrated that CDR3β hypervariability regulated MAIT TCR recognition via changing TCR flexibility and contacts with MR1 and antigens[75]. Collectively, these studies suggest that MAIT cells may be able to discriminate microbial antigens and selectively expand by fine-tuning their TCR.

Cytokine Secretion

In response to phorbol 12-myristate 13-acetate (PMA) and ionomycin, peripheral blood MAIT cells are able to secrete TNF-α, IFN-γ, IL-17, and IL-2 but not IL-10, or T_H2 cytokines, whereas stimulation with *E. coli*-infected monocytes induces mainly IFN-γ production[18,61]. Similar cytokine mRNA profile was also observed in hepatic MAIT cells[61]. Moreover, intracellular staining showed that MAIT cells represented most of IL-17 producing cells in the liver and IL-17$^+$MAIT also co-produced IFN-γ but not IL-22[61]. In addition, Lepore et al. suggested that circulating MAIT cells comprise sub-populations with distinct cytokine expression profiles. In the three tested donors, most of the subsets secreted IFN-γ, MIP-1β, TNF-α, and IL-2 while IL-4 and IL-10 producer were less frequent[48]. In this study, MAIT cells were identified as Vα7.2$^+$CD161$^+$ cells, herein CD8$^+$ MAIT cells cannot be distinguished from the CD4 subset. Whether a unique cytokine profile is linked to a specific co-receptor usage remains to be determined. Study on Vα7.2-Jα12/33 clones showed that upon stimulation with *E. coli*-infected THP-1 cells, these MAIT clones released T_H2 cytokines (IL-4, 5, 10 and 13) together with T_H0 (GM-CSF), T_H1 (IFN-γ, TNF-α) cytokines but not IL-17[48]. T_H2 cytokine responses to TCR ligation was also observed in MAIT cells from Vα19 transgenic mice[77]. Furthermore, following stimulation with PFA-fixed *E.coli* and anti-CD28 mAb, fetal intestinal MAIT cells released IL-22 and IFN-γ, while fetal liver and lung solely elicited IFN-γ[54]. In contrast, MAIT cells from fetal thymus, spleen and MLN produced IFN-γ in response to PMA/ionomycin but not *E. coli* stimulation[54]. The production of IL-22 was also reported in blood MAIT cells from patients with inflammatory bowel disease[78]. Collectively, MAIT cells have a $T_H1/17$ cytokine secretion profile and, to a much less extent, are capable to produce T_H2 cytokine. Their cytokine secretion pattern may reflect the maturation state, antigen exposure history, their tissue distribution, as well as microenviromental cues. How different cytokine releases is regulated and their physiological relevance in health and disease remain to be addressed.

Cytotoxicity

One of the most important features of MAIT cells is their anti-microbial activity. In murine models, their contribution in controlling bacterial infections has been demonstrated in many reports, included *E.coli, Mycobacterium abscessus, Klebsiella pneumonia, Mycobacterium bovis* bacillus Calmette-Guérin *(BCG) as well as*

Francisella tularensis infections, in which cytokine release from MAIT cells were proved essential[20,79–81]. In addition to cytokine secretion, human MAIT cells were also reported to be cytotoxic as they produced granzyme B in response to bacteria stimulation[18]. A recent study demonstrated that MAIT cells could detect and kill epithelial cells infected with invasive *Shigella flexneri,* suggesting their function in control of bacteria dissemination[58]. A second report supports the above study[59]. Kurioka et al. showed that upon stimulation, MAIT cells exchanged their cytotoxic granule contents (granzyme A and K in resting cells; granzyme B and perforin in stimulated cells) and are licensed to kill cognate target cells, including APC, with greater efficiency. Moreover, this report suggested that in addition to TCR, a second signal, such as cytokine, was required for potent cytotoxicity as the blocking of IL-12 compromised the induction of granzyme B and perforin. This exquisite regulation may be important to prevent unnecessary host damage[59].

MAIT Activation

Freshly isolated blood MAIT cells are in a nonproliferating state, as they barely express Ki67[18]. Similar feature was also described in adult liver MAIT cells[61]. However, MAIT cells from fetal tissues express considerable levels of Ki67 and readily proliferate in response to fixed *E.coli* and its supernatant[54]. Increased levels of proliferation were also observed in cord blood following TCR stimulation[62]. The high proliferation rate of MAIT cells found in fetal tissues and cord blood may reflect their developmental stages. Although adult MAIT cells poorly respond to TCR stimulation, their proliferative responses could be induced by costimulation with anti-CD28 or innate cytokines[59,62]. Moreover, MAIT cells also respond to *E.coli* and are ready to proliferate, being $Ki67^+$ for about 60% of the population[59]. Their proliferating capacity are inhibited by blocking with anti-MR1 antibody.

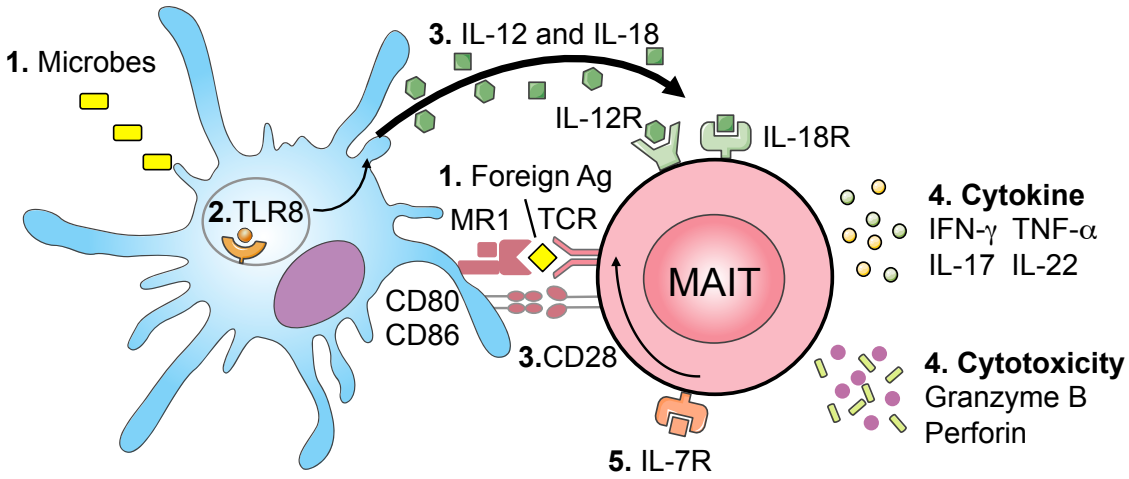

Figure 5. Activation of MAIT cells[82,83]**. (1)** APCs uptake microbes and present foreign antigen – vitamin B2 metabolites – to MAIT cells via MR1-iTCR interaction. **(2)** Microbial components also trigger pathogen recognition receptors (e.g., TLR8) resulting in the release of innate cytokines (e.g., IL-12, IL-18). **(3)** The responsiveness of MAIT cells can be enhanced by costimulation with coreceptor CD28 or innate cytokines. **(4)** Activated MAIT cells produce $T_H1/17$ cytokines and exhibit cytotoxicity. **(5)** IL-7 enhances cytokine secretion of hepatic MAIT cells through the regulation of TCR-signaling components. Figures were generated using images from Servier Medical Art (www.servier.com), licensed under the Creative Commons Attribution 3.0 Unported License (http://creativecommons.org/license/by/3.0/).

MR1-dependent MAIT activation to bacteria was initially studied, in which blockade of MR1 abrogates the upregulation of early activation marker CD69 and diminishes the production of IFN-γ by MAIT cells[20]. However, MAIT cells poorly respond to TCR stimulation, showing low cytokine production compared to mitogen stimulation[18,61,62,84]. This raised the question of whether MAIT activation could also be induced by a TCR-independent manner (as shown in iNKT cells, Figure 2). The low responsiveness of MAIT cells to TCR stimulation is due to the down- or up-regulation of genes encoding positive and negative regulators in TCR signaling pathway that are yet distinct from those of exhausted and anergic T cells[62]. Similar to their induction of proliferative response, low cytokine production by MAIT cells can also be restored by costimulation with anti-CD28 or innate cytokines[59,62]. Given that resting MAIT cells express high levels of IL-7R, IL-12R, and IL-18R, the role of corresponding cytokines has been established in a number of studies. A recent study on human liver MAIT cells showed that IL-7 – a cytokine produced by hepatocytes during inflammation – enhanced cytokine production of MAIT cells through the regulation of TCR-signaling components[61]. Yet this observation requires further confirmation as bulk liver mononuclear cells were incubated with IL-7. Therefore,

whether this was a specific effect or a bystander consequence remains to be determined. Using recombinant cytokines IL-12, IL-18, and Toll-like receptor (TLR) agonists, Ussher et al. demonstrated that MAIT cells respond to innate cytokine stimulation in an TCR-independent manner[19]. The subsequent study on liver MAIT cells showed that MAIT cells indirectly responded to TLR8 agonist depending on secretion of IL-12 and IL-18 by ssRNA-activated intrahepatic monocytes[84]. These results broaden the potential responsiveness of MAIT cells to non-riboflavin-synthesizing bacteria, virus, as well as inflammatory stimuli. Responses to innate cytokines were also reported in iVα19-Tg murine models where innate cytokine IL-12 rather than MR1 dominated MAIT activation and their effector functions in control of BCG infection[80]. Similar results were showed in pulmonary *Francisella tularensis* infection[81]. Collectively, these studies suggest that multiple factors regulate MAIT responsiveness during infection and infer their potential role in inflammatory diseases.

MAIT Cell in Human Diseases

Bacterial Infection

The role of MAIT cells in bacterial infection was initially studied in *Mycobacterium tuberculosis* infection. MAIT cells are present in human lung and react to *Mycobacterium tuberculosis in vitro*[21]. In individuals with active tuberculosis (TB), the frequency of MAIT cells decreases in the peripheral blood and pleural effusions compared with healthy subjects, suggesting that they may migrate to the inflamed lung and contribute to the local responses[20,21,85]. The subsequent functional study showed that in response to BCG but not *E.coli* stimulation, MAIT from TB individuals produced moderately higher amount of IFN-γ and TNF-α compared to healthy individuals[85]. This finding led the authors to propose that MAIT cells might selectively expand upon antigen exposure in TB patients, as suggested in reference[76]. Moreover, as MAIT from TB individuals expressed elevated levels of inhibitory receptor PD-1, blockade of PD-1 resulted in a higher production of cytokines following BCG activation, therefore PD-1 on MAIT cells could be a potential target for TB immunotherapy[85].

Decreased frequency of circulating MAIT cells was also observed in a clinical trial testing the efficacy of an oral *Shigella* vaccine[58]. A specific reduction of MAIT cells

was observed on day 11 post vaccination. When analyzing vaccine responder and non-responder separately (based on specific IgA responses), increased MAIT proportion and upregulation of activation marker HLA-DR were only observed in responder group. However, the relation between MAIT activation and specific IgA response remains to be addressed.

Similarly, reduction of circulating MAIT cells in bacterial infection has also been addressed in many other reports, including *Pseudomonas aeruginosa* pulmonary infection, *Vibrio cholerae* infection in children, as well as septic patients with severe bacterial infections[86–88].

Viral Infection

In addition to bacterial infections, decreased circulating $CD161^{hi}$ Tc17 cells, mostly MAIT cells, were also reported in patients with chronic hepatitis C (HCV)[51]. Instead, these cells were found enriched in liver and their prevalence was inversely correlated with the clinical disease score, suggesting that they may contribute to the control of disease progression[51]. As previously discussed, hepatic MAIT cells indirectly respond to TLR8 agonist ssRNA and produce IFN-γ[84]. Similar responses were also present in pathologic livers, such as those with HBV and HCV infections[84]. This raises the question of whether MAIT can act as a therapeutic target for the treatment of liver diseases.

Likewise, in early and chronic human immunodeficiency virus (HIV) infection, circulating MAIT population was found to be severely decreased and failed to recover following anti-retroviral therapy, whereas their number in rectal mucosa was relatively preserved[89–91]. In addition, the residual circulating MAIT cells were functionally impaired from individuals infected with HIV for 6-8 years[90]. It has been reported that HIV impaired mucosal epithelial barrier integrity resulting in microbial translocation and therefore systemic immune activation[92]. Accordingly, the loss of MAIT cells and their functional impairment may contribute to the increased susceptibility to microbial infection in HIV patients, thus rescue of MAIT cells may help restore host defense in immunodeficient patients.

Autoimmune Diseases

As discussed above, MAIT responsiveness to innate cytokines and their localization at mucosal surface implicate that they may play a role in autoimmune diseases. The frequency and potential function of MAIT cells in different autoimmune diseases are summarized in table 2. Although MAIT cells have been associated with various autoimmune diseases, how they function and contribute in these diseases is an open question that warrants further investigation. A physiologically relevant mouse model will indeed benefit the understanding of MAIT cells under (patho-)physiological conditions.

Table 2. MAIT cells in inflammatory diseases

Disease	Blood	Inflamed Site	Function
MS[93]	➔	↑	ND
MS[94]	↑	ND	Pathogenetic potential through IFN-γ production
MS[95]	↓	ND	Protective potential: Suppress IFN-γ produced by pathogenic T_H1 cells
Psoriasis[96]	ND	Slightly increase in dermis, but decrease in epidermis (ns)	Pathogenetic potential through IL-17 production
Asthma[97]	↓	↓	Protective potential: Their deficiency correlates with clinical severity
Type I diabetes[98]	$CD27^-$ MAIT ↑	ND	Pathogenetic potential through IL-17 production
Type II diabetes and obesity[99]	↓	➔, but higher than in blood	Pathogenetic potential through IL-17 production
Inflammatory Bowel Disease (IBD)[78]	↓	↑	Pathogenetic potential through IL-17 production
Systemic lupus erythematosus (SLE) and rheumatoid arthritis (RA)[100]	↓	In RA patient, higher in synovial fluid than blood	Their deficiency correlates with clinical severity.
Kidney and brain tumor[101]	ND	$CD56^-$MAIT infiltration	Anti-tumor potential through $T_H1/17$ cytokine production

↓↑➔, deceased, increased or preserved MAIT levels in patients, compared with healthy donors; **ND**, not determined; **ns**, not significant

Laboratory Mouse Strains

Mice are commonly used model organism and experimental tool in immunological research and in many respects they mirror human biology. Notably, mouse genome sequencing revealed about 30,000 genes, with 99% having analogues in human[102]. Among many reasons to use mouse as an experimental model, the most important ones are: their genetic isogenicity, ease of genetic manipulation, possibility to perform *in vivo* analyses, and the limited accessibility to human samples[103]. The use of such model shed lights on human immunology. However, as mouse and human diverged millions of years ago, significant differences exist between the two species. The differences include lifespan, body size, and ecological niche, which have huge impact on immune system[104]. Hence, such differences should be taken into account when interpreting and translating murine findings to human.

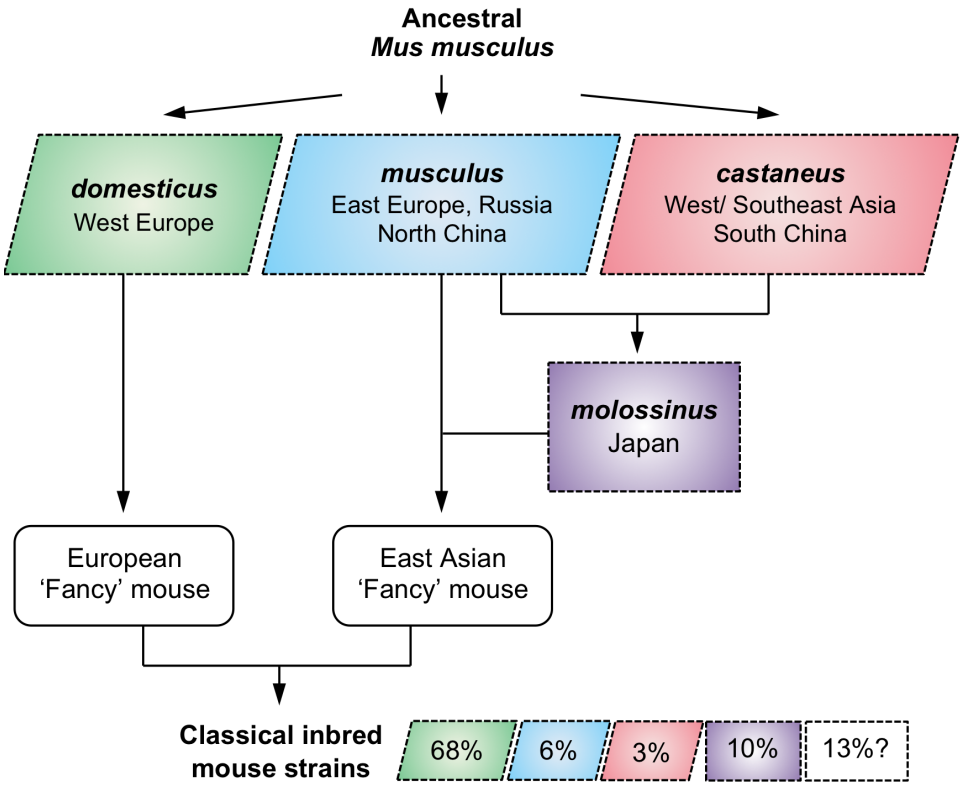

Figure 6. Origin of classical inbred laboratory mouse strains. Classical inbred mouse strains were bred in early 20th century from a limited number of founding 'fancy' mice. The genetic contributions of *Mus musculus* subspecies to the haplotypes of laboratory strains are indicated.

Classical Inbred Strains

Most laboratory mouse strains, including commonly used C57BL/6, BALB/c, C3H/He, and 129/Sv strains, were derived from *Mus musculus (M.m.) domesticus, M. m. musculus, M. m. castaneus,* and the hybrid *M. m. molossinus*. The genetic contributions of each subspecies are 68%, 6%, 3% and 10%, respectively[105]. The ancestral origin of the remaining 13% of haplotypes is unknown (Figure 6)[105]. Due to the limited number of founder mice, these inbred strains represent only a small proportion of the genetic diversity of their ancestors.

TCR-Transgenic Strains and MAIT Cells

Unlike in human, the frequency of MAIT cells in classical inbred mouse strains is exceedingly low[7]. The lack of iTCR Vα19 specific antibody or surrogate makers has made it more challenging to study these cells in mice. Therefore, studies on mouse MAIT cells were mostly performed in TCR-transgenic (Tg) mice (i.e., Vα19-Tg, Vβ6-Tg, and Vα19-Vβ6-Tg) in which the MAIT iTCRα chains or/and its preferential pairing TCRβ chains were overexpressed. These Tg strains have been used to investigate MAIT development[49,64], microbial reactivity[20], and their implication in bacteria infections[20,80] and inflammatory diseases[106,107]. Notably, these Tg MAIT cells do not adequately recapitulate the phenotype of human MAIT cells as they lack the expression of transcription factor PLZF and exhibit a naïve phenotype whereas MAIT cells in human are memory and express PLZF[49]. Tg MAIT cells were derived from T-T hybridoma using peripheral T cells form $TAP^{-/-}$ $Ii^{-/-}$ mice and were selected based on TCRα usage[7]. Therefore they may not be fully tolerant to MHC-I or II molecules. Moreover, in the absence of exogenous ligand, a number of hybridoma were found to react against MR1-overexpressing cells lines suggesting that they may exhibit autoreactivity to MR1-expressing cells or respond to the riboflavin metabolites antigen from the culture media uptaken by MR1[71]. In addition, the newly defined MR1-tetramer identified that more than 40% of $tetramer^{+}$ cells from Vα19-Tg mice are $CD4^{+}$, in contrast to human MAIT cells in which only a small population expresses CD4[50]. Unexpectedly, MR1-tetramer also detects $tetramer^{+}$ cells in Vα19-Tg $MR1^{-/-}$ mice in which the restriction molecule MR1 is absent[50]. In some studies, TAP and Ii knockout genes were introduced, leading to a low frequency of conventional T cells. Such models lack the physiologic integrity, therefore are

inappropriate to address the immunoregulatory or nonredundant role of MAIT cells. Thus, it remains to be determined whether these inconsistencies between Tg and human MAIT hold true for naturally occurring mouse MAIT cells.

Wild-derived Inbred Strains

In addition to above classical inbred strains, there are also wild-derived inbred strains, which represent more divergent genetic origins compared to the classical ones. Wild-derived inbred mice were established from mice captured in the wild at different times and locations, which were then inbred to homozygosity[105]. They are derived directly from major taxonomic groups of *Mus musculus* subspecies, such as CAST/Ei (*M.m.castaneus*), MOLF/Ei (*M.m.molossinus*), PWD/Ph (*M.m.musculus*), and WSB/Ei (*M.m.domesticus*). Among wild-derived inbred strains, CAST/Ei represent the lowest genetic contribution to the haplotype of classical strains (3%), resulting in a higher density of DNA polymorphisms than other strains[108]. Thus, there is a higher possibility to identify natural variation in CAST/Ei. Indeed, CAST/Ei have been used to identify loci affecting on various phenotypes, such as growth and obesity[109], B lymphocyte deficiency[110], hearing loss[111], and axonal regeneration in CNS[112]. Identification of these loci requires genetic mapping approach which links phenotype of interest to polymorphic makers of known chromosomal location, such as single nucleotide polymorphism (SNP)[113]. Moreover, among common inbred strains, densely distributed SNPs (average density of 1 SNP per 311 base pairs) facilitate the identification of causative genetic changes[105].

Results

Aim of the study

The aim of the study in this thesis was to identify natural (non TCR Tg) mouse MAIT cells, to analyze their phenotypic and functional features and ultimately to generate a mouse model to study MAIT cells in health and disease.

Findings and conclusions

Due to the scarcity of MAIT cells in classical inbred mice, we set up a screen for MAIT iTCR Vα19-Jα33 expression in wild-derived inbred strains, among which, CAST/Ei (CAST) harbor 20 fold higher of MAIT iTCR than that of classical C57BL/6 (B6) mice.

The crossing of CAST mice to the B6 background caused a dichotomous segregation of MAIT iTCR Vα19-Jα33 expression in the N2 progeny. Genetic mapping identified a single locus on the TCRα region accounting for the expression of Vα19-Jα33 and allowed the generation of a B6-*MAIT*^{CAST} congenic strain. Although the exact molecular mechanism was not elucidated, the TCRα repertoire analysis revealed that the usage of distal Vα segments was increased in CAST mice while Jα remained unchanged compared with those of B6 mice. Notably, Vα19 is the most distal Vα, thus the general increase of distal Vα usage contributed to the higher frequency of MAIT cells in CAST mice.

Given that human MAIT cells express the transcription factor RORγt[18,51,55], we introgressed Rorc(γt)-Gfp^{TG} reporter gene[114] onto B6-*MAIT*^{CAST} congenic mice and used RORγt-GFP as a surrogate maker to label MAIT cells.

Using this tool, we have characterized that natural mouse MAIT cells are CD4^{-}CD8$^{-/lo}$ and display an effector memory phenotype (CD44^{+} CD62L^{-}) and tissue-homing properties (CCR6^{+}CCR7^{-}). Higher frequency of MAIT cells are present in non-lymphoid tissues such as liver, lung, skin, and gut than in lymphoid organs including spleen and MLN.

Similar to their human counterparts, mouse MAIT cells express high levels of cytokine receptors (IL-7R, IL-18Rα, IL-12Rβ) and coexpress transcription factors PLZF and RORγt. Moderate levels of NK1.1 and CXCR6 are also expressed by hepatic but not splenic MAIT cells.

Upon TCR ligation, $T_H1/2/17$ type cytokines are detected in the supernatant of purified MAIT cell culture. Intracellular cytokine staining showed that in response to anti-CD3/CD28 beads or PMA/ionomycin, MAIT cells exclusively secrete IL-17 whereas stimulation with *E.coli*-infected bulk splenocytes mainly induce IFN-γ releases.

In addition, mouse MAIT cells specifically respond to bacterial-derived antigens (i.e., semi-purified *E.coli* supernatant or 5-OP-RU) in an MR1-dependent manner. During experimental urinary tract infection, MAIT cells migrate to the bladder and display a protective anti-bacterial activity.

Collectively, the "MAIT" congenic strain allows the phenotypic and functional study of naturally occurring mouse MAIT cells in health and disease.

Paper

Mucosal-associated invariant T cell–rich congenic mouse strain allows functional evaluation

Yue Cui[1]*, Katarzyna Franciszkiewicz[1]*, Yvonne K. Mburu[1], Stanislas Mondot[1], Lionel Le Bourhis[1], Virginie Premel[1], Emmanuel Martin[1], Alexandra Kachaner[1], Livine Duban[1], Molly A. Ingersoll[2], Sylvie Rabot[3,4], Jean Jaubert[5], Jean-Pierre De Villartay[6], Claire Soudais[1], Olivier Lantz[1,7,8,9]

[1] *Institut Curie, Inserm U932, Paris, France.*
[2] *Dendritic cell immunobiology Unit and Inserm U818, Institut Pasteur, Paris France*
[3] *INRA, UMR1319, Micalis, Jouy-en-Josas, France.*
[4] *AgroParisTech, Micalis, Jouy-en-Josas, France*
[5] *Mouse Functional Genetics Unit, Institut Pasteur, Paris France*
[6] *INSERM U768, Hôpital Necker, Paris, France*
[7] *Center of Clinical Investigations CICBT507 IGR/Curie, Paris, France*
[8] *Equipe labellisée de la ligue de lutte contre le cancer, Institut Curie, Paris, France*
[9] *Département de biopathologie, Institut Curie, Paris, France*
* These authors contributed equally to this study.

Correspondance to:
Olivier Lantz
Laboratoire d'Immunologie and Inserm U932,
Institut Curie, 26 rue d'Ulm, 75005 Paris, France.
Phone: +33 144324218
Fax: + 331 53 10 26 52
Email: olivier.lantz@curie.fr

J Clin Invest. doi:10.1172/JCI82424.

Mucosal-associated invariant T cell–rich congenic mouse strain allows functional evaluation

Yue Cui,[1] Katarzyna Franciszkiewicz,[1] Yvonne K. Mburu,[1] Stanislas Mondot,[1] Lionel Le Bourhis,[1] Virginie Premel,[1] Emmanuel Martin,[1] Alexandra Kachaner,[1] Livine Duban,[1] Molly A. Ingersoll,[2] Sylvie Rabot,[3,4] Jean Jaubert,[5] Jean-Pierre De Villartay,[6] Claire Soudais,[1] and Olivier Lantz[1,7,8,9]

[1]Institut Curie, INSERM U932, Paris, France. [2]Dendritic Dell Immunobiology Unit and INSERM U818, Institut Pasteur, Paris, France. [3]INRA, UMR1319, Micalis, Jouy-en-Josas, France. [4]AgroParisTech, Micalis, Jouy-en-Josas, France. [5]Mouse Functional Genetics Unit, Institut Pasteur, Paris, France. [6]INSERM U768, Hôpital Necker, Paris, France. [7]Center of Clinical Investigations CIC BT507 IGR/Curie, Paris, France. [8]Equipe Labellisée de la Ligue de Lutte Contre le Cancer, Institut Curie, Paris, France. [9]Département de Biopathologie, Institut Curie, Paris, France.

Mucosal-associated invariant T cells (MAITs) have potent antimicrobial activity and are abundant in humans (5%–10% in blood). Despite strong evolutionary conservation of the invariant TCR-α chain and restricting molecule MR1, this population is rare in laboratory mouse strains (≈0.1% in lymphoid organs), and lack of an appropriate mouse model has hampered the study of MAIT biology. Herein, we show that MAITs are 20 times more frequent in clean wild-derived inbred CAST/EiJ mice than in C57BL/6J mice. Increased MAIT frequency was linked to one CAST genetic trait that mapped to the TCR-α locus and led to higher usage of the distal Vα segments, including Vα19. We generated a MAIT^{hi} congenic strain that was then crossed to a transgenic *Rorcgt-GFP* reporter strain. Using this tool, we characterized polyclonal mouse MAITs as memory (CD44$^+$) CD4$^-$CD8$^{lo/neg}$ T cells with tissue-homing properties (CCR6$^+$CCR7$^-$). Similar to human MAITs, mouse MAITs expressed the cytokine receptors IL-7R, IL-18Rα, and IL-12Rβ and the transcription factors promyelocytic leukemia zinc finger (PLZF) and RAR-related orphan receptor γ (RORγt). Mouse MAITs produced Th1/2/17 cytokines upon TCR stimulation and recognized a bacterial compound in an MR1-dependent manner. During experimental urinary tract infection, MAITs migrated to the bladder and decreased bacterial load. Our study demonstrates that the MAIT^{hi} congenic strain allows phenotypic and functional characterization of naturally occurring mouse MAITs in health and disease.

Introduction

Mucosal-associated invariant T cells (MAITs) express an invariant TCR-α (iTCR-α) chain (iVα7.2-Jα33 in human and iVα19-Jα33 in mouse) restricted by the major histocompatibility complex (MHC) class I–related protein 1 (MR1) (1–4). MAITs recognize bacteria-infected cells (5, 6) and display antimicrobial activity in several experimental infection models (6–8). There is a strict correlation between the capacities of a bacterial strain to activate MAITs and to synthesize riboflavin (vitamin B2) (rib) (6, 9). Indeed, MAITs specifically recognize derivatives of the rib biosynthetic pathway, which is absent from mammals, but present in most bacteria and in yeasts (9, 10).

MAITs are decreased in the blood of patients suffering from subacute (5, 6) or acute infections (11) and are detected at the site of infection. The frequency of MAITs is also modified in nonbacterial diseases: increased in recently diagnosed multiple sclerosis patients (12, 13), but decreased in obesity, type-2 diabetes (14), inflammatory bowel disease (15), and HIV (16–19).

MAITs are CD4$^-$CD8$^-$ (DN) (and also CD8αα in humans) or CD8αβ^{int}. They are abundant in the blood (1%–10%), gut (3%–5%), and liver (20%–50%) of humans, but are extremely rare in laboratory mouse strains (20–22). The disparity in frequency between species contrasts with the high conservation of both the TCR-α and MR1 molecules, which indicates a strong evolutionary selection pressure and thereby important functions (23).

The phenotype and functional properties of MAITs are much better known in humans than in mice. Human MAITs from adult peripheral blood display an effector memory phenotype (CD45RO$^+$, CD62L$^-$, CD95$^+$) and tissue-homing features (CCR2$^+$, CCR5+, CCR6$^+$, CXCR6$^+$, CCR9$^+$, CCR7$^-$) (21, 24). They secrete high amounts of IFN-γ, TNF-α, and granulocyte-macrophage CSF (GM-CSF) and have the potential to secrete IL-17 and IL-22 (21, 24–26), but not Th2 cytokines (21, 27). MAITs are cytotoxic for epithelial cells infected by invasive bacteria (28, 29). In addition to TCR triggering, MAITs can be activated by innate cytokines such as IL-12 and IL-18 (25, 30). Consistent with their innate-like features and IL-17 secretion capacity, MAITs express the transcription factors ZBTB16 (promyelocytic leukemia zinc finger [PLZF]) and RAR-related orphan receptor γ (RORγt) (21, 24, 31, 32).

In the cord blood, human MAITs display a naive phenotype, and their TCR-β repertoire is diverse (21, 22). After birth, MAITs expand to reach high clonal size (20, 33). This contrasts with the low cell-division rate of MAITs in human adult blood, shown by low Ki-67 expression (21, 34). Taken together, these data indicate that MAITs either proliferated during childhood or undergo division in the tissues and recirculate to the blood once resting.

Authorship note: Yue Cui and Katarzyna Franciszkiewicz contributed equally to this work.
Conflict of interest: The authors have declared that no conflict of interest exists.
Submitted: April 17, 2015; **Accepted:** September 3, 2015.
Reference information: *J Clin Invest*. doi:10.1172/JCI82424.

Table 1. Fine mapping of the MAIT^{hi} locus in informative recombinant mice generated during backcrossing MAIT^{CAST} phenotype to B6

	Mbp (on chromosome 14)								
Vα19-Jα33[A]	53.70	54.25	54.40	54.70	54.83	54.86	55.00	56.00	57.00
0.7	B6	B6	B6	B6	B6	B6	B6	Het	Het
0.44	B6	B6	B6	B6	B6	B6	Het	Het	Het
2.35	B6	B6	B6	B6	B6	**Het**	Het	Het	Het
0.95	Het	**Het**	B6	B6	B6	B6	B6	B6	B6
6.99	Het	Het	Het	Het	**Het**	B6	B6	B6	B6
10.74	Het	Het	Het	Het	Het	Het	Het	B6	B6

[A]Vα19-Jα33 mRNA levels measured by RT-qPCR in blood or MLNs. Fold change relative to B6 MLNs, after normalization to Cα. Bold indicates the most informative recombination point.

In contrast to human, mouse MAITs are extremely rare in common laboratory mouse strains. So far, the study of MAIT physiology has mostly relied on mice that are Tg for the MAIT TCR chains. Several iVα19 TCR-α Tg strains have been produced (32, 35, 36). In iVα19 Tg *Ca*$^{-/-}$ (to prevent the expression of endogenous TCR-α chains) mice, on an MR1-sufficient background, the DN and CD8^{lo} T cells display an increased usage of the Vβ6 and Vβ8 TCR-β segments (32, 36, 37). Most of these Vβ6^{+} or Vβ8^{+} T cells are activated by bacteria (6, 38). These TCR-α Tg models allow the study of MAIT specificity and antibacterial activity in vitro and in vivo (6, 39, 40), even if, in contrast to humans, most MAITs display a naive CD44^{lo} phenotype (32). This is probably related to the forced premature expression of the TCR-α chain transgene, which also greatly modifies the functionality of the Tg T cells (41). This casts doubt on the relevance of these TCR Tg laboratory mouse models for studying the physiological functions of MAITs. Likewise, in non-TCR Tg mouse models, antibody-mediated (8) or genetic (6) depletion of conventional T cells was necessary to evidence the role of MAITs in experimental infections. Thus, the phenotype as well as the function of naturally occurring mouse MAITs in health and disease remains to be addressed.

Two possibilities arise to explain the low frequency of MAITs in laboratory mice: (a) mice from animal facilities lack specific bacterial strains or communities in their microbiota that are necessary to sufficiently expand MAITs or (b) during the genetic bottleneck that occurred upon their establishment, laboratory mice lost an allele necessary for MAIT peripheral activation, expansion, or survival. We first studied the environmental hypothesis and then found that laboratory mouse strains have lost one genetic element implicated in MAIT development. A "MAIT^{hi}" congenic strain was generated and further crossed to a *Rorcgt-GFP*^{TG} reporter strain. Most of the GFP^{+} memory DNCD8^{lo} T cells were identified as MAIT, according to the expression of the iVα19 TCR-α chain and MR1 dependence. Using this tool, we analyzed the phenotype, peripheral expansion, and functions of naturally occurring mouse MAITs in health and in experimental urinary tract infection (UTI).

Results

Reconstitution of germ-free mice with human microbiota is insufficient to increase the number of MAITs above that found in specific pathogen–free-raised mice. We previously showed that colonization of germ-free (GF) mice with 1 microbial species is sufficient to increase the number of MAITs to the levels found in mice of specific pathogen–free (SPF) facilities (6). However, the number of MAITs was still much lower than that found in humans. This could be due to a lack of a specific bacterial strain or combination thereof that is only found in humans.

To test this hypothesis, we reconstituted breeding GF mice with a human microbiota and examined the frequency of MAITs in the pups 4 to 8 weeks after weaning. To increase the reliability of our experiment, we used *Tap*$^{-/-}$ *Ii*$^{-/-}$ mice, which harbor 10-fold more MAITs than C57BL/6J (B6) mice (32). We verified that the human microbiota had implanted (Supplemental Figure 1; supplemental material available online with this article; doi:10.1172/JCI82424DS1) and measured MAIT frequency in the colon lamina propria (LP) by quantitative reverse-transcription PCR (RT-qPCR) of the specific Vα19-Jα33 (iVα19) TCR-α chain transcripts. We found that the frequency of MAITs in mice reconstituted with human microbiota was similar to that found in mice from our SPF facility (Figure 1A). This result suggests that the small number of MAITs found in mice from SPF animal facilities is probably not due to the absence of specific microbes or combinations thereof.

The CAST/EiJ mouse strain harbors 20 times more MAITs than B6 mice. To test the genetic hypothesis that would explain the low number of MAITs in laboratory mice, we next measured MAIT frequency in SPF inbred mouse strains harboring a wider genetic diversity than conventional laboratory mice. Among 7 wild mouse strains tested (data not shown), we found 2 with increased frequency of MAITs: *Mus musculus castaneus* (CAST/EiJ abbreviated CAST) and *Mus musculus musculus* PWK (Figure 1B). We focused on the CAST strain that harbored the highest frequency of MAITs (15.4 ± 7.3 AU, mean ± SD). To assess the genetic basis of this phenotype, we crossed CAST (MAIT^{hi}) to B6 (MAIT^{lo}) to generate F1 mice. The frequency of MAITs in F1s was intermediate (Figure 1B). To determine the number of loci involved, we crossed the F1s to B6s to generate N2s (Figure 1B). The N2s segregated into 2 groups of roughly equal size with either low or intermediate frequency of MAITs, suggesting that only 1 locus is responsible for the MAIT^{hi} phenotype. This result allowed a straightforward linkage analysis on 66 N2s using 4,700 informative SNPs distinguishing B6 and CAST. We identified a single locus in a 20-Mb region on chromosome 14 (Figure 1C) linked with the MAIT^{hi} phenotype. To confirm this analysis, we also generated F2s and correlated the iVα19 levels in mesenteric lymph nodes (MLNs) with the genotypes (B6/B6, B6/CAST, CAST/CAST) of the previously mapped regions (Figure

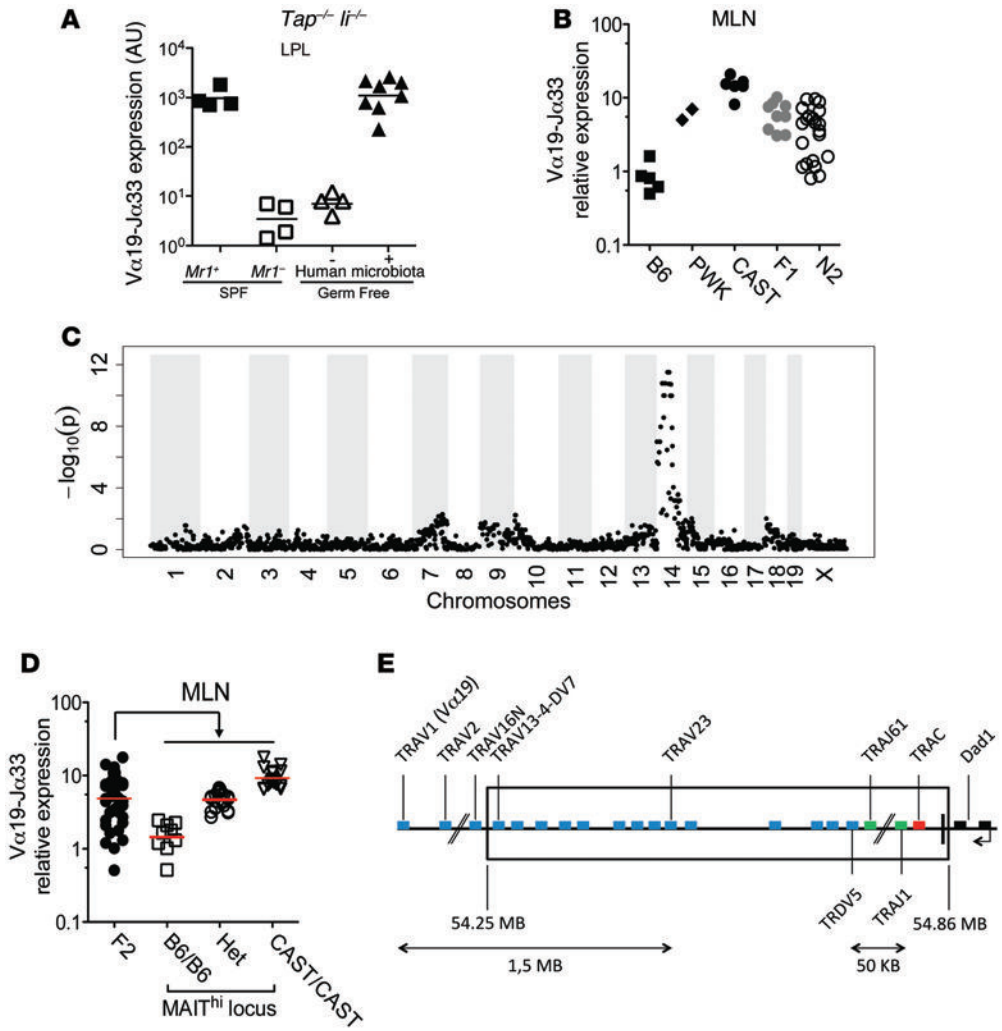

Figure 1. MAIT abundance in mouse is determined by genetic background rather than a limited microbiota. (**A**) Normalized Vα19-Jα33 mRNA levels in the LP of the progeny of GF *Mr1*$^{+}$ *Tap*$^{-/-}$ *Ii*$^{-/-}$ breeding pairs reconstituted or not with human microbiota. *Mr1*$^{+}$ or *Mr1*$^{-/-}$ *Tap*$^{-/-}$ *Ii*$^{-/-}$ SPF mice are shown as controls. (**B**) Normalized Vα19-Jα33 mRNA expression in the MLNs of B6, PWK, CAST, F1 (B6 × CAST), and N2 (F1 × B6). (**C**) Manhattan plot of SNP call significance ($-\log_{10}[P]$) of MAIT^{hi} versus MAIT^{lo} (BC2 or BC3) ordered by chromosomal location. (**D**) Normalized Vα19-Jα33 mRNA expression in the MLNs of F2 (F1 × F1) mice, grouped by genotype of the MAIT^{hi} locus: B6/B6, Het, CAST/CAST. (**E**) Genomic map of the chromosome 14 TCR-α region encompassing the MAIT^{CAST} locus (boxed).

1D). The results fully confirmed the linkage analysis and indicate a strong gene-dosage effect.

Increased frequency of MAIT-specific iTCR-α rearrangement in CAST mice. As only 1 locus was involved in the MAIT^{CAST} phenotype, we generated a B6-MAIT^{CAST} congenic strain that would have a high number of MAITs on a B6 background by backcrossing the MAIT^{CAST} trait to B6 for more than 10 generations. The additional recombinants generated during this process allowed us to narrow down the MAIT^{hi} locus to the TCR-α region (Table 1). This 0.6-Mb region does not include the iVα19 (TRAV1)segments, but encompasses the 3′ end of the Vα locus, TCR-δ, Jα, and Cα segments (Figure 1E). This TCR-α location suggested that the higher frequency of MAITs found in the CAST strain might be related to an increased generation of the iVα19-Jα33 rearrangements.

Since MAITs do not accumulate in the thymus (see ref. 32 and below), the increased generation of the iVα19-Jα33 rearrangement was consistent with the higher frequency of iVα19 transcripts in the thymus of CAST mice in comparison with B6 (Figure 2A). This hypothesis is further supported by the strict segregation of the iVα19 levels in the thymus of the F2s according to the MAIT locus genotype (Figure 2A). To determine whether expression of the MAIT^{CAST} trait by hematopoietic cells was sufficient to increase MAIT frequency, T cell–depleted BM from B6-MAIT^{B6} or B6-MAIT^{CAST} mice was used to reconstitute irradiated CD45.1 congenic mice. In these chimeras, the presence of the MAIT^{CAST} trait in the hematopoietic compartment resulted in increased MAIT frequency in the different organs (Figure 2B), indicating that the MAIT^{CAST} phenotype is hematopoietic intrinsic.

To better investigate the mechanisms leading to the increased rate of Vα19-Jα33 usage, we quantified the usage of the different Vα and Jα segments in the thymus of B6, BALB/c, and CAST strains. We used a 5′ RACE TCR-α amplification step followed by deep sequencing (42). Because the Vα segments rearrange to the Jα segments in a sequential and orderly fashion beginning with the most 3′ Vα and 5′ Jα segments and the Vα19 segment is the most 5′, the frequency of the iVα19-Jα33 rearrangements might be proportional to the usage of the most distal (5′) Vα segments. We indeed observed a much higher usage of the distal Vα segments in CAST mice as compared with B6 mice (Figure 2C), while no difference was found with regards to Jα usage (Supplemental Figure 2A). The increased usage of distal Vα segment in CAST could result from the lack of a Vα triplication that is exclusively present in B6 mice (Figure 2C and ref. 43). Hence, we quantified the Vα segments in thymocytes from BALB/c mice, which also lack this triplication: the distal Vα usage was slightly increased, but did not reach CAST levels (Figure 2C), in agreement with MAIT iTCR-α frequency

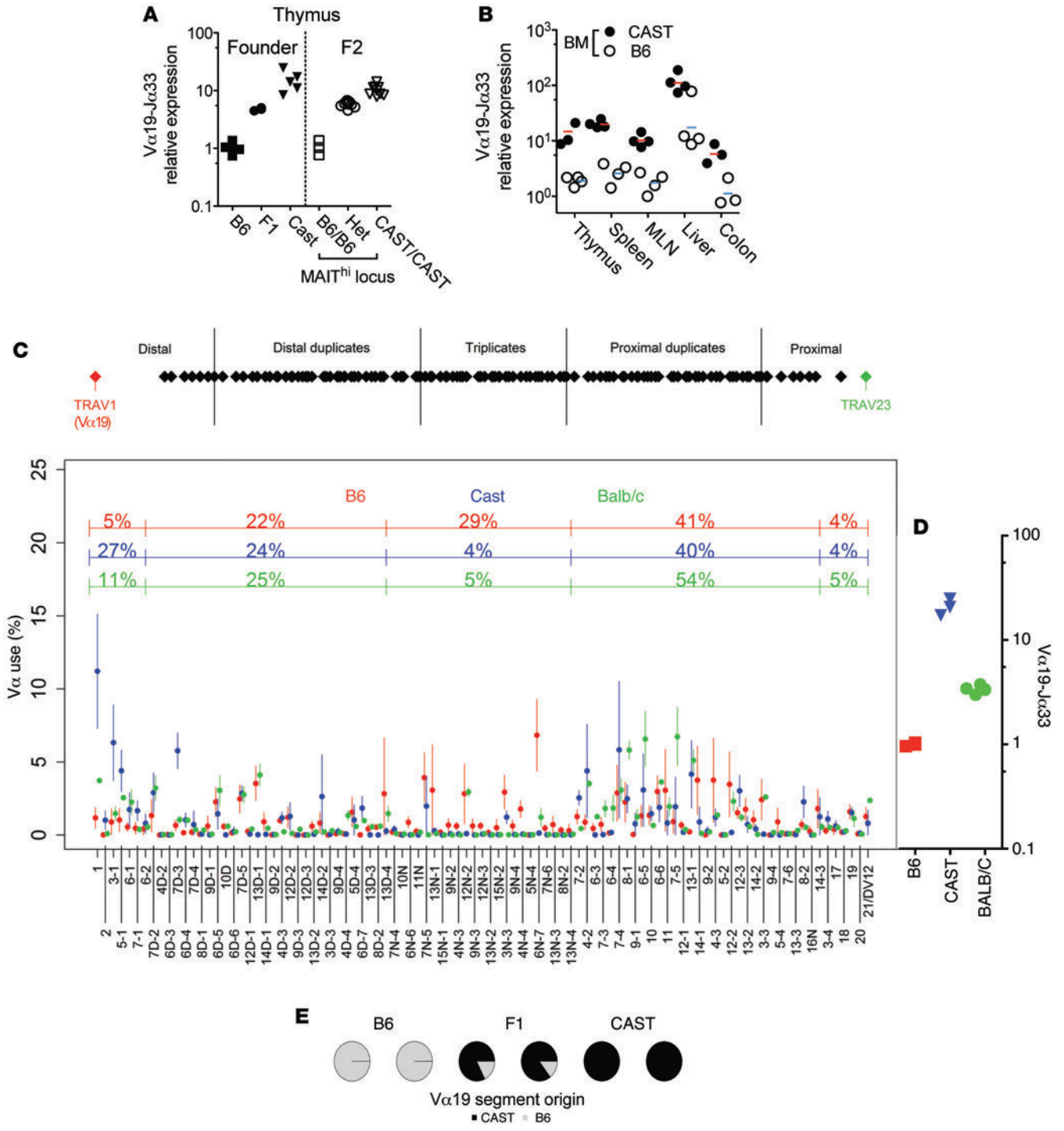

Figure 2. The MAIT^{CAST} locus determines iVα19 levels in the thymus, is hematopoietic intrinsic, and leads to an increased usage of the distal Vα segments. (**A**) Normalized Vα19-Jα33 mRNA levels in the thymus of the indicated mice. (**B**) Normalized Vα19-Jα33 mRNA levels in irradiated B6 recipients 60 days after reconstitution by T cell–depleted BM from B6-MAIT^{B6} (B6) or B6-MAIT^{CAST} (CAST) donors. (**C**) Top: map of the TCR-Vα locus. Bottom: Vα segment usage by thymocytes from the indicated mice (mean ± SD) (2–3 individual mice of each genotype were studied). (**D**) Normalized Vα19-Jα33 mRNA levels in the thymus of the indicated mice. (**E**) The effect of the MAIT^{CAST} locus is chromosome 14 intrinsic: the Vα19^{+} TCR-αs were sequenced in thymocytes from F1 (B6 × CAST) mice. Their B6 or CAST origin was determined according to 2 polymorphic nt in the Vα19 segment. B6 and CAST mice were used as controls.

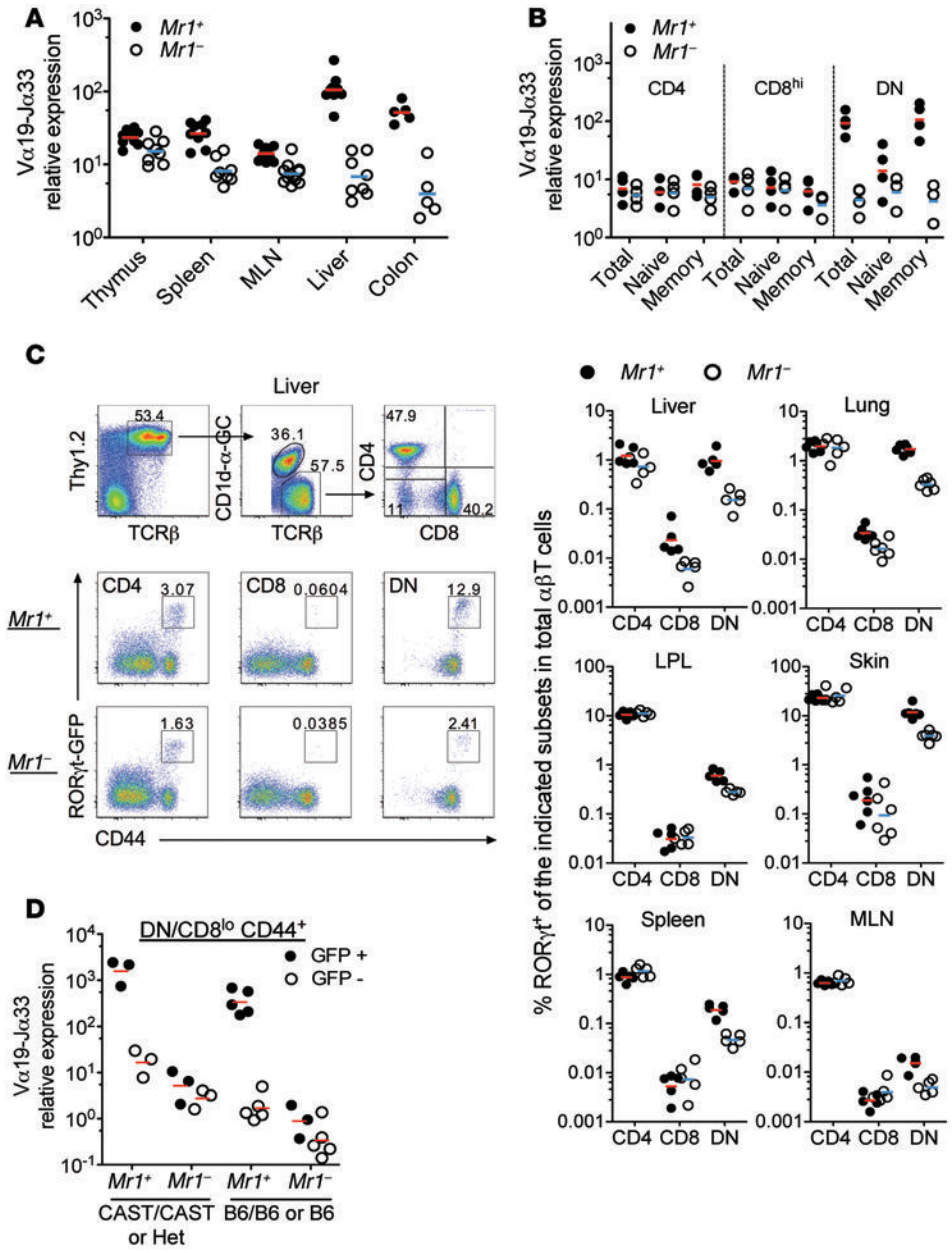

Figure 3. MAITs in *Rorcgt-GFP*^{TG} B6-MAIT^{CAST} mice are GFP$^+$CD44^{hi}DN/CD8^{lo}. (**A**) Normalized Vα19-Jα33 mRNA expression in the indicated organs from *Mr1*$^+$ or *Mr1*$^{-/-}$ B6-MAIT^{CAST} mice. (**B**) Normalized Vα19-Jα33 mRNA levels in the indicated subsets isolated from pooled spleen and MLNs. CD4$^+$ (CD4$^+$CD8$^-$), CD8^{hi} (CD4$^-$CD8^{hi}), DN (CD4$^-$CD8$^{lo/neg}$), total (unseparated), naive (CD44^{lo}), and memory (CD44^{hi}) cells are shown. Each dot represents an independent sort from pools of 2 to 5 mice studied in 5 independent experiments. (**C**) Gating strategy and staining (left, liver) and frequency (right) in the indicated organs of TCR-β$^+$Thy1.2$^+$CD1d-αGC-Tet^{neg}GFP$^+$CD4$^+$, CD8^{hi} or DN (CD4$^-$CD8$^{lo/neg}$) cells in *Rorcgt-GFP*^{TG} B6-MAIT^{CAST} mice. Representative of 3 independent experiments with 3 to 5 mice per group. For skin and lungs, 6 mice in each group were studied in 1 experiment. (**D**) Normalized Vα19-Jα33 mRNA levels in FACS-sorted TCR-β$^+$Thy1.2$^+$CD4^{neg}CD8$^{lo/neg}$CD44^{hi}GFP$^+$ cells (black circles) and GFP$^-$ cells (white circles) from the MLNs and spleen of *Rorcgt-GFP*^{TG} B6-MAIT^{CAST} (CAST/CAST, CAST homozygote; Het, heterozygote; for the MAIT locus), *Rorcgt-GFP*^{TG} B6-MAIT^{B6} (B6/B6), or *Rorcgt-GFP*^{TG} B6 (B6) mice. Each dot represents an independent sort from pools of 2 to 5 mice.

(Figure 2D): MAIT iTCR-α frequency was 3.4 ± 0.3 AU in BALB/c as compared with 1.03 ± 0.26 in B6 (Figure 2D). Altogether, these results suggest that a higher usage of distal Vα segments contributes to the higher frequency of MAITs observed in CAST mice.

The origin of the higher use of the distal Vα segments in CAST is not clear. The mapped region includes part of the 3′ UTR of *Dad1*, a gene with antiapoptotic function (Figure 1E). Because any decrease of the life span of the CD4$^+$CD8$^+$ (DP) thymocytes leads to a decrease in the use of the Vα19 segment (44), we quantified *Dad1* mRNA in B6 and CAST mice and observed similar expression (Supplemental Figure 2B). We also did not find any differences in the recombination signal sequences of the Jα33 segments between B6 and CAST (45). Notably, the higher rate of Vα19-Jα33 rearrangements found in CAST was chromosome intrinsic. Indeed, in B6/CAST F1 thymocytes, more than 80% of the Vα19$^+$ TCR-α transcripts were encoded by the CAST chromosome (Figure 2E).

Altogether, these results further argue against the involvement of disparities in DP thymocyte life span or other cell biology processes between the 2 strains that would explain the high MAIT frequency in CAST mice. Differences in the molecular mechanism of the Vα to Jα recombination between B6 and CAST strains are certainly involved.

Identification and tissue distribution of MAITs in B6-MAIT^{CAST} congenic mice. The increased number of MAITs in B6-MAIT^{CAST} congenic mice allowed us to further characterize their tissue distribution and phenotype. Using RT-qPCR, we quantified MAITs in the different organs of B6-MAIT^{CAST} mice on an *Mr1*$^+$ or *Mr1*^{neg} background. In *Mr1*$^+$ thymus, the amount of iVα19 transcripts was higher (23.9 ± 5.5 AU) than in B6 or BALB/c (Figure 2, A and D, and Figure 3A). Notably, the iVα19 levels were barely decreased on an *Mr1*^{neg} background, further confirming that MAITs do not accumulate in the thymus. In the periphery, MAITs were abundant in the liver, with a strong difference between *Mr1*$^+$ and *Mr1*$^-$ mice (117 ± 62 AU versus 8.1 ± 5.2 AU) (Figure 3A). A similar pattern was observed in the colon LP (53 ± 17 AU versus 5.3 ± 5.2 AU). The iVα19 levels in the MLNs (14.4 ± 2.7 AU) and spleen (28 ± 9.3 AU) (Figure 3A) were not significantly different from the levels observed in the thymus. Nevertheless, the absence of MR1 expression resulted in slightly lower iVα19 levels in these latter

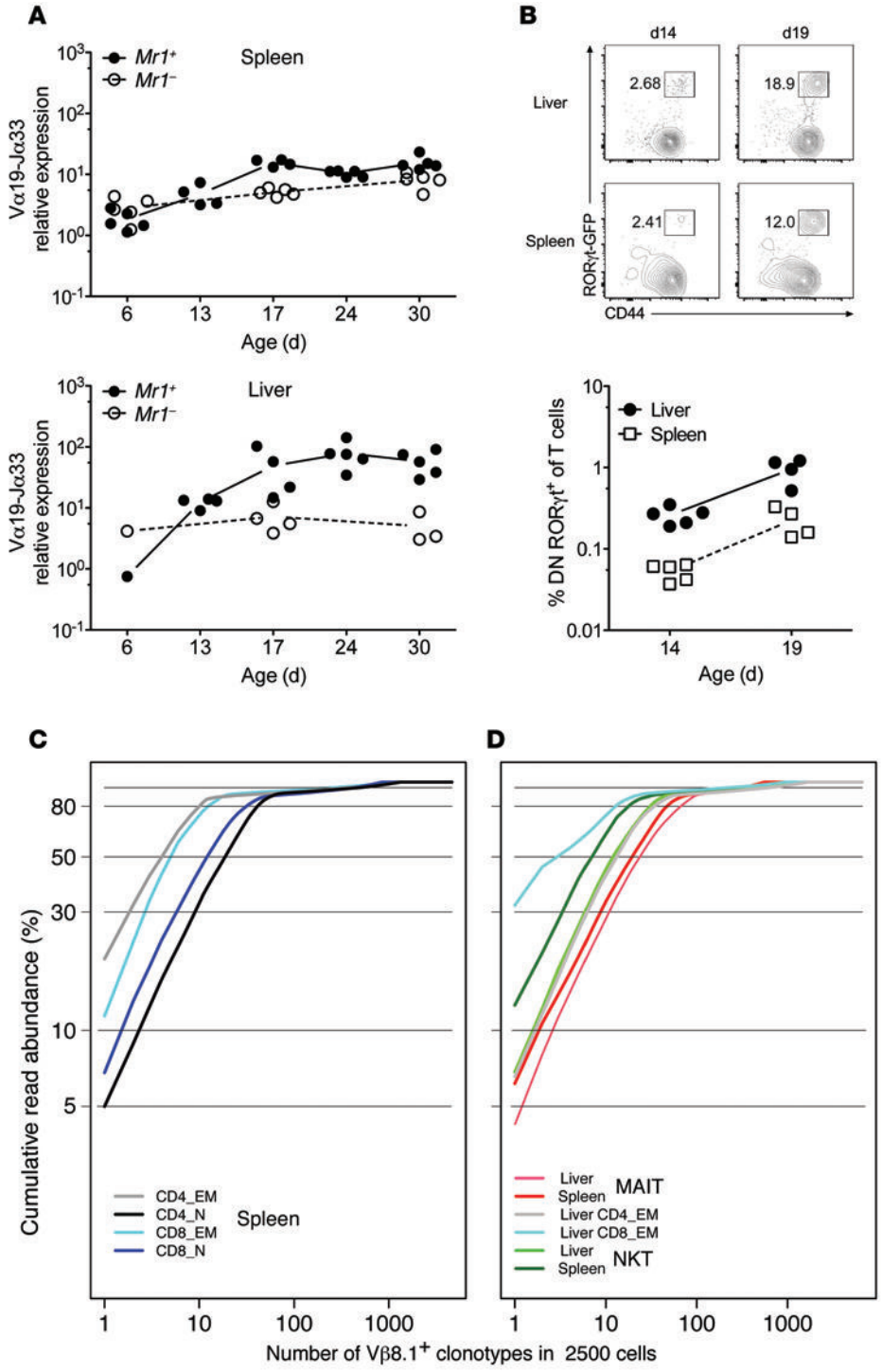

Figure 4. Development of MAITs after birth and TCR-β repertoire analysis of mouse MAITs. (**A** and **B**) Quantitation of MAITs by (**A**) RT-qPCR or (**B**) flow cytometry in the indicated organs at different time points after birth. Dot plots are gated on DNCD8^{lo} T cells. (**C** and **D**) The indicated mouse cell subsets were FACS sorted from *Rorcgt-GFP*^{TG} B6-MAIT^{CAST} mice, and Vβ8.1 TCR-β repertoire analysis was performed by deep sequencing. The cumulative frequency of productive TCR-β rearrangement is plotted for individual clonotypes ranked according to decreasing frequency. (**C**) Naive (CD62L^{hi}CD44^{lo}) and memory (CD62L^{lo}CD44^{hi}) CD4$^+$ or CD8$^+$ subsets were included as controls. (**D**) Control populations, NKT (CD1d-αGC-Tet$^+$), and MAIT (CD4^{neg}CD8$^{lo/neg}$CD44^{hi}GFP$^+$) from the indicated organs were analyzed. Two to three (except for the liver) replicates were studied for each condition, and representative results are shown. Analysis of Vβ8.2 TCR-β segments showed similar results (not depicted).

organs (8.72 ± 3.7 AU and 7.8 ± 3 AU, respectively). Thus, in mice, although MAITs do not significantly accumulate in the peripheral lymphoid organs, they are still more abundant in the liver and colon, as observed in humans. However, the overall number of MAITs in mice was much lower than in humans, suggesting that mouse MAITs do not considerably expand in the periphery.

The poor peripheral accumulation might be related to differences in naive/memory status of mouse versus human MAITs, as we have previously observed that MAITs from Vβ6 Tg and *Tap*$^{-/-}$ *Ii*$^{-/-}$ mice display a naive (CD44^{lo}) phenotype (32). We therefore sorted T cells from the spleen and the MLNs of B6-MAIT^{CAST} congenic mice according to CD4/CD8 and CD44 expression and quantified the iVα19 transcripts. The iVα19 mRNA was found mostly in DN, CD8^{lo}, and CD44^{hi} fractions (Figure 3B), indicating that mouse MAITs are CD4^{neg} (DN/CD8^{lo}) and display a CD44^{hi} memory phenotype as in humans. The absence of CD8αβ^{hi} expression by mouse MAITs is consistent with the CD8αβ^{lo} and CD8αα/DN phenotype of human adult MAITs (21, 22, 32).

Until MR1 tetramers become widely available, mouse MAIT study will remain hampered by the lack of specific markers, as there is no mouse equivalent to human CD161 or another surface marker that would be specific for MAITs. Because all human MAITs express the transcription factor RORγt (21, 24), we introgressed a *Rorcgt-GFP*^{TG} reporter Tg (46) into B6-MAIT^{CAST} congenic mice based on the hypothesis that most GFP$^+$ cells in the DN/CD8^{lo} T cell subsets would be MAITs. The number of CD44^{hi}GFP$^+$ cells in the CD8^{hi} or CD4$^+$ subsets did not vary significantly in *Mr1*$^+$ versus *Mr1*$^{-/-}$ backgrounds (Figure 3C). In contrast, an MR1-dependent subset of CD44^{hi}GFP$^+$ DN/CD8^{lo} T cells was observed in the different organs of B6-MAIT^{CAST} mice, with higher frequencies in nonlymphoid tissues such as liver, lung, skin, and gut LP than in lymphoid organs, including spleen and MLNs (Figure 3C).

To verify that CD44^{hi}GFP$^+$DN/CD8^{lo} T cells are mostly MAI-

Ts in *Mr1*$^{+}$ *Rorcgt-GFP*^{TG} B6-MAIT^{CAST} mice, iVα19 chain mRNA was quantified in spleen T cells from *Mr1*$^{+}$ and *Mr1*$^{-/-}$ mice sorted according to GFP, CD44, and CD4/CD8 expression. iVα19 expression was MR1-dependent and strongly correlated with RORγt-GFP expression (Figure 3D). The level of iVα19 mRNA in GFP-expressing CD44^{hi}DN/CD8^{lo} cells from MR1-sufficient B6-MAIT^{CAST} mice (1783 ± 908 AU) was 90 times higher than in the GFP-negative counterparts and 280 times higher than in MR1-deficient B6-MAIT^{CAST} mice (6.4 ± 4.3 AU for GFP^{+} and 3 ± 1.3 AU for GFP^{-} cells) (Figure 3D). This pattern of iVα19 expression also occurs in B6-MAIT^{B6} or B6 mice (350-fold higher in CD44^{hi}GFP^{+}DN/CD8^{lo} T cells from *Mr1*$^{+}$ than from *Mr1*$^{-/-}$ mice) (Figure 3D). The iVα19 mRNA levels found in CD44^{hi}GFP^{+}DN/CD8^{lo} T cells from *Mr1*$^{+}$ *Rorcgt-GFP*^{TG} B6-MAIT^{CAST} mice (1,000 times higher than in unseparated MLN cells from B6 mice and 10 times higher than in MLN cells from Vβ6 Tg *Tap*$^{-/-}$ *Ii*$^{-/-}$ mice) indicate that 80% to 100% of these cells were MAITs. These results show that in mice as in humans, most, if not all, MAITs display a CD44^{hi}GFP^{+} DN/CD8^{lo} phenotype.

Expansion versus accumulation of MAITs in mice. In humans, MAITs are very few in the thymus and cord blood (21, 22) and expand after birth to reach high clonal size (20, 33). To determine the dynamics of MAITs after birth in mice, we quantified the iVα19 transcripts at 6 to 30 days of age in the thymus, spleen, and liver of *Mr1*$^{+}$ or *Mr1*$^{-/-}$ *Rorcgt-GFP*^{TG} B6-MAIT^{CAST} mice. In the spleen and liver, the MAIT frequency was very low in neonates (day 6) and progressively increased after day 13 to day 17 (Figure 4A). We did not observe any accumulation of MAITs in the thymus, as the difference in iVα19 levels between *Mr1*$^{+}$ and *Mr1*$^{-/-}$ mice was less than 2-fold at all time points (Supplemental Figure 3 for young and Figure 3A for adult mice). To determine whether MAITs appearing in young mice express RORγt, we measured GFP^{hi}CD44^{hi}DN/CD8^{lo} T cell frequency in the spleen and liver 14 and 19 days after birth (Figure 4B). The frequency of MAITs (GFP^{hi}CD44^{hi}DN/CD8^{lo} T cells) increased by 3- to 4-fold between these 2 time points, in accordance with iVα19 mRNA quantitation. Together, these results indicate that MAITs do not accumulate in the thymus, as previously suggested by the study of TCR Tg mice and human thymus (21, 32). After birth and up to weaning time, MAIT frequency in the spleen and liver gradually increased to represent approximately 0.1% and 1% of total T cells, respectively (Figure 4B).

The increased frequency of MAITs observed in the liver could be related either to peripheral proliferation or to an accumulation of MAITs in this organ. In the first hypothesis, the TCR-β repertoire should be less diverse than in the second, as the clonal size would be higher in the case of proliferation. We therefore analyzed the diversity of the MAIT TCR-β chains using Vβ segment–specific primers in PCRs followed by deep sequencing. The MAIT (CD44^{hi}GFP^{+}DN/CD8^{lo}) repertoire was compared with that of NKT (CD1d-αGC-Tet^{+}), effector memory (EM) (CD44^{hi}CD62L^{lo}), and naive (CD44^{lo}) CD4^{+}or CD8^{+} T cells. The analysis of the rarefaction curves (plots relating the cumulative frequency of individual clonotypes ranked by decreasing frequency) of Vβ8.1^{+} T cells from the spleen and liver showed that, although using specific Vβ segments, mouse MAITs harbor a rather diverse repertoire, similar in diversity to that of NKT cells, without real oligoclonality (Figure 4, C and D). Similar data were obtained with a Vβ8.2-specific primer (data not shown). Together, these results indicate that murine MAITs do not extensively proliferate in the periphery and that the higher proportion of MAITs found in the liver is the result of accumulation rather than proliferation.

Phenotype and functionality of mouse MAITs. *Rorcgt-GFP*^{TG} B6-MAIT^{CAST} mice harbor sufficient numbers of GFP-tagged MAITs to enable the analysis of their phenotype and functionality. We found that MAITs isolated from the spleen and liver express high levels of IL-7Rα (CD127), IL-18Rα, and IL-12Rβ1 (CD212), as their human counterparts do (Figure 5A, Supplemental Figure 4A, and ref. 21), whereas the IL-2Rβ (CD122) chain was not detectable. A subpopulation of spleen MAITs expressed NKG2D, while NK1.1 expression was only found on a subset of MAITs from the liver. CD26, a dipeptidase highly expressed by human MAITs, was expressed by most mouse MAITs (Figure 5B). CD103 was detected on a substantial percentage of spleen MAITs, indicating their tissue tropism. In line with this, mouse MAITs did not express CCR7 and many are CCR6^{+}. A subpopulation of liver MAITs expressed CXCR6. CCR5 expression was not detected. In summary, naturally occurring mouse MAITs are very similar to their human counterparts and express several markers distinguishing them from conventional T or NKT cells, including RORγt, IL-18Rα, and CCR6.

Importantly, all MAIT (CD44^{hi}GFP^{+} DN/CD8^{lo}) cells from *Mr1*$^{+}$ B6-MAIT^{CAST} mice expressed the transcription factor ZBTB16 (PLZF), as observed in humans (Figure 5C and ref. 31). In contrast, ZBTB16 was expressed by only a small proportion (approximately 3%) of the Vβ6/8^{+} DN T cells found in iVα19 Tg mice (Supplemental Figure 4B) despite the fact that more than 50% of these cells are bacterial reactive and MR1 restricted (6, 32). These results probably explain the lack of *Zbtb16* detection by RT-qPCR in our previous report that examined *Zbtb16* levels in CD8^{+}and DN T cells isolated from iVα19/Vβ6 double-Tg mice (32). In addition, 100% of the GFP^{+} cells found in the DN T cell subset from Vβ6 Tg B6-MAIT^{CAST} mice expressed ZBTB16 (Supplemental Figure 4C). These results suggest that the premature expression of the iTCR-α chain or saturation of the selecting niches (47) does not allow the acquisition of the full MAIT differentiation program in TCR Tg mice.

To assess the functionality of mouse MAITs, we sorted them together with control populations: mainstream memory (CD44^{hi}) CD4^{+}and CD8^{+} T cells as well as NKT cells (the sorting strategy is shown in Supplemental Figure 5). We then assessed the production of lymphokines after stimulation with anti-CD3/CD28 beads (Figure 5D). We found that MAITs produced small amounts of IFN-γ, but high levels of TNF-α, GM-CSF, and IL-17. Contrary to human MAITs, mouse MAITs secreted measurable amounts of IL-4 and IL-10 and low levels of IL-5. This particular lymphokine secretion pattern was similar in Vβ6^{+}, Vβ6/8^{+}, or Vβ6^{-} MAITs, suggesting that the presence of Th2 cytokines was not due to a contamination by type 1 NKT cells, which do not express the Vβ6 segment. However, the presence of type 2 NKT cells could not be completely excluded, since they harbor a diverse TCR-β repertoire and do not bind CD1d-αGC tetramers. We therefore repeated this experiment using GFP^{+}CD44^{+} DN/CD8^{lo} T cells from *Cd1d*$^{-/-}$ B6-MAIT^{CAST} mice that are devoid of any kind of NKT cells. Importantly,

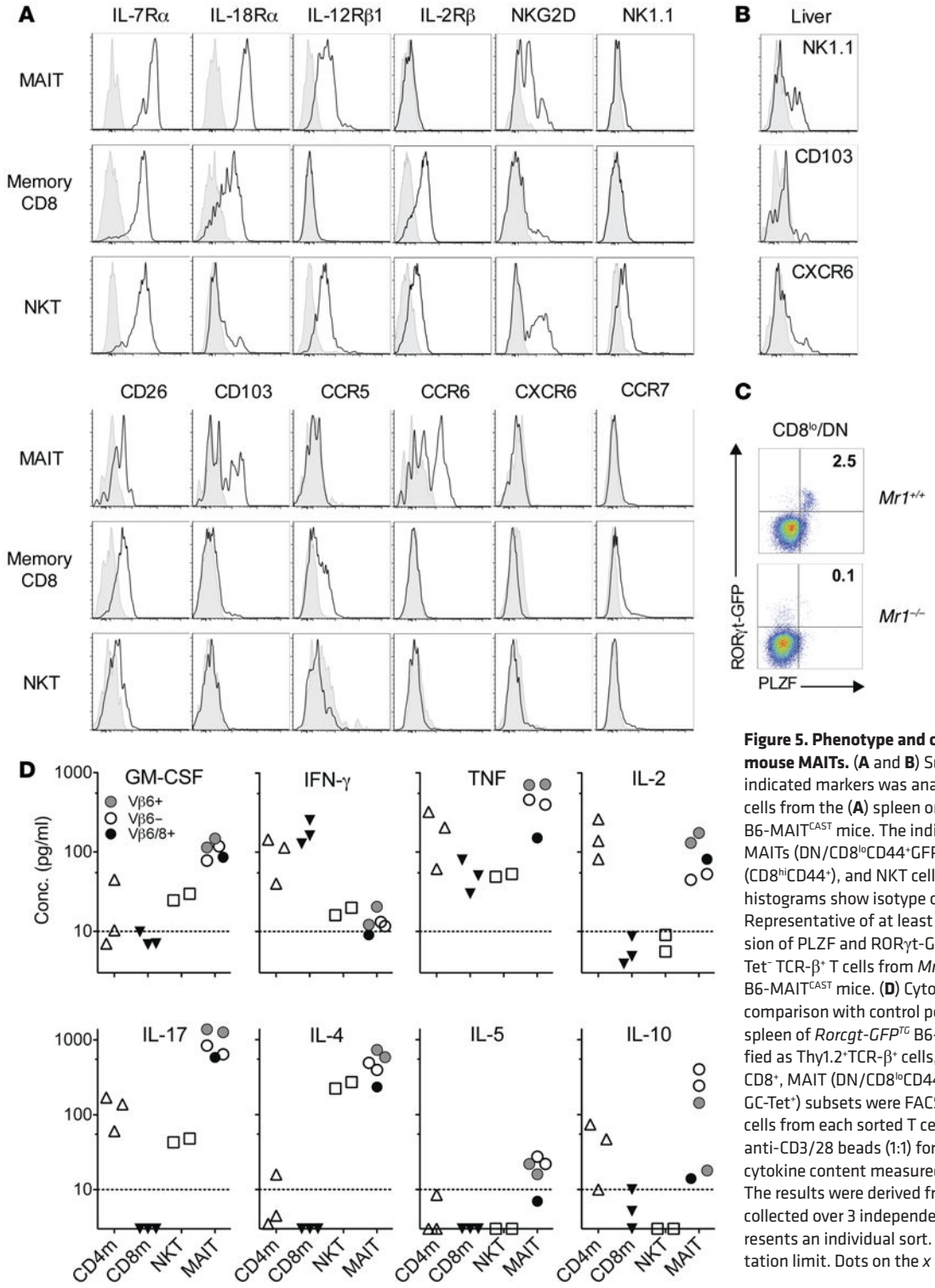

Figure 5. Phenotype and cytokine production by mouse MAITs. (**A** and **B**) Surface expression of the indicated markers was analyzed on Thy1.2$^+$TCR-β$^+$ T cells from the (**A**) spleen or (**B**) liver of *Rorcgt-GFP*^{TG} B6-MAIT^{CAST} mice. The indicated subsets were studied: MAITs (DN/CD8^{lo}CD44$^+$GFP$^+$), memory CD8$^+$ T cells (CD8^{hi}CD44$^+$), and NKT cells (CD1d-αGC-Tet$^+$). Shaded histograms show isotype or FMO control (CD103). Representative of at least 3 experiments. (**C**) Expression of PLZF and RORγt-GFP by DN/CD8^{lo}CD1d-αGC-Tet$^-$ TCR-β$^+$ T cells from *Mr1*$^{+/+}$ or *Mr1*$^{-/-}$ *Rorcgt-GFP*^{TG} B6-MAIT^{CAST} mice. (**D**) Cytokine secretion by MAITs in comparison with control populations. T cells from the spleen of *Rorcgt-GFP*^{TG} B6-MAIT^{CAST} mice were identified as Thy1.2$^+$TCR-β$^+$ cells, and memory (CD44$^+$) CD4$^+$ or CD8$^+$, MAIT (DN/CD8^{lo}CD44$^+$GFP$^+$), and NKT (CD1d-α-GC-Tet$^+$) subsets were FACS sorted. Eight-thousand cells from each sorted T cell subset were cultured with anti-CD3/28 beads (1:1) for 42 to 45 hours and the cytokine content measured in the culture supernatant. The results were derived from 4 to 7 separate cultures collected over 3 independent experiments. Each dot represents an individual sort. Dashed line indicates quantitation limit. Dots on the *x* axis indicate not detected.

the frequency of GFP$^+$CD44$^+$ DN/CD8^{lo} T cells in *Cd1d*$^{-/-}$ *Mr1*$^{-/-}$ B6-MAIT^{CAST} mice was extremely low (Supplemental Figure 6, A and B), indicating that more than 90% to 95% of the GFP$^+$ CD44$^+$ DN/CD8^{lo} T cells found in *Cd1d*$^{-/-}$ *Mr1*$^+$ B6-MAIT^{CAST} mice are MR1 dependent. MAITs from *Cd1d*$^{-/-}$ *Mr1*$^+$ B6-MAIT^{CAST} mice displayed a pattern of lymphokine secretion (low IFN-γ, high IL-17, and measurable levels of IL-4 and IL-10; Supplemental Figure 6C) similar to that observed in CD1d-sufficient *Mr1*$^+$ B6-MAIT^{CAST} mice, excluding the possibility that the Th2 cytokines were produced by contaminating NKT cells. Collectively, these data indicate that, in addition to Th1/17 type cytokines, mouse MAITs secrete low amounts of Th2 cytokines. To determine whether Th1/2/17 cytokines were produced by different MAIT subsets or concurrently secreted by a single MAIT, we analyzed IFN-γ, IL-4, and IL-17

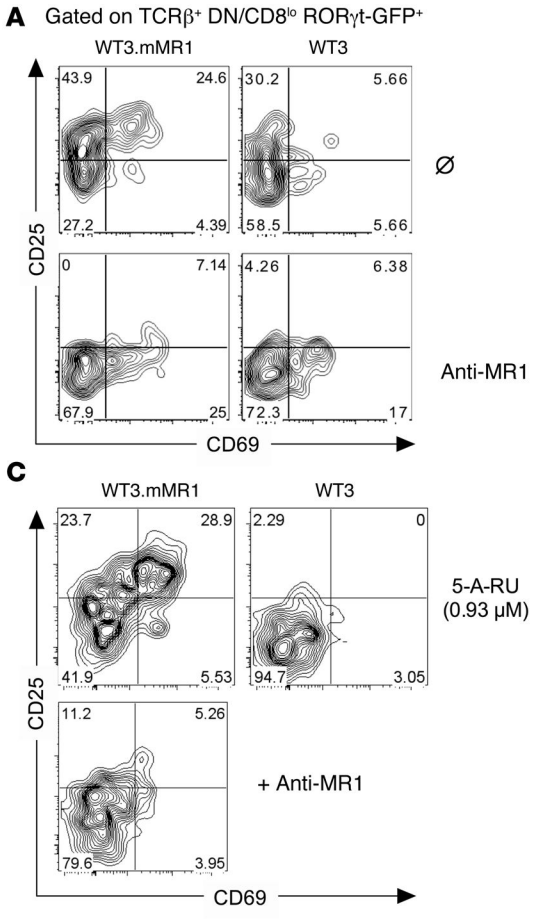

Figure 6. Natural MAITs are activated by bacteria-derived compound in an MR1-dependent manner. (**A**) Activation of *Rorcgt-GFP*^{TG} B6-MAIT^{CAST} splenocytes after overnight coculture with SPB (2 AU) and WT3 cells overexpressing MR1 (WT3.mMR1) or the parental cell line (WT3). (**B**) Dose-response curves of MAIT activation in the presence or absence of anti-MR1 (26.5) blocking antibody. The results were pooled from 3 independent experiments (mean ± SD). (**C**) Activation of *Rorcgt-GFP*^{TG} B6-MAIT^{CAST} splenocytes with 0.93 μM of 5-A-RU extemporaneously mixed with MeG (1:1 ratio) after overnight incubation with WT3 or WT3.mMR1 cells together with anti-MR1 antibody (bottom panel). (**D**) Dose-response curves of MAIT activation in the presence or absence of anti-MR1 blocking antibody. Results represent a pool of 3 mice. (**C** and **D**) Representative of 2 independent experiments.

expression by intracytoplasmic staining of splenocytes after several stimulations, namely, anti-CD3/CD28 beads, PMA/ionomycin, or paraformaldehyde-fixed (PFA-fixed) *E. coli* (Supplemental Figure 7). PMA/ionomycin or TCR ligation induced substantial IL-17 expression by MAITs, while IFN-γ and IL-4 were undetectable, in line with the recently published results of cytokine production by MAITs from B6 mice identified with MR1-5-OP-RU tetramers (48). Interestingly, IFN-γ was detected in MAITs only after activation with *E. coli*, suggesting that MAITs require additional innate signals to efficiently produce IFN-γ. Whether Th1/2/17 cytokines are produced by different MAIT subsets remains to be addressed, since we have been unable to define stimulation conditions in which all the cytokines are reliably detectable by intracytoplasmic staining.

To determine whether the presence of MAITs influences antibody production, we measured the serum levels of IgA and IgG isotypes in *Mr1*$^{+}$ and *Mr1*$^{-}$ B6-MAIT^{CAST} mice (Supplemental Figure 8). Serum IgA levels were slightly decreased in the absence of MAITs, but the levels of all the other Ig isotypes tested were similar. These results suggest that MAITs are probably not involved in the regulation of systemic humoral responses, but may modify local immune responses.

To further verify the antigen specificity of GFP^{+}CD44^{hi}DN/CD8^{lo} T cells, we measured their activation after stimulation with graded amounts of a MAIT-activating semipurified bacterial fraction (SPB) (49) loaded on MR1-overexpressing WT3 cells (50). We found that MAITs (GFP^{+}CD44^{hi}DN/CD8^{lo}), but not GFP^{lo}CD44^{hi} CD8^{+} T cells from the same culture dish, were specifically activated by the SPB fraction, as shown by the upregulation of the activation markers CD69 and CD25 (Figure 6, A and B). This activation was MR1 dependent, since it was blocked by an anti-MR1 antibody (Figure 6, A and B). In line with this, incubation of the SPB fraction with the parental WT3 cell line (which expresses very low levels of MR1) did not activate MAITs. The active compound or compounds in this bacterial fraction derive from the rib biosynthesis pathway (10, 49) through a reaction between the rib intermediate 5-amino-6-D-ribityl-uracil (5-A-RU) and methyl-glyoxal (MeG) generating the 5-(2-oxopropylideneamino)-6-D-ribitylaminouracil (5-OP-RU) pyrimidine adduct. The 5-OP-RU binds to and is stabilized by MR1 and activates MAITs. We therefore measured the activation of polyclonal MAITs by MR1-overexpressing WT3 cells incubated with serial dilutions of 5-A-RU extemporaneously mixed with MeG. MAITs were activated by this compound when incubated with MR1-overexpressing cells but not the MR1^{lo} parental cell line (Figure 6C). The activation was also decreased in the presence of an anti-MR1 antibody. These results demonstrate that the GFP^{+}CD44^{hi}DN/CD8^{lo} T cells found in *Mr1*$^{+}$ B6-MAIT^{CAST} mice are bona fide MAITs, recognizing a bacterial ligand derived from the rib biosynthesis pathway in an MR1-dependent manner.

Polyclonal mouse MAITs are protective and migrate to the infection site in an experimental model of UTI. The availability of a MAIT-rich mouse model allowed us to investigate the role of MAITs in antimicrobial immunity. Because we detected MAITs in the urine of 10 out of 12 patients with leukocyturia associated with UTI (Figure 7, A and B), we studied an experimental model of UTI. Female *Rorcgt-GFP*^{TG} B6-MAIT^{CAST} mice with (*Mr1*$^{+}$) or without MAITs (*Mr1*$^{-/-}$) were intravesically instilled with uro-

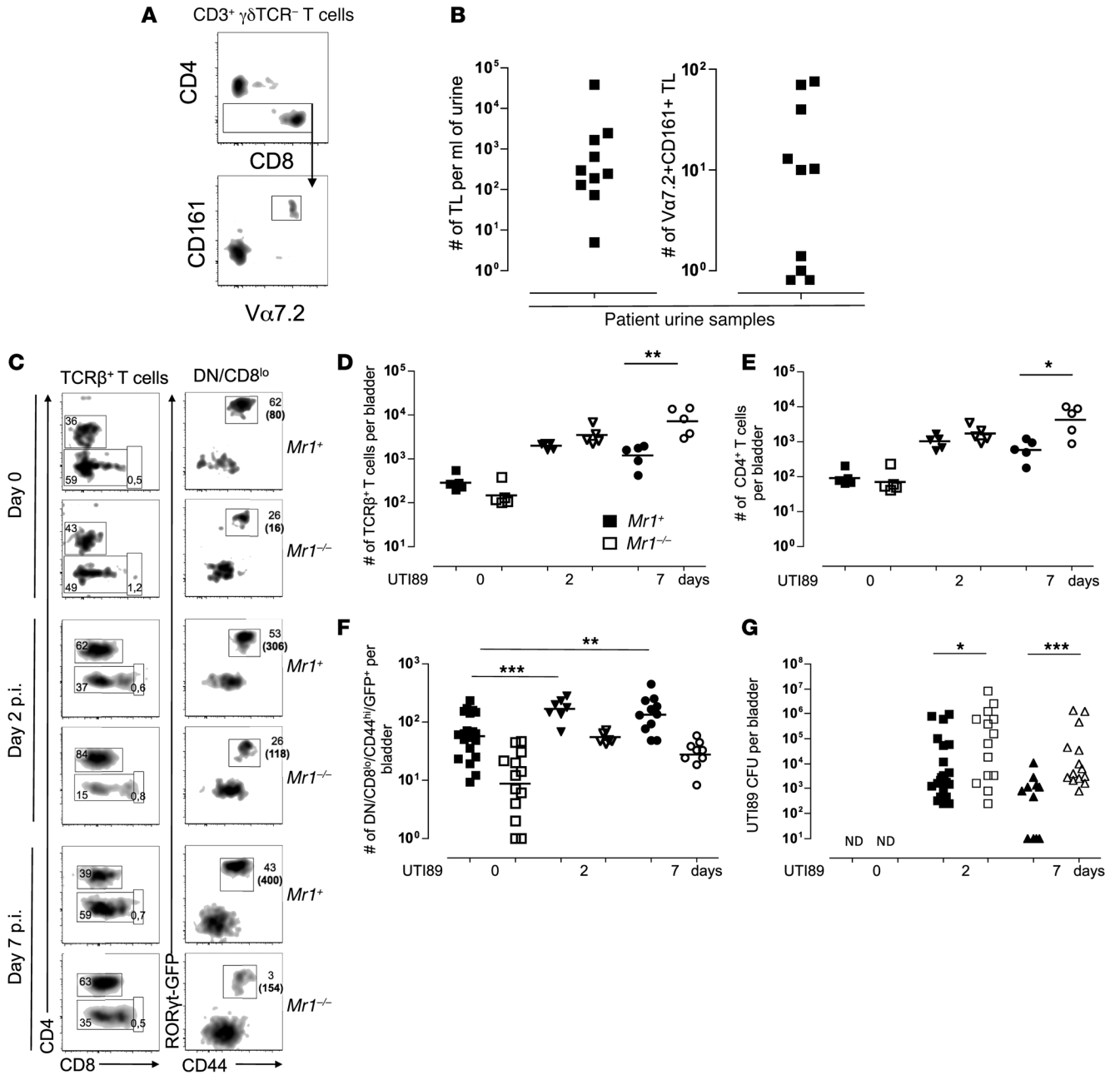

Figure 7. MAITs are recruited to the bladder upon UTI in humans and mice and contribute to bacterial clearance in mice. (**A**) Gating strategy on TCR-γδ$^-$CD3$^+$ T cells isolated from urine samples collected from patients with UTI. (**B**) Enumeration of MAITs in the urine: number of T lymphocytes (TL) (left panel) and MAITs (right panel) per ml of urine. (**C**) Flow cytometry analysis of T cells infiltrating bladder from *Mr1*$^+$ or *Mr1*$^{-/-}$ *Rorcgt-GFP*^{TG} B6-MAIT^{CAST} mice at day 0 (naive) or 2 or 7 days after infection with UTI89. Representative FACS plots and gating strategy are shown. Numbers in parentheses correspond to total number of cells. (**D**–**F**) Quantitation of bladder-infiltrating total T cells (**D**), CD4$^+$ T cells (**E**), and MAITs (**F**) at the indicated time points post infection (p.i.). (**G**) UTI89 bacterial load in mouse bladders at indicated time points. Pooled data from 2 to 3 independent experiments. *P < 0.05; **P < 0.01; ***P < 0.001.

pathogenic *E. coli* (UPEC) strain UTI89 (51). The lymphoid cells infiltrating the bladder were analyzed by flow cytometry. We observed robust recruitment of αβT cells (Figure 7, C and D), including CD4$^+$ conventional T cells (Figure 7E) and MAITs (Figure 7F), starting 2 days after infection. Indeed, a significant increase in GFP$^+$CD44^{hi}DN/CD8^{lo} T cell numbers was detected in the infected bladders of *Mr1*$^+$ mice at day 2 and was sustained for at least 7 days (Figure 7F). As we observed an overall accumulation of T cells in the bladder upon infection, we also detected an increase in the absolute number of GFP$^+$CD44^{hi}DN/CD8^{lo} T cells in *Mr1*^{neg} mice, but this was always substantially lower than in *Mr1*$^+$ littermates. To investigate the antibacterial activity of the infiltrating MAITs, we assessed the bacterial load in infected bladders at different time points. The presence of MAIT in the bladders of *Mr1*$^+$ B6-MAIT^{CAST} mice was associated with more efficient bacterial clearance than in *Mr1*$^{-/-}$ littermates (Figure

7G). Furthermore, a sustained presence of MAITs during the late phase of infection (day 7) correlated with lower numbers of conventional T cells in infected bladders, suggesting more efficient resolution of the inflammation and the potential to enhance the subsequent adaptive immune response, although we did not study this directly. These data indicate that MAITs are present in the bladder and display protective antimicrobial activity.

Discussion

Although MAIT frequency is modified in several diseases, the role of MAITs in health and disease is still elusive, as no clear evidence associates them with a specific pathology. This can be addressed by studying animal models, but the number of MAITs in SPF-raised conventional laboratory mice is close to the detection limits. Tg mice for the TCR-α or TCR-β chains of MAITs are very useful for assessing MAIT reactivity and also to some extent for the study of MAIT selection (32, 36). However, the use of TCR Tg mice for functional studies is more challenging because the premature overexpression of the iTCR-α chain leads to artifactual features (41). These caveats are difficult to overcome even with the comparison to an *Mr1*^{neg} control, as discussed in the supplementary text of ref. 32. On the other hand, for the available TCR-β Tg mice (Vβ6 and Vβ8), both chains were isolated from iVα19$^+$ T-T hybridoma recognizing MR1-overexpressing fibroblastic cell lines. Therefore, the potential for autoreactivity of these TCRs against MR1 itself or MR1 loaded with a culture medium component cannot be excluded. Whether this putative autoreactivity affects the selection and functions of the T cells found in these Tg mice is currently being studied.

Given the high conservation between species of both the restricting element MR1 and the iTCR-α chain, the disparity between the number of MAITs in humans and laboratory mice is intriguing. Although it was recently shown that MAITs can tremendously expand in B6 mice during bacterial infection by *Francisella tularensis* and display protective activity after depletion of conventional T cells (8), it is rather difficult to envision how such a minor subset would drive innate-like response and display protection during natural infection or infections in unmanipulated settings. We set out to understand the reasons for this apparent paradox. Because the reconstitution of germ-free mice with human microbiota did not lead to higher frequency of MAITs than that found in SPF mice, we hypothesized that laboratory mice may have lost an allele or alleles important for the defense against common pathogens due to the absence of selection pressures in the clean animal facilities. Indeed, laboratory mice are not representative of the existing mouse species, as they harbor less than 25% of the genetic diversity of wild mice (45).

We found 2 wild-derived inbred SPF mouse strains with higher frequency of MAITs. Given the naive phenotype of MAITs we had observed in iTCR-α Tg mice, we expected that the gene or genes involved in the MAIT^{hi} phenotype would be implicated in the activation, survival, and/or expansion of MAITs. To our surprise, the 20-fold increase in MAIT frequency found in the CAST strain was linked to 1 locus located at the 3′ end of the TCR-α region, leading to higher production of the specific rearrangement. Although the exact molecular mechanism is not elucidated, the increased number of MAITs was CAST chromosome (Figure 2E) and hematopoietic (Figure 2B) intrinsic and was already observed in the thymus (Figure 2A). The small difference in MAIT frequency found in the thymus of *Mr1*$^+$ versus *Mr1*$^{-/-}$ animals (Figure 3A) is consistent with the absence of MAIT accumulation in this organ (32). Indeed, the occurrence of the restricting MHC allele during thymic selection has a small impact on the frequency of naive T cells specific for many nominal antigens (52).

The lower frequency of iVα19$^+$ cells in the periphery of *Mr1*$^{-/-}$ in comparison with *Mr1*$^+$ animals suggests that MR1 expression in the periphery is necessary for their activation and/or their peripheral expansion and survival. Nevertheless, the peripheral expansion in mice is much lower than in humans, as indicated by the diverse MAIT TCR repertoire in the liver of B6-MAIT^{CAST} mice, which suggests that MAITs accumulate rather than proliferate in this organ. We also observed that both NKT and EM T cells expanded less in the SPF mice we studied than in humans (Figure 4 and refs. 20, 53). This might be a general difference of effector cells between the 2 species and would suggest that the turnover of NKT and MAITs is slower in humans than in mice.

The smaller number of MAITs in SPF B6-MAIT^{CAST} mice in comparison with humans might be related to differences in the gut microbiota between these 2 species. Although the similar number of MAITs in the LP of SPF mice and germ-free mice colonized by human microbiota (Figure 1A) argues against this hypothesis, it remains to be determined whether MAIT numbers would increase after implantation of human microbiota into B6-MAIT^{CAST} mice. Although the proportion of type 2 NKT is higher in humans, NKT cells are much more abundant in mice than in humans. Therefore, a competition between MAIT and NKT cells during intrathymic development or for peripheral niches could also be involved. However, NKT cell numbers were not increased in the spleen, MLNs, liver, and LP of *Mr1*$^{-/-}$ mice (data not shown), while MAITs were only slightly increased in *Cd1d*$^{-/-}$ B6-MAIT^{CAST} mice (Supplemental Figure 6), arguing against this hypothesis.

In the absence of available MR1 tetramers or anti-Vα19 antibody, we relied on RT-qPCR of the iVα19-Jα33 iTCR-α chain to track MAITs. The iTCR-α chain was only found in the CD44^{hi}CD8^{lo}DN subset (Figure 3B), confirming that mouse MAITs are not found in the CD4$^+$ or CD8^{hi} subset, as observed in humans. Similarly to what occurs in humans, MAITs were mostly found in tissues such as liver and colon LP (Figure 3A). To facilitate phenotype analysis and allow functional studies, we introgressed an *Rorcgt-GFP* reporter into the B6-MAIT^{CAST} congenic strain. Almost all CD44^{hi}GFP$^+$CD8^{lo}DN T cells in adult B6-MAIT^{CAST} mice expressed the iVα19-Jα33 TCR-α chain (Figure 3D). However, since this subset might also encompass a few CD1d-restricted NKT cells, we verified our lymphokine secretion studies using MAITs from *Cd1d*$^{-/-}$ *Rorcgt-GFP*^{TG} B6-MAIT^{CAST} mice. Overall, with regard to phenotypic features, mouse MAITs are similar to human ones, assuming that mouse DN/CD8^{lo} T cells are orthologous to human DN/CD8αα and CD8αβ^{lo} T cells. The presence of IL-18Rα and IL-12Rβ1 indicates that mouse MAITs can be activated by innate signals, as are human MAITs (25).

Although MAITs were discovered by identifying an iTCR-α chain in a particular T cell subset (20), in our opinion, MAITs should be defined as T cells educated by MR1 in the thymus to acquire a specific differentiation program. Whether MR1-restricted T cells are limited to T cells expressing iVα19-Jα33 iTCR-α (and iVα7.2-Jα33/12/20 in

humans, ref. 38) is not yet clear. The data above indicate that if other MR1 restricted T cells with a distinct repertoire exist, they would have to be distinct from the CD44^{hi}RORγt^{+}CD8^{lo}DN subset. In addition, it remains to be determined whether all MR1-restricted T cells would be labeled with MR1 tetramers loaded with one given ligand. This is true for adult human MAITs (38). In humans, the presence in the cord blood of T cells expressing high levels of CD161^{hi}IL-18Rα^{+} (22) that are not Vα7.2^{+} suggests that T cells with a distinct repertoire can follow a development pathway similar to that of MAITs (54), probably linked to the selection on DP thymocytes (55). Whether all these T cells are MR1 restricted remains to be determined. (22, 56)

In *Mr1*$^{+}$ iVα19 Tg *Ca*$^{-/-}$ mice, we observed that most CD4^{+} T cells are neither bacterial reactive nor MR1 restricted (6, 32). In contrast, a significant number of MR1-dependent MR1-Tet^{+} Vβ6/8.1-2^{+} T cells were CD4^{+} in another iVα19 Tg line (38). In the current study, in a polyclonal model, in the organs we studied, we did not observe CD4^{+} MR1-restricted T cells, confirming our previous reports (6, 32). The origin of these discrepancies between different iVα19 Tg *Ca*$^{-/-}$ lines might be due to differences in the microbiota of the animal facilities or TCR-α Tg timing or level of expression. Nevertheless, the polyclonal B6-MAIT^{CAST} mouse model described herein is not subjected to this TCR Tg artifact and largely recapitulates the features of human MAITs.

This new model allowed us to study the phenotype and function of MAITs in mice. Our results are concordant with the MR1-5-OP-RU tetramer–based characterization of the rare MAITs found in C57BL/6 mice that has recently been published (48) and confirm the interest of the *Rorcgt-GFP*^{TG} B6-MAIT^{CAST} mouse strain. Overall, mouse and human MAITs were very similar with regard to phenotype and lymphokine secretion (21).The few differences we observed were a more diverse repertoire related to a lower peripheral expansion, low CXCR6 expression, and secretion of IL-4 and IL-10. We (21) and others (25, 26, 30) have never observed such a lymphokine secretion pattern in humans. The impact of MAITs on antibacterial mucosal IgA responses suggested by the slightly lower level of serum IgA will be addressed in further studies. Importantly, like human MAITs, polyclonal mouse MAITs from B6-MAIT^{CAST} mice expressed both ZBTB16 and RORγt transcription factors in contrast to our study on iVα19-Vβ6 double-Tg mice (32). The changes in T cell ontogeny imparted by the premature expression of a TCR-α Tg probably explain these differences.

The origins of the differences between mouse and human MAITs are unclear. With regard to repertoire, all the memory T cell subsets, whether innate-like or conventional effector, seem to display lower oligoclonality in mice in comparison with humans (Figure 4B and refs. 20, 33). Thus, MAITs would be similar to other memory subsets in mice. However, it should be stressed that, in humans, only blood MAITs were studied, whereas the mouse MAITs were isolated from lymphoid organs or tissues.

The availability of a mouse model harboring polyclonal MAITs allowed us to study their putative involvement during an experimental UTI. In line with the human data (Figure 7A), we observed the presence of MAITs in the mouse bladder during UTI. Moreover, MR1-deficient mice exhibited higher bacterial load, in particular at late time points (Figure 7G). The larger conventional T cell infiltration in the bladder during infection in the absence of MAITs may be related to higher bacterial load or to a direct effect of MAITs on conventional T cell accumulation or survival. Therefore, this model will be very useful to study, for instance, the mechanisms of bacillus Calmette-Guérin (BCG) antitumor activity during the treatment of bladder carcinoma (57). This MAIT-rich mouse model will also allow the test of MAIT stimulation with synthetic ligand as a therapeutic tool in various diseases or as an adjuvant for vaccine development.

Methods

Mice. B6 mice were obtained from Charles Rivers Laboratories. The *Mus musculus castaneus* (CAST/EiJ) and *Mus musculus musculus* PWK strains were provided by X. Montagutelli (Institut Pasteur). The *Rorcgt-GFP*^{TG} (46) and *Cd1d*$^{-/-}$ lines, both on a B6 background, were provided by G. Eberl (Institut Pasteur) and A. Lehuen (INSERM U1016, Institut Cochin, Paris, France), respectively. The 3 strains were transferred as embryos into our animal facility at Institut Curie. *Tap*$^{-/-}$ *Ii*$^{-/-}$ *Mr1*$^{+}$ (and *Mr1*$^{-/-}$) mice have been previously described (32). B6-MAIT^{CAST} congenic mice were obtained by selecting mice expressing a MAIT^{hi} phenotype in the blood to be bred to B6 mice for more than 10 generations.

Germ-free *Tap*$^{-/-}$ *Ii*$^{-/-}$ mice were obtained by Cesarean section at the CNRS Central Animal Facility (Orléans, France) and then housed at the ANAXEM Animal Facility, INRA (Jouy-en-Josas, France). The reconstitution with human microbiota was carried out at INRA. Colonization was verified several times during the experiments. At 2 to 3 months after reconstitution, colon LP lymphocytes were collected and MAITs were quantified by real-time RT-qPCR.

Mouse cell preparation. Thymus, spleen, and MLNs were collected into cold PBS with 0.5% BSA. Lymphocytes were liberated by mechanical disruption over a cell strainer. Livers and lungs were perfused with 10 ml of PBS to remove circulating blood cells. Livers were then dissociated by passing through a 100-μm cell strainer and resuspended in PBS with 0.5% BSA. Lung lobes and chopped skins were digested in CO_2-independent media containing 0.5 Wünsch units/ml liberase (Roche) and 0.1 mg/ml DNase I (Roche) at 37°C for 30 minutes (lung) to 1 hour (skin) and further dissociated using gentleMACS Dissociator according to the manufacturer's instructions (Miltenyi Biotec). The cell suspensions were filtered through a 100-μm cell strainer. The released cells from liver, lung, and skin were layered on a 40%/80% Percoll gradient (GE Healthcare) and spun at 800 *g* for 20 minutes at room temperature. Mononuclear cells were recovered from the interface. Intestinal lymphocytes were isolated as previously described (20, 57, 58). Briefly, large intestines were collected in cold PBS. The intestines were carefully flushed and opened longitudinally. Intestinal epithelium was removed by shaking in 60 ml of PBS with 3 mM EDTA for 10 minutes (twice) followed by 15 minutes incubation in 15 ml of CO_2-independent medium containing 1.5 mM $MgCl_2$ and 1 mM EGTA (twice) at 37°C. The remaining tissue was cut into 1- to 2-mm pieces and digested in 30 ml of CO_2-independent medium containing 20% FCS, 100 U/ml collagenase (type VIII, Sigma-Aldrich), and 5 U/ml DNase I (DN25, Sigma-Aldrich) and shaken for 90 minutes at 37°C. The tissue suspension was dissociated by syringe aspirations and passed through a cell strainer. Cell suspension was pelleted followed by density gradient centrifuge at 1,000 *g* for 25 minutes at room temperature (lympholyte; Cedarlane). LPLs were recovered from the interface.

Cells were cultured in DMEM or RPMI 1640 medium supplemented with 10% heat-inactivated FCS, 100 U/ml penicillin, 100 μg/

ml streptomycin, 2 mM L-glutamine, 10 mM HEPES, and 1 mM sodium pyruvate (Gibco; Thermo Fisher Scientific).

Hematopoietic chimera. Donor BM was flushed from tibia and femur of 2 B6-MAIT^{CAST} or B6-MAIT^{B6} *Mr1*$^{+}$ *Rorcgt-GFP*^{TG} mice. T cells were depleted using autoMACS Pro (Miltenyi) after labeling with anti-CD3 microbeads. Two million T cell–depleted BM cells from either donor group were injected into the tail veins of 4 to 5 irradiated CD45.1 recipients (1.2 Gys). Two months after reconstitution, mice were sacrificed and organs were collected for FACS and RT-qPCR analysis.

Mouse Universal Genotyping Array. DNA was extracted from ear punches of 35 MAIT^{lo} and 31 MAIT^{hi} mice using the Wizard SV Genomic DNA Purification System according to the manufacturer's instructions (Promega). DNA was then sent to GenSeek (Neogen) for genotyping using the Mouse Universal Genotyping Array (MUGA) chip. Genotyping data were analyzed using an in-house R script. Briefly, MUGA data were filtered for both sample call rate (≥0.90) and SNP call frequency (≥0.90). A Wilcoxon test was performed to compare heterozygosity at each SNP's location according to MAIT^{lo} and MAIT^{hi} groups. Then *P* values were $-\log^{10}$ transformed and plotted according to chromosomal location.

Mouse TCR-α and TCR-β repertoire analysis. TCR-α repertoire study was performed using a 5′ rapid amplification of cDNA end adapted to deep sequencing using an Ion PGM system (Life Technologies, Ion 318 Chip vx; 400 base reads) as described previously (42). TCR-β repertoire was analyzed using Vβ-specific primers and Cβ primers that included CS1 and CS2 sequences at their 5′ end to enable Illumina Sequencing. TCR-β repertoires were obtained by sequencing using MiSeq (Illumina, v3 kit; 2 × 300 bases paired-end reads, ICGEX platform). Each data set was demultiplexed and trimmed for base quality (>25) and read length (>250 bp). Paired reads were merged using the flash v1.2.10 program (-m30-M135-t10-x0.1) (59). The data have been deposited in the NCBI's Sequence Read Archive (SRA) database (SRR2218429-SRR2218460). Resulting fasta files were then uploaded onto the IMGT/high V-Quest webserver (60) (allele*01 only), and the Junction file was parsed using an in-house R script to extract information regarding the V-J combination and the CDR3 nucleotide composition. Only predicted productive TCR rearrangements were kept for downstream analysis. The TCR-α and TCR-β repertoire sequencing data were analyzed using R and vegan packages. To normalize for uneven numbers of reads, each data set was subsampled 100 times at a depth of 5,000 reads. Then an average rarefaction matrix was computed from the 100 subsampled tables to draw the rarefaction plots.

Flow cytometry. Flow cytometry was performed with directly conjugated antibodies according to standard techniques and analyzed on FACSAria, Fortessa, and LSRII flow cytometers (BD). DAPI and a 405-nm excitation were used to exclude dead cells. The list of antibodies is available in the Supplemental Methods section.

For transcription factor staining, cells were incubated with the LIVE/DEAD fixable violet stain (Life Technologies) and Fc block antibody prior to cell-surface marker staining. Cells were then fixed and permeabilized overnight using the BD Cytofix/Cytoperm kit (BD), after which they were incubated with either anti-PLZF or anti-RORγt antibody

For the detection of cytokines, 8,000 (Figure 5D) or 30,000 (Supplemental Figure 6C) sorted splenocytes were cultured in 50 μl RPMI 1640 complete medium in the presence of anti-CD3/CD28 Dynabeads (1:1; Gibco, Thermo Fisher Scientific) for 42 to 45 hours at 37°C. Cytokines in the supernatant were detected using the Cytometric Bead Array Flex Set (BD Biosciences).

MAIT stimulation with bacteria-derived compound. The preparation of the SPB was previously described (49). Briefly, the bacterial lysate was prepared by growing *E. coli*, DH5α ATCC strain, to saturation. The bacteria pellet was resuspended in water at 4°C for a week to induce the release of the MAIT ligand. Supernatant was collected, filtered, and phenol-cloroform extracted before being aliquoted and lyophilized for further use. One AU corresponds to 25 μl bacterial supernatant. 5-A-RU synthesis and 5-OP-RU preparation have been described elsewhere (49).

Splenocytes from *Rorcgt-GFP*^{TG} B6-MAIT^{CAST} mice were depleted of APCs and CD4^{+} T cells using anti-CD19, anti-CD11c, anti-CD11b, and anti-CD4 MicroBeads (Miltenyi Biotech). Then 3 × 10^5 MAIT-enriched splenocytes were cultured with 10^5 WT3 or mouse MR1–transfected WT3 (WT3.mMR1) cells (50) that had been preincubated with serial dilutions of semipurified bacterial supernatant or 5-A-RU plus MeG for 30 minutes at 37°C. Under some conditions, 10 μg/ml of anti-MR1 blocking Ab (clone 26.5; ref. 61), provided by T. Hansen (Washington University, St. Louis, Missouri, USA), was added before adding the T cells. After overnight culture, activation was analyzed using flow cytometry.

UTI. Urine samples from patients with UTI were obtained from the Microbiology Department of Curie Institute after cytobacteriologic analysis. Samples that tested positive for both bacteria and leukocytes were included in the study.

For the experimental UTI, clinical UPEC, cystitis isolate UTI89, was grown statically for 20 hours in LB broth, washed in PBS, and resuspended for use at 1 to 2 × 10^7 CFUs per 50 μl (62). Seven- to ten-week-old B6-MAIT^{CAST} female mice were anesthetized with ketamine (125 mg/kg) and xylazine (12.5 mg/kg) intraperitoneally, and a 24-gauge catheter (BD Insyte Autoguard, BD) containing either PBS or UTI89 was inserted through the urethra; 50 μl of bacterial suspension or PBS was instilled at a slow rate to avoid vesicoureteral reflux.

At indicated time points, bladders, spleens, and bladder-draining LNs were harvested. Bladder-infiltrating lymphocytes were isolated from tissue digested in CO_2-independent medium (Invitrogen) containing Liberase TM (0.17 U/ml) (Roche), collagenase D (1 mg/ml) (Roche), and deoxyribonuclease 1 (1 U/ml) (Invitrogen). After 40 minutes incubation at 37°C in a shaking incubator, tissue suspensions were pressed through a 40-μm cell strainer (Falcon), washed in PBS with 0.5% BSA and 2 mM EDTA, and pelleted for FACS staining

Quantitative PCR and SNP genotyping. Real-time qPCR was performed as previously described (20). The primers were specific for regions that are identical in B6 and CAST strains. Real-time PCR was performed using a LightCycler 480 (Roche). Fold change in expression was determined by the 2-ΔΔCT method after normalizing to the TCR-α constant region (*Cα*).

SNP genotyping assays were custom designed using TaqMan Assay Design Tool (Life Technologies) on the reference assembly NCBI37/mm9. SNP queries were performed using the Mouse Genomes Project database (http://www.sanger.ac.uk/sanger/Mouse_SnpViewer/rel-1505) and the UCSC Genome Browser (http://genome.ucsc.edu/cgi-bin/hgGateway).

Statistics. All data were analyzed with the 2-tailed nonparametric Mann-Whitney *U* test using GraphPad Prism v5.0c (GraphPad Software Inc.). Data were considered significant at a *P* value of less than 0.05. All data are reported as the arithmetic or geometric mean ± SD as appropriate.

Study approval. All animal experiments were performed in an accredited mouse facility in accordance with the guidelines of the French Veterinary Department. The animal protocol was approved by the Animal Ethical Committee of Paris Centre (CEEA-59): file #2012-0067. Urine from patients with UTIs was obtained at Institut Curie. Following French regulations, all patients were informed that leftovers of specimens obtained for diagnosis or through therapeutic procedures may be used for research purposes.

Author contributions

YC, KF, YKM, SM, LLB, AK, VP, EM, LD, SR, JPV, and CS performed experiments. MI and JJ contributed essential reagents or tools. All authors interpreted the data. OL supervised the work, interpreted the data, and wrote the manuscript.

Acknowledgments

We thank M. Sarkis for synthesizing 5-A-RU; C. Daviaud and I. Grandjean for managing the mouse colony; Z. Maciorowski, S. Grondin, and A. Viguier for cell sorting; T. Rio Frio of the Next-Generation Sequencing (NGS) platform for advice; D. Laubreton for technical help; A. Lehuen, X. Montagutelli, and G. Eberl for mice; and T. Hansen for the 26.5 antibody and MR1 transfectants. We thank P. Matzinger for her suggestions. We also thank L. Teyton, S. Amigorena, and K. Benlagha for their helpful discussions and review of the manuscript. This work was supported by grants from INSERM, Agence Nationale de la Recherche (ANR), DIM Ile de France, Association pour la Recherche sur la Sclérose En Plaques (ARSEP), Institut Mérieux, and Institut Curie. Y.K. Mburu is a recipient of the Lloyd J. Old Memorial Award and is supported by an Irvington Institute postdoctoral fellowship from the Cancer Research Institute.

Address correspondence to: Olivier Lantz, Laboratoire d'Immunologie and INSERM U932, Institut Curie, 26 rue d'Ulm, 75005 Paris, France. Phone: 33.144324218; E-mail: olivier.lantz@curie.fr.

1. Le Bourhis L, Guerri L, Dusseaux M, Martin E, Soudais C, Lantz O. Mucosal-associated invariant T cells: unconventional development and function. *Trends Immunol*. 2011;32(5):212–218.
2. Le Bourhis L, Mburu YK, Lantz O. MAIT cells, surveyors of a new class of antigen: development and functions. *Curr Opin Immunol*. 2013;25(2):174–180.
3. Treiner E, et al. Selection of evolutionarily conserved mucosal-associated invariant T cells by MR1. *Nature*. 2003;422(6928):164–169.
4. Treiner E, Duban L, Moura IC, Hansen T, Gilfillan S, Lantz O. Mucosal-associated invariant T (MAIT) cells: an evolutionarily conserved T cell subset. *Microbes Infect*. 2005;7(3):552–559.
5. Gold MC, et al. Human mucosal associated invariant T cells detect bacterially infected cells. *PLoS Biol*. 2010;8(6):e1000407.
6. Le Bourhis L, et al. Antimicrobial activity of mucosal-associated invariant T cells. *Nat Immunol*. 2010;11(8):701–708.
7. Georgel P, Radosavljevic M, Macquin C, Bahram S. The non-conventional MHC class I MR1 molecule controls infection by Klebsiella pneumoniae in mice. *Mol Immunol*. 2011;48(5):769–775.
8. Meierovics A, Yankelevich WJ, Cowley SC. MAIT cells are critical for optimal mucosal immune responses during in vivo pulmonary bacterial infection. *Proc Natl Acad Sci U S A*. 2013;110(33):E3119–E3128.
9. Kjer-Nielsen L, et al. MR1 presents microbial vitamin B metabolites to MAIT cells. *Nature*. 2012;491(7426):717–723.
10. Corbett AJ, et al. T-cell activation by transitory neo-antigens derived from distinct microbial pathways. *Nature*. 2014;509(7500):361–365.
11. Grimaldi D, et al. Specific MAIT cell behaviour among innate-like T lymphocytes in critically ill patients with severe infections. *Intensive Care Med*. 2014;40(2):192–201.
12. Abrahamsson SV, et al. Non-myeloablative autologous haematopoietic stem cell transplantation expands regulatory cells and depletes IL-17 producing mucosal-associated invariant T cells in multiple sclerosis. *Brain*. 2013;136(pt 9):2888–2903.
13. Annibali V, et al. CD161^{high}CD8$^+$ T cells bear pathogenetic potential in multiple sclerosis. *Brain*. 2010;134(pt 2):542–554.
14. Magalhaes I, et al. Mucosal-associated invariant T cell alterations in obese and type 2 diabetic patients. *J Clin Invest*. 2015;125(4):1752–1762.
15. Serriari NE, et al. Innate mucosal-associated invariant T (MAIT) cells are activated in inflammatory bowel diseases. *Clin Exp Immunol*. 2014;176(2):266–274.
16. Cosgrove C, et al. Early and nonreversible decrease of CD161++/MAIT cells in HIV infection. *Blood*. 2013;121(6):951–961.
17. Leeansyah E, et al. Activation, exhaustion, and persistent decline of the antimicrobial MR1-restricted MAIT-cell population in chronic HIV-1 infection. *Blood*. 2013;121(7):1124–1135.
18. Wong EB, et al. Low levels of peripheral CD161++CD8+ mucosal associated invariant T (MAIT) cells are found in HIV and HIV/TB co-infection. *PLoS One*. 2013;8(12):e83474.
19. Fernandez CS, Kelleher AD, Finlayson R, Godfrey DI, Kent SJ. NKT cell depletion in humans during early HIV infection. *Immunol Cell Biol*. 2014;92(7):578–590.
20. Tilloy F, et al. An invariant T cell receptor alpha chain defines a novel TAP-independent major histocompatibility complex class Ib-restricted α/β T cell subpopulation in mammals. *J Exp Med*. 1999;189(12):1907–1921.
21. Dusseaux M, et al. Human MAIT cells are xenobiotic resistant, tissue-targeted, CD161hi IL-17 secreting T cells. *Blood*. 2011;117(4):1250–1259.
22. Walker LJ, et al. Human MAIT and CD8αα cells develop from a pool of type-17 precommitted CD8$^+$ T cells. *Blood*. 2012;119(2):422–433.
23. Huang S, et al. MR1 antigen presentation to mucosal-associated invariant T cells was highly conserved in evolution. *Proc Natl Acad Sci U S A*. 2009;106(20):8290–8295.
24. Billerbeck E, et al. Analysis of CD161 expression on human CD8+ T cells defines a distinct functional subset with tissue-homing properties. *Proc Natl Acad Sci U S A*. 2010;107(7):3006–3011.
25. Ussher JE, et al. CD161++ CD8+ T cells, including the MAIT cell subset, are specifically activated by IL-12$^+$IL-18 in a TCR-independent manner. *Eur J Immunol*. 2014;44(1):195–203.
26. Tang XZ, et al. IL-7 licenses activation of human liver intrasinusoidal mucosal-associated invariant T cells. *J Immunol*. 2013;190(7):3142–3152.
27. Havenith SH, et al. Analysis of stem-cell-like properties of human CD161++IL-18Rα$^+$ memory CD8$^+$ T cells. *Int Immunol*. 2012;24(10):625–636.
28. Le Bourhis L, et al. MAIT cells detect and efficiently lyse bacterially-infected epithelial cells. *PLoS Pathog*. 2013;9(10):e1003681.
29. Kurioka A, et al. MAIT cells are licensed through granzyme exchange to kill bacterially sensitized targets. *Mucosal Immunol*. 2015;8(2):429–440.
30. Turtle CJ, et al. Innate signals overcome acquired TCR signaling pathway regulation and govern the fate of human CD161(hi) CD8α semi-invariant T cells. *Blood*. 2011;118(10):2752–2762.
31. Savage AK, et al. The transcription factor PLZF directs the effector program of the NKT cell lineage. *Immunity*. 2008;29(3):391–403.
32. Martin E, et al. Stepwise development of MAIT cells in mouse and human. *PLoS Biol*. 2009;7(3):e54.
33. Lepore M, et al. Parallel T-cell cloning and deep sequencing of human MAIT cells reveal stable oligoclonal TCRβ repertoire. *Nat Commun*. 2014;5:3866.
34. Turtle CJ, Swanson HM, Fujii N, Estey EH, Riddell SR. A distinct subset of self-renewing human memory CD8$^+$ T cells survives cytotoxic chemotherapy. *Immunity*. 2009;31(5):834–844.
35. Croxford JL, Miyake S, Huang YY, Shimamura M, Yamamura T. Invariant V(alpha)19i T cells regulate autoimmune inflammation. *Nat Immunol*. 2006;7(9):987–994.
36. Kawachi I, Maldonado J, Strader C, Gilfillan S. MR1-restricted Vα 19i mucosal-associated invariant T cells are innate T cells in the gut lamina propria that provide a rapid and diverse cytokine

response. *J Immunol*. 2006;176(3):1618–1627.
37. Shimamura M, Huang YY, Migishima R, Yokoyama M, Saitoh T, Yamamura T. Localization of NK1.1(+) invariant Vα19 TCR(+) cells in the liver with potential to promptly respond to TCR stimulation. *Immunol Lett*. 2008;121(1):38–44.
38. Reantragoon R, et al. Antigen-loaded MR1 tetramers define T cell receptor heterogeneity in mucosal-associated invariant T cells. *J Exp Med*. 2013;210(11):2305–2320.
39. Chua WJ, Truscott SM, Eickhoff CS, Blazevic A, Hoft DF, Hansen TH. Polyclonal mucosa-associated invariant T cells have unique innate functions in bacterial infection. *Infect Immun*. 2012;80(9):3256–3267.
40. Sakala IG, et al. Functional heterogeneity and antimycobacterial effects of mouse mucosal-associated invariant T cells specific for riboflavin metabolites. *J Immunol*. 2015;195(2):587–601.
41. Terrence K, Pavlovich CP, Matechak EO, Fowlkes BJ. Premature expression of T cell receptor (TCR) αβ suppresses TCRγΔ gene rearrangement but permits development of γΔ lineage T cells. *J Exp Med*. 2000;192(4):537–548.
42. Vera G, et al. Cernunnos deficiency reduces thymocyte life span and alters the T cell repertoire in mice and humans. *Mol Cell Biol*. 2013;33(4):701–711.
43. Bosc N, Lefranc MP. The mouse (Mus musculus) T cell receptor α (TRA) and Δ (TRD) variable genes. *Dev Comp Immunol*. 2003; 27(6–7):465–497.
44. Guo J, et al. Regulation of the TCRα repertoire by the survival window of CD4(+)CD8(+) thymocytes. *Nat Immunol*. 2002;3(5):469–476.
45. Keane TM, et al. Mouse genomic variation and its effect on phenotypes and gene regulation. *Nature*. 2011;477(7364):289–294.
46. Lochner M, et al. In vivo equilibrium of proinflammatory IL-17$^+$ and regulatory IL-10$^+$ Foxp3$^+$ RORγt$^+$ T cells. *J Exp Med*. 2008;205(6):1381–1393.
47. Bautista JL, et al. Intraclonal competition limits the fate determination of regulatory T cells in the thymus. *Nat Immunol*. 2009;10(6):610–617.
48. Rahimpour A, et al. Identification of phenotypically and functionally heterogeneous mouse mucosal-associated invariant T cells using MR1 tetramers. *J Exp Med*. 2015;212(7):1095–1108.
49. Soudais C, et al. In vitro and in vivo analysis of the gram-negative bacteria-derived riboflavin precursor derivatives activating mouse MAIT cells. *J Immunol*. 2015;194(10):4641–4649.
50. Huang S, et al. MR1 uses an endocytic pathway to activate mucosal-associated invariant T cells. *J Exp Med*. 2008;205(5):1201–1211.
51. Mulvey MA, Schilling JD, Hultgren SJ. Establishment of a persistent Escherichia coli reservoir during the acute phase of a bladder infection. *Infect Immun*. 2001;69(7):4572–4579.
52. Legoux F, Debeaupuis E, Echasserieau K, De La Salle H, Saulquin X, Bonneville M. Impact of TCR reactivity and HLA phenotype on naive CD8T cell frequency in humans. *J Immunol*. 2010;184(12):6731–6738.
53. Dellabona P, Padovan E, Casorati G, Brockhaus M, Lanzavecchia A. An invariant Vα24-Jα Q/Vβ11 T cell receptor is expressed in all individuals by clonally expanded CD4-8$^-$ T cells. *J Exp Med*. 1994;180(3):1171–1176.
54. Fergusson JR, et al. CD161 defines a transcriptional and functional phenotype across distinct human T cell lineages. *Cell Rep*. 2014;9(3):1075–1088.
55. Seach N, et al. Double-positive thymocytes select mucosal-associated invariant T cells. *J Immunol*. 2013;191(12):6002–6009.
56. Leeansyah E, Loh L, Nixon DF, Sandberg JK. Acquisition of innate-like microbial reactivity in mucosal tissues during human fetal MAIT-cell development. *Nat Commun*. 2014;5:3143.
57. Biot C, et al. Preexisting BCG-specific T cells improve intravesical immunotherapy for bladder cancer. *Sci Transl Med*. 2012;4(137):137ra72.
58. Arstila T, et al. Identical T cell clones are located within the mouse gut epithelium and lamina propia and circulate in the thoracic duct lymph. *J Exp Med*. 2000;191(5):823–834.
59. Magoc T, Salzberg SL. FLASH: fast length adjustment of short reads to improve genome assemblies. *Bioinformatics*. 2011;27(21):2957–2963.
60. Li S, et al. IMGT/HighV QUEST paradigm for T cell receptor IMGT clonotype diversity and next generation repertoire immunoprofiling. *Nat Commun*. 2013;4:2333.
61. Huang S, et al. Evidence for MR1 antigen presentation to mucosal-associated invariant T cells. *J Biol Chem*. 2005;280(22):21183–21193.
62. Hung CS, Dodson KW, Hultgren SJ. A murine model of urinary tract infection. *Nat Protoc*. 2009;4(8):1230–1243.

Figure S1

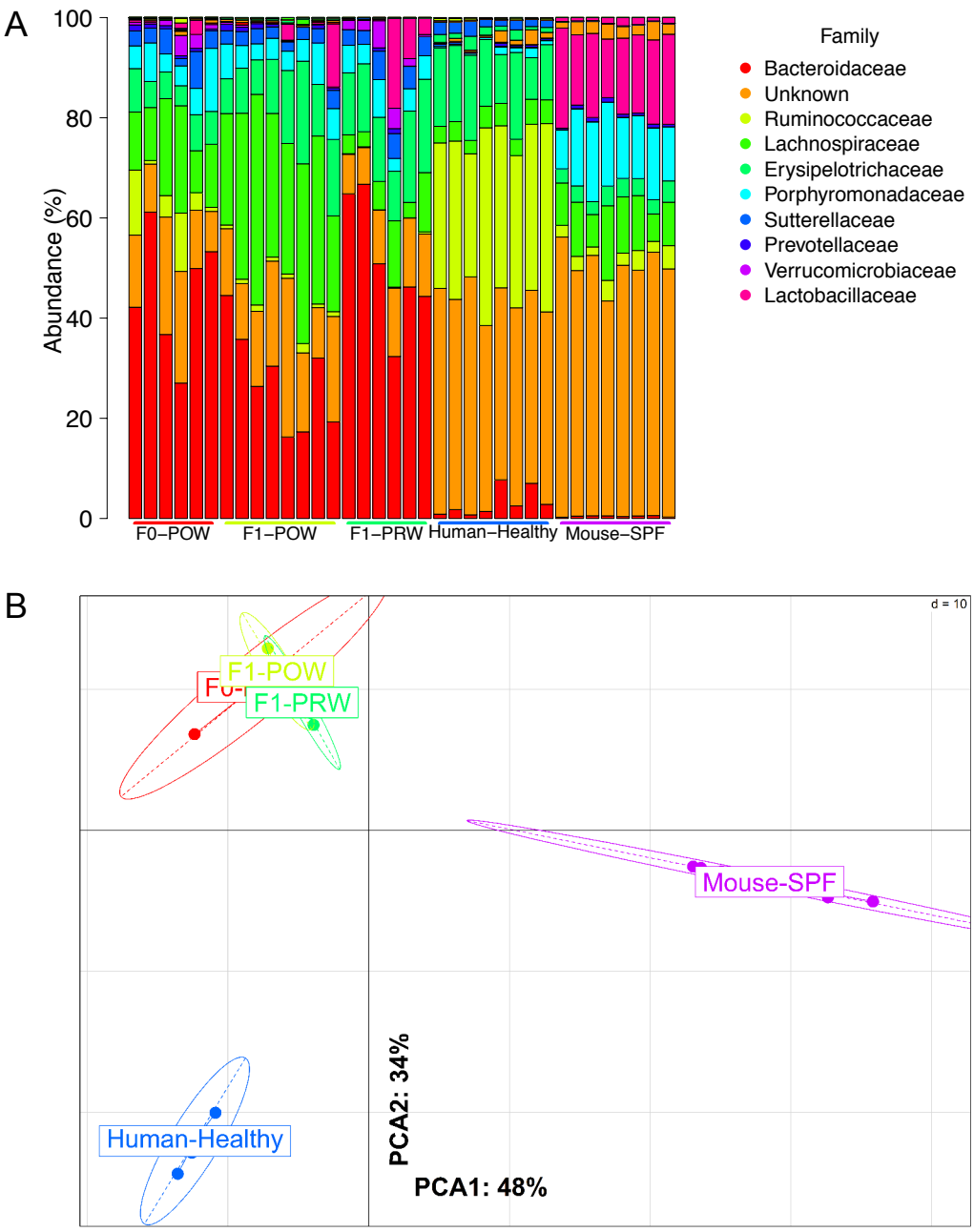

Fig. S1. Human microbiota reconstitution of breeding TAP li double KO mice. (A) Microbiota composition at the family level inferred for human replicates (H), SPF mice (SPF) and breeding mice reconstituted with human microbiota (F) before (F1-PRW) and after weaning (F1-POW) of the pups and mothers (FO). **(B)** Between class analysis (BCA) computed with the principal components analysis of the whole microbiota composition dataset and constrained with H, SPF and F instrumental variables.

Figure S2

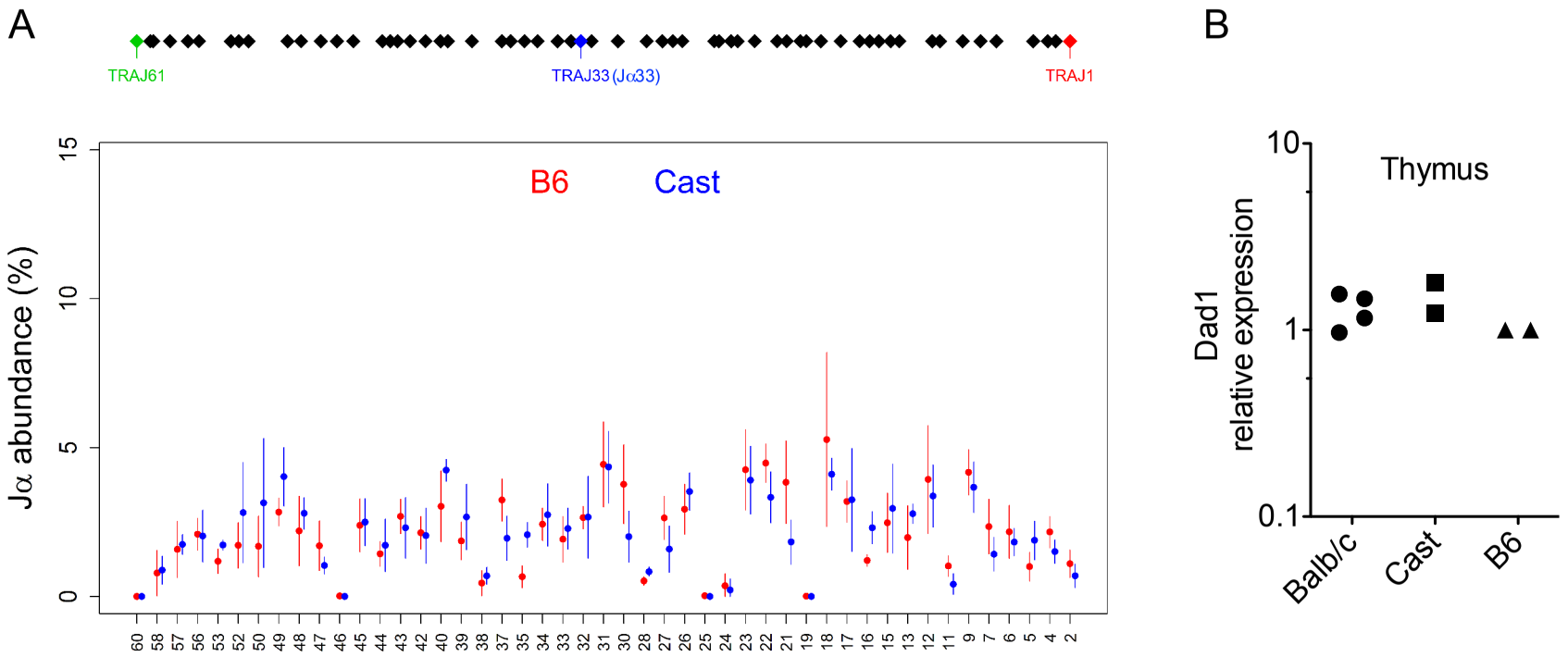

Fig. S2. TCR Jα usage and *Dad1* expression in CAST/EiJ mice. (A) Thymic TCR Jα repertoire analysis from C57Bl/6J (red) and CAST/EiJ (blue) mice using 5'RACE and NGS sequencing. Proximal 5' to distal 3' Jα segments were plotted as mean± SD. **(B)** Thymic *Dad1* (*defender against cell death 1*) mRNA expression analysis using TaqMan Gene Expression assay (Applied Biosystems). Fold change relative to C57Bl/6J is plotted, after normalizing to Cα.

Figure S3

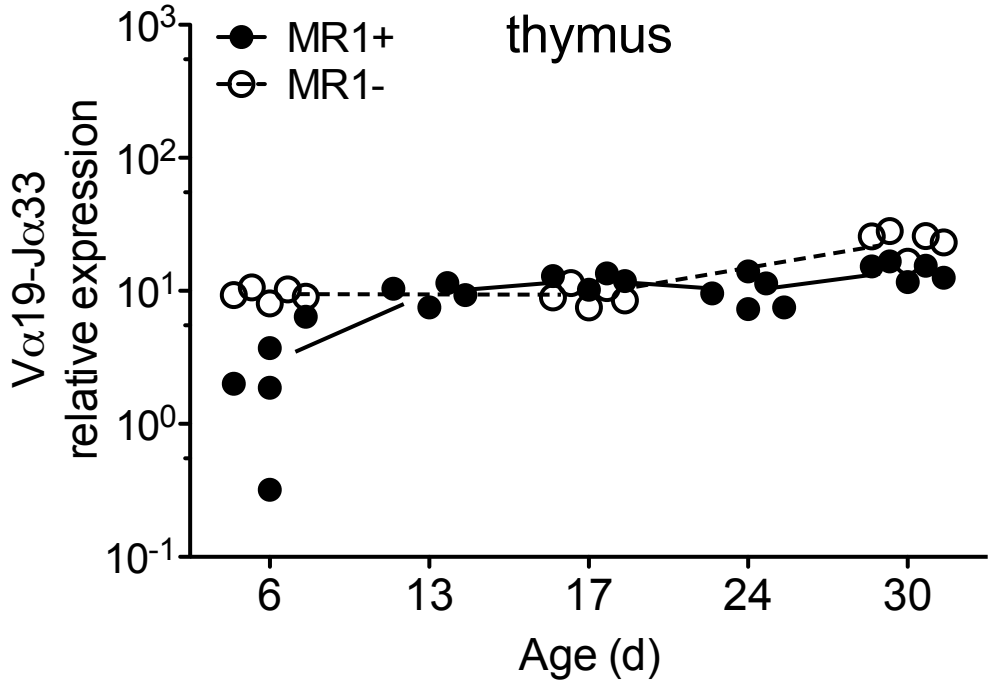

Fig. S3. No accumulation of MAIT cells in the thymus after birth. Vα19-Jα33 transcripts were quantified by RT-qPCR at the indicated time points after birth.

Figure S4

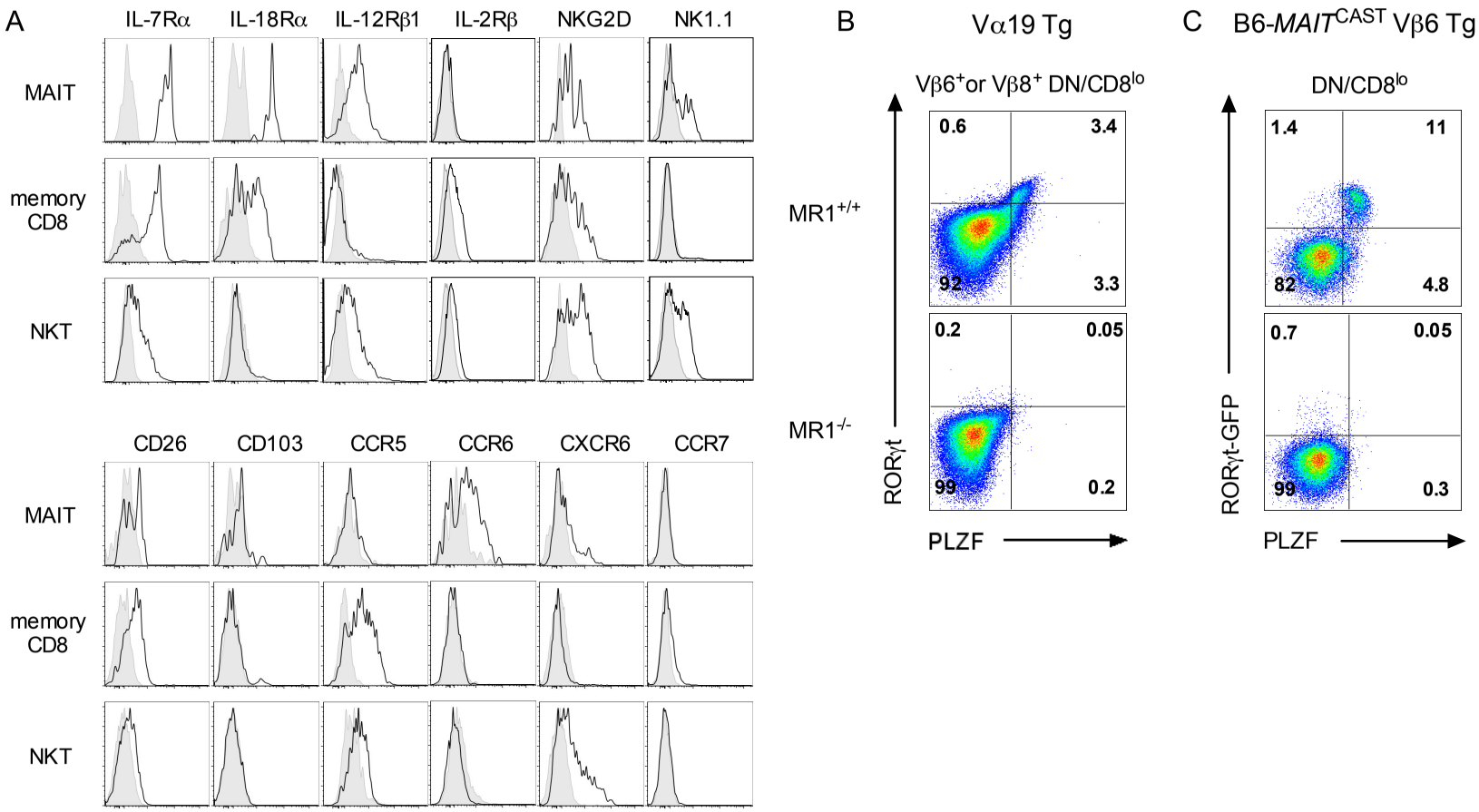

Fig. S4. Phenotype of murine MAIT cells. (A) Surface expression of indicated markers on liver MAIT cells, **(B)** Expression of PLZF and RORγt by Vβ6+ or Vβ8+ DN/CD8^{lo} T cells from iVα19 Tg Cα$^{-/-}$ mice on MR1$^{+/+}$ or MR1$^{-/-}$ background, **(C)** Expression of PLZF by RORγt-GFP+ DN/CD8lo TCRβ+ T cells from Vβ6 Tg B6-MAIT^{CAST} on a MR1$^{+/+}$ or MR1$^{-/-}$ background.

Figure S5

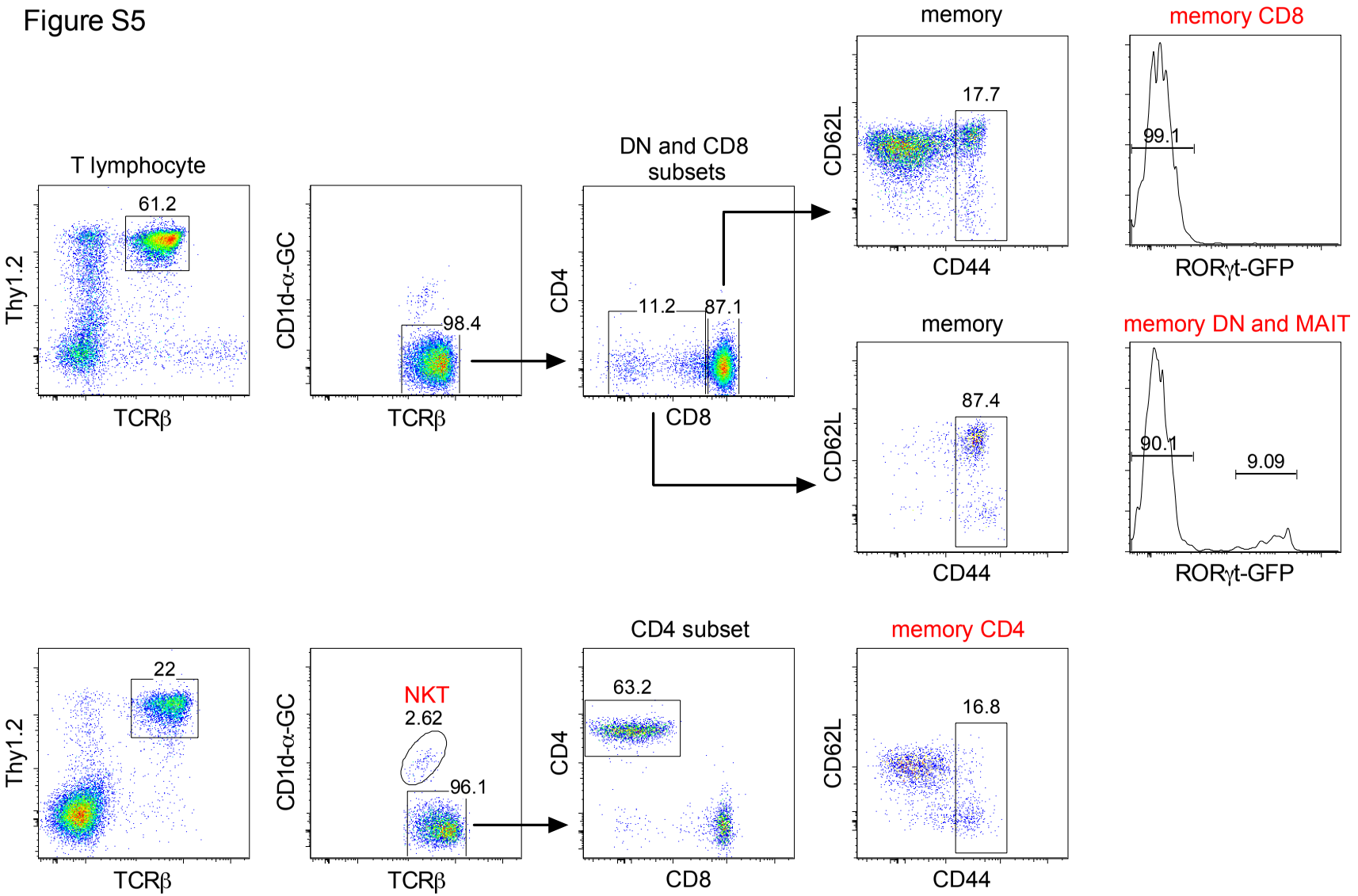

Fig. S5. Gating strategy of splenocyte sorting. Pools of 5-10 spleen were subjected to anti-CD19, -CD11c, -CD11b and -CD4 microbeads depletion to enrich DN and CD8+ T cells before separation of memory CD8 ($CD8^{hi}CD44^{+}GFP^{-}$), memory DN ($CD8^{lo/neg}CD44^{+}GFP^{-}$) and MAIT ($CD8^{lo/neg}CD44^{+}GFP^{+}$) subsets by FACS sorting (top). Memory CD4 ($CD4^{+}CD44^{+}$) and NKT ($CD1d\text{-}\alpha\text{-}GC^{+}$) subsets were sorted from pool of splenocytes before microbead-enrichment (bottom).

Figure. S6

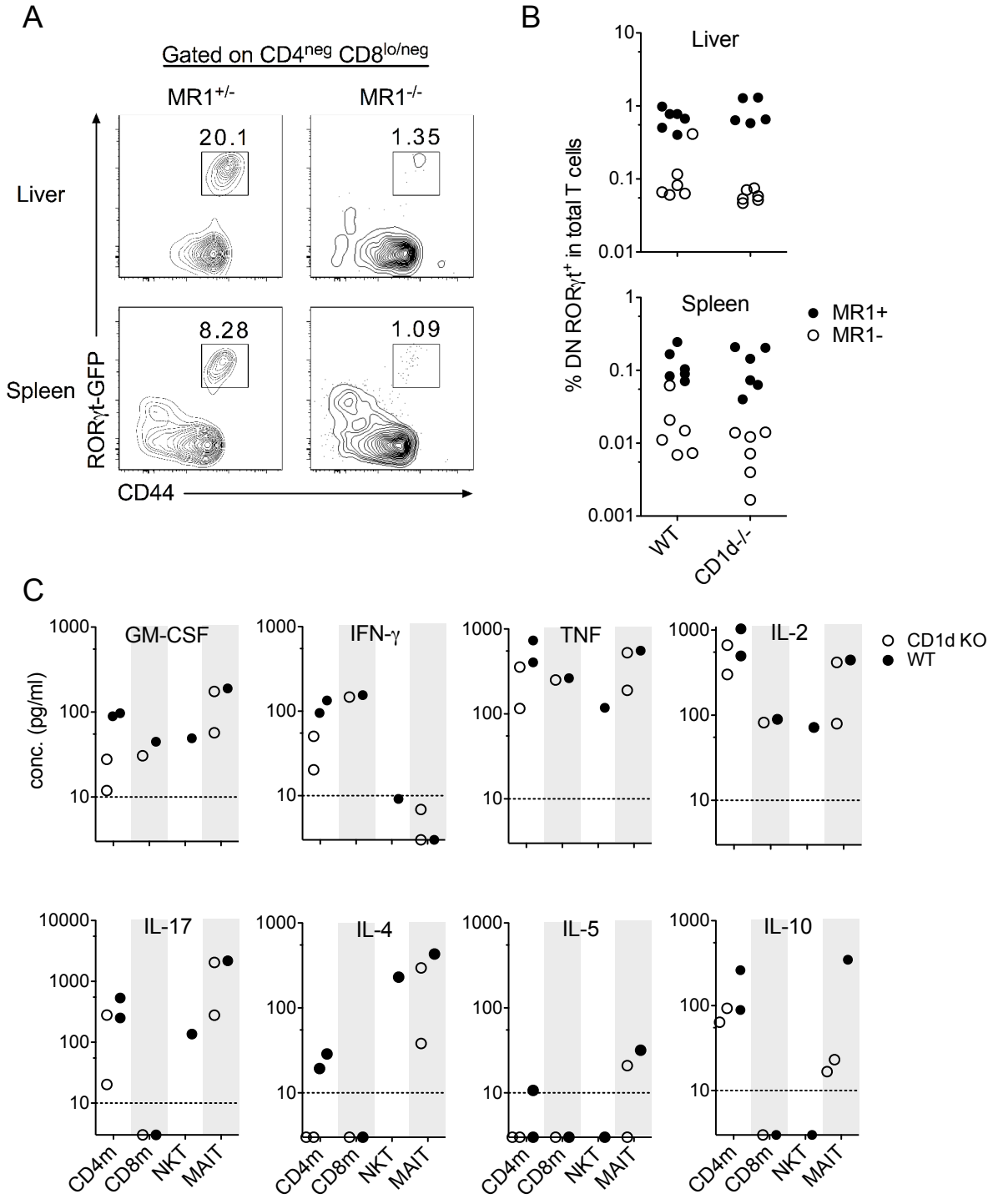

Fig. S6. Frequency and cytokine secretion pattern of MAIT cells in CD1d$^{-/-}$ ROR(γt)-Gfp^{TG} B6-MAIT^{CAST} mice. Gating strategy and staining **(A)** and frequency **(B)** of TCRβ^{+}Thy1.2^{+} CD4^{neg}CD8$^{lo/neg}$GFP^{+} cells in CD1d$^{-/-}$ Rorc(γt)-Gfp^{TG}-B6-*MAIT*^{CAST} mice. Compilation of 3 independent experiments. **(C)** Cytokine secretion of the indicated subsets isolated from CD1d$^{-/-}$ or WT (Rorc(γt)-Gfp^{TG}-B6-*MAIT*^{CAST}) mice as described in Fig. S5. NKT cells were sorted from WT mice using CD1d-α-GC tetramer. Compilation of 2 independent experiments.

Figure. S7

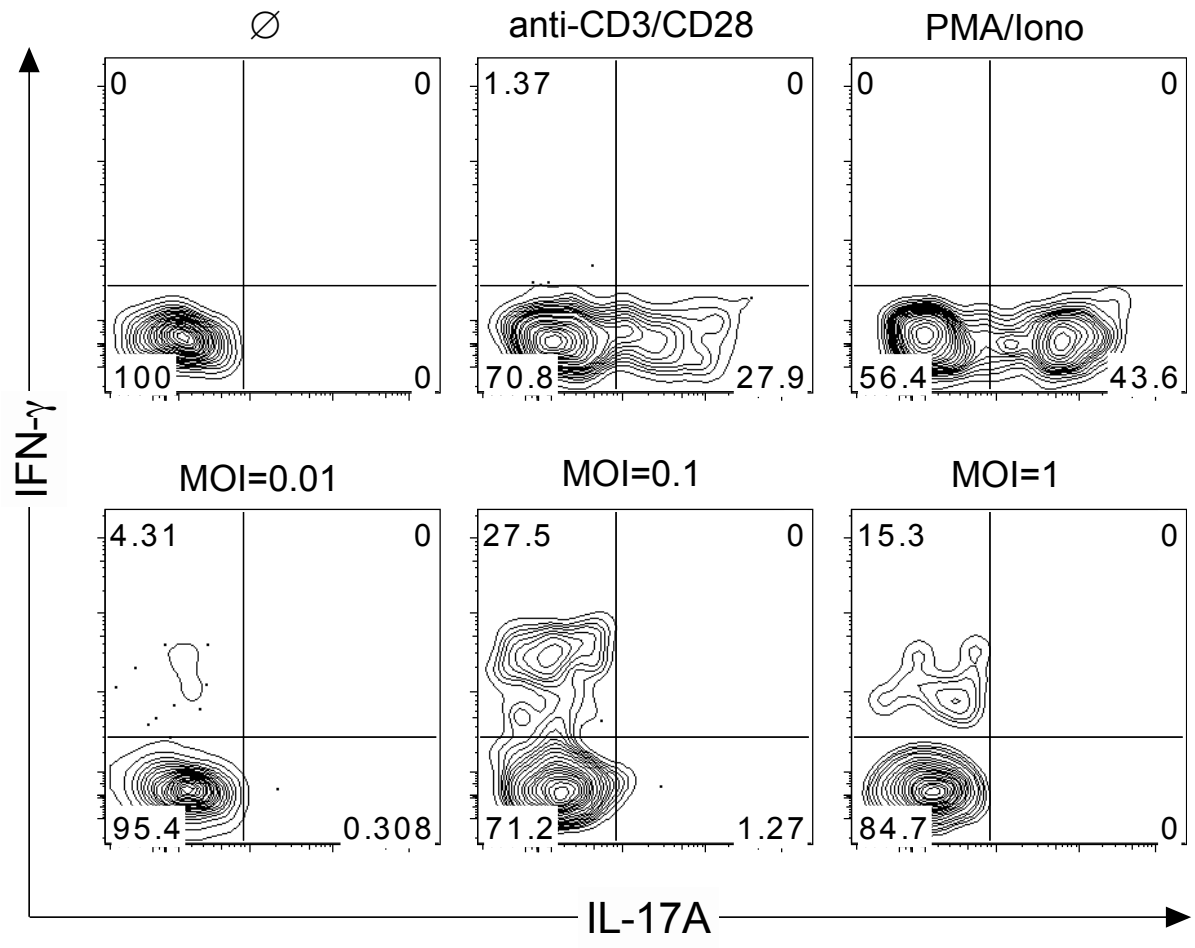

Figure S7. Cytokine production by mouse MAIT cells. Splenocytes from CD1d$^{-/-}$ Rorc(γt)-Gfp^{TG}-B6-*MAIT*^{CAST} mice were stimulated with anti-CD3/CD28 beads (9 h), PMA/Ionomycin (5 h), or PFA fixed *E.coli* (overnight, lower panel) and stained for intracellular IL-17A and IFN-γ. Representative plots from three independent experiments are shown gating on TCRβ^{+}DN/CD8^{lo}CD44^{+}GFP^{+} cells.

Figure S8

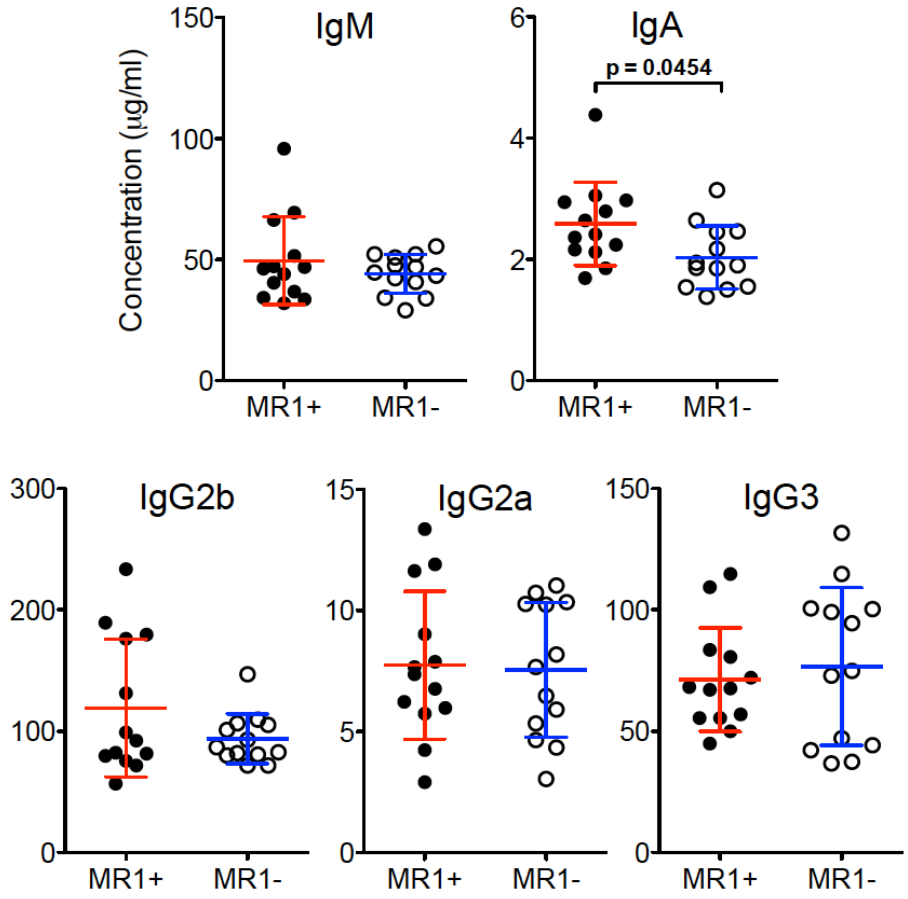

Figure S8. In the absence of MAIT cells, serum immunoglobulin isotype levels remain unchanged. ELISA was used to measure total IgM, IgG2a, IgG2b, IgG3 and IgA in sera drawn from the indicated unchallenged 7-9 week old mice. Bars indicate mean ± SD.

Cui et al supplementary materials and methods

Antibody list

All Abs were purchased from BioLegend, BD Pharmingen, eBioscience unless otherwise stated. The antibody clones used included: CD19 (1D3), TCRβ (H57-597), CD90.2 (53-2.1, 30-H12), CD4 (RM4-5), CD8 (53-6.7), CD44 (IM7), CD62L (MEL-14), CD25 (PC61), CD69 (H1.2F3), mCD1d-α-GC tetramers (ProImmune), IL-7Rα (A7R34), IL-18Rα (BG/IL18RA), IL-12Rβ (114), IL-2Rb (TM-Beta 1), NKG2D (CX5), NK1.1 (PK136), CD26 (H194-112), CD103 (2E7), CCR5 (HM-CCR5), CCR6 (29-2L17), CXCR6 (221002, R&D systems), CCR7 (4B12), PLZF (Mags.21F7), RORγt (AFKJS-9), IL-17A (TC11-18H10.1), IFN-γ (XMG1.2), IL-4 (11B11).

***In vitro* stimulation**

E.coli were cultured overnight at 37°C in Luria Broth, pelleted and washed in PBS before fixation for 20 min in 1% of PFA. For intracellular cytokine staining, 2 x 10^6 splenocytes were stimulated with 10 ng/ml PMA (Sigma) and 1 μg/ml ionomycin (Sigma) for 5 h, anti-CD3/CD28 Dynabeads (1:1, Gibco) for 9 h or fixed E.coli overnight. Golgi Plug (1 μg/ml, BD) was added for the final 3-4 h of culture. Prior to surface marker staining, cells were incubated with live/dead violet fixable cell stain (Life Technologies) and Fc block. Cells were then fixed and permeabilized for 20 min using Cytofix/Cytoperm kit (BD) and subjected to intracellular IFN-γ, IL-4 and IL-17A staining.

ELISA

Blood samples were collected by retro-orbital bleeding from naïve B6-*MAIT*^{CAST} MR1^{+} or MR1$^{-/-}$ mice (n=13 for each genotype, 7-9 weeks old). Total serum IgM, IgG1, IgG2a, IgG2b, IgG3 and IgA titers were determined using Ready-Set-Go® ELISA kits, according to the manufacturer's instructions (eBioscience). Data were analyzed using second-order polynomial model (Prism GarphPad 5.0) and plotted as concentration.

Fecal samples

DNA was extracted from stool as previously published (1, 2). DNA quality and quantity were checked using NanoDrop and Qubit together with BR assay.

16S rDNA Barcoding PCR

Barcoded PCR was carried out using barcoded primers targeting V4-V5 variable part of the 16S rRNA gene. iProof High fidelity master mix (Bio-Rad) was used to perform the PCR following manufacturer's recommendations. Mix for one PCR reaction was made up of 12.5 µL of iProof High fidelity master mix, 0.5 µL of both 563F and 924R primers (0.2 µM), 10 µL of RNase DNase free water and 1.5 µL of DNA (10 ng). The PCR program applied was 95°C for 5 min followed by 30 cycles (95°C for min, 41°C for min and 72°C for min) and a final step at 72°C for min. PCR reactions (25 µL) were then quantified using Qubit BR DNA assay kit. Equal amount of amplicon DNA were pooled and thoroughly mixed. The resulting amplicon pool was loaded on an agarose gel (1.5%) and electrophoresis run for 45 min at 100 V. The band corresponding to 16S amplicon was excised from the gel and purified using Qiaquick gel extraction kit (Qiagen). After gel extraction the amplicon quantity and intergrity were both checked on agarose gel electrophoresis and Qubit BR DNA assay kit. Amplicon was stored at -20°C until use.

16S rDNA sequencing and statistics

Sequencing of the amplicon pool was performed at Institut Curie NGS platform on an Ion Torrent PGM machine using the 318 chips. Raw sequencing output was demultiplexed and trimmed using in-house analysis pipeline (BCmm = 0, Pmm = 2, W = 50 bp, Q = 20, MinL = 200 bp and MaxL = 335 bp). Reads were clustered at 97% of identity using vsearch pipeline (http://zenodo.org/record/15524#.VPIujy4f2J8). Chimeric OTU were identified using UCHIME (3) and discarded from downstream analysis. Taxonomy of representative OTU sequences was determined using RDP classifier (4). OTU sequences were aligned using ssu-align (5). The phylogenetic tree was inferred from the OTUs multiple alignments using Fattree2 (6).

Statistical analyzes were performed using R program (7) and different related packages (Ade4 (8), Vegan (9), ape, phyloseq). Weighted unifrac distances (10, 11) were computed using microbiota abundance table and phylogenetic tree. Statistical tests were performed using the Wilcoxon test (p-value). Multiple tests were corrected using the False Discovery Rate method (q-value).

References

1. Yu Z, Morrison M. Improved extraction of PCR-quality community DNA from digesta and fecal samples. [Internet]. *Biotechniques* 2004;36(5):808–12.

2. Ó Cuív P et al. The effects from DNA extraction methods on the evaluation of microbial diversity associated with human colonic tissue. [Internet]. *Microb. Ecol.* 2011;61(2):353–62.

3. Edgar RC, Haas BJ, Clemente JC, Quince C, Knight R. UCHIME improves sensitivity and speed of chimera detection. *Bioinformatics* 2011;27:2194–2200.

4. Cole JR et al. The Ribosomal Database Project: improved alignments and new tools for rRNA analysis. [Internet]. *Nucleic Acids Res.* 2009;37(Database issue):D141–5.

5. Nawrocki EP. Structural RNA Homology Search and Alignment using Covariance Models 2009;

6. Price MN, Dehal PS, Arkin AP. FastTree 2--approximately maximum-likelihood trees for large alignments. [Internet]. *PLoS One* 2010;5(3):e9490.

7. R Development Core Team. R: A Language and Environment for Statistical Computing 2012;

8. Dray S, Dufour AB. The ade4 Package: Implementing the Duality Diagram for Ecologists. *J. Staistical Softw*. 2007;22(4):1–20.

9. Oksanen J et al. vegan: Community Ecology Package [Internet][published online ahead of print: 2013];http://cran.r-project.org/package=vegan. cited

10. Lozupone C, Hamady M, Knight R. UniFrac--an online tool for comparing microbial community diversity in a phylogenetic context. *BMC Bioinformatics* 2006;7:371.

11. Lozupone C, Knight R. UniFrac: A new phylogenetic method for comparing microbial communities. *Appl. Environ. Microbiol.* 2005;71:8228–8235.

Discussion

Although MAIT cells have been implicated in a number of infectious and autoimmune diseases (Table 2), their exact roles remain elusive, in part due to their scarcity in mice which hampers *in vivo* studies and therefore the understanding of MAIT cell biology. In this study, we describe a congenic mouse model with naturally increased frequency of MAIT cells. Together with reporter RORγt-GFP, we were able to study the characteristics of natural mouse MAIT cells.

Like human MAIT cells, resting mouse MAIT cells are effector memory cells ($CD44^{+}CD62L^{-}$) and express the transcription factors RORγt and PLZF. In contrast, Tg MAIT cells were reported having a $CD44^{lo}$ $PLZF^{lo}$ naïve phenotype[49]. This implicates that the locus responsible for increased MAIT iTCR rearrangement may also have an impact on MAIT development. Thus, we studied the phenotype of MAIT cells from B6 and Vα19-Tg mice and found that B6 MAIT cells were memory ($CD44^{hi}$) while Tg MAIT were mostly $CD44^{lo}$ with a small subset expressed PLZF, in agreement with recent results obtained using MR1-5-OP-RU tetramer[65]. The phenotypic differences of MAIT cells between WT and Tg mice may be due to the disrupted thymic development of T cells in Tg mice resulting from the prematuration and overexpression of the iTCRα[115]. Thus, MAIT cells from both CAST and B6 mice have a memory phenotype and the introduced CAST locus drives increases of MAIT cells.

Regardless, the frequency of MAIT cells within T cell population in mouse is far lower compared to those in human. In contrast, the other invariant αβT cells population, iNKT cells are more abundant in mice. Both MAIT cells and iNKT cells are selected by DP thymocytes and they share functional similarities (Table 1). Thus, their competition during intra-thymic development or for peripheral niches may lead to the low frequency of MAIT cells in mice. However, we did not observe significant increases of NKT or MAIT cells from $MR1^{-/-}$ or $CD1d^{-/-}$ mice respectively.

Microbiota plays an essential role in shaping immune system and regulating immune homeostasis[116]. Obviously, inbred mice raised in specific pathogen-free (SPF) conditions are exposed to a relatively restricted set of microbes whereas human

immune systems repetitively encounter a large variety of microbes. The importance of microbiota for MAIT development has been implicated in a number of studies[11,18,20]. Thus, the paucity of MAIT cells in mice may be due to the lack of specific human microbiota species. However, we performed the human microbiota reconstitution into $TAP^{-/-}Ii^{-/-}$ germ free mice and did not observe increases of MAIT cells than those of SPF mice. In addition, in contrast to their oligoclonality in human, MAIT cells in mice express a polyclonal repertoire suggesting a lack of expansion of these cells. Of note, MAIT cells readily expand in response to pulmonary bacteria infection in B6 mice and proliferate following bacterial stimulation in human[54,59,81]. It is possible that the rarity of MAIT cells in mice from SPF condition is due to the lack of microbial stimulation in the clean environment. In addition to MAIT cells, other memory T cell subsets (i.e., conventional CD4, CD8 T cells and NKT cells) also show diverse repertoires compared with those of human. The differences of lifespan and body size between human and mice may explain such common disparity.

Given that human MAIT cells express the transcription factor RORγt, we therefore hypothesized that mouse MAIT cells also express this marker. By comparing $MR1^{+}$ to $MR1^{-}$ mice, we observed a selectively larger RORγt-GFP^{+} population in the DN compartment and confirmed that iTCR Vα19-Jα33 chains were enriched in this population. Consistent with the expression of RORγt, mouse MAIT cells produce high levels of IL-17 following TCR or mitogen stimulation. Intracellular IFN-γ was solely observed in response to *E.coli* stimulation suggesting that a second signal, such as innate cytokine, is necessary for efficient IFN-γ production. Identification of mouse MAIT cells using MR1 tetramer revealed two MAIT populations: RORγt^{+} T-bet^{lo} IL-17 producing subset and a minor RORγt^{lo} T-bet^{+} IFN-γ producing subset[65]. As RORγt was used as a surrogate marker in our study, we mainly characterized RORγt^{+} DN subset. However, the release of IFN-γ we observed was from the RORγt^{hi} cells, which is reminiscent of the finding in human. In human, Turtle et. al showed that IL-12-stimulated $CD8\alpha^{+}$ $CD161^{hi}$ $CD62L^{lo}$ cells, including MAIT cells, expressed higher T-bet and IFN-γ, lost IL-17 secretion but preserved their RORγt expression[62]. This suggests that MAIT cells may retain functional plasticity and they can change their effector phenotype to cope with diverse immunological challenges.

In addition to iTCR Vα7.2, CD161 has been generally used as a surrogate maker to identify human MAIT cells. CD161 is encoded by *NKRP1A* and its ligand is lectin-like transcript 1 (LLT1). The mouse ortholog of *CD161* is a family of genes *Nkrp1a-g*.

Although NK1.1 (NKR-P1C) has been used as a mouse CD161 in B6 mice, NKRP-1B and D may represent a closer relation to CD161 as they bind to C-type lectin-related ligand, Clr-b, which is the mouse ortholog of LLT1[57]. Nevertheless, NK1.1 was reported to be expressed on a large proportion of Vα19 Tg MAIT cells[77]. We therefore examined its expression on natural mouse MAIT cells and found that a subset of hepatic but not splenic MAIT cells expressed NK1.1. In contrast, by using MR1-5-OP-RU tetramer, Rahimpour et al. showed that NK1.1 was expressed by MAIT cells in thymus and spleen, but not in lung, which was in agreement with the CD4 expression by MAIT cells from these organs[65]. This is reminiscent of the phenotypes of different NKT functional subsets, in which NKT1 (T-bet$^+$) cells express NK1.1 and are mostly CD4$^+$, whereas NKT17 (RORγt$^+$) cells lack both receptors (Figure 1)[27]. Due to the limitation of our study, we mainly characterized RORγt$^+$ DN MAIT cells, which are NK1.1$^-$ in spleen. Thus, one can speculate that the expression of NK1.1 by MR1 tetramer$^+$ cells in spleen may derive from CD4$^+$ MAIT cells. Together with the expression of NK1.1, we also observed CXCR6 expression by hepatic MAIT cells. Critical roles of CXCR6 in homeostasis and activation of NKT cells have been documented[117]. Interestingly, in the liver of CXCR6$^{-/-}$ mice, NK1.1$^+$ NKT cells were specifically reduced suggesting this liver-homing chemokine receptor may be important for NKT cell maturation[117]. Whether CXCR6 regulates NK1.1 expression on hepatic MAIT in a similar manner remains to be determined. Similarly, PLZF was also reported to promote the local residence of hepatic NKT cells by inducing the expression of adhesion molecule lymphocyte function-associated antigen-1 (LFA-1). Whether PLZF plays a role on homing and adhesion properties of MAIT cells warrants further investigation.

Like other innate-like T cells, MAIT cells have been shown to respond to innate cytokines, such as IL-12 and IL-18[19,80,81,84]. Given that mouse MAIT cells express high level of IL-12R and IL-18R, these findings may also hold true for mouse MAIT cells. We showed that mouse MAIT cells specifically respond to bacterial-derived antigens (i.e., semi-purified *E.coli* supernatant or 5-OP-RU) in an MR1-dependent manner. However, when stimulated with whole *E.coli*, MAIT cells exhibited higher expression of activation makers (CD25$^+$CD69$^+$) and this activation cannot be blocked using anti-MR1 antibody (not depicted). Moreover, in transwell culture with either WT or MR1$^-$ bone marrow-derived dendritic cells infected with *E.coli*, MAIT cells were able to upregulate activation markers CD69 and CD25, suggesting these cells

responded to soluble factors, possibly IL-12, because their activation was compromised by IL-12 blocking antibody (not depicted). In contrast, blocking MR1 had no effect on such stimulation. Their response to cytokine-mediated stimulation may be important to ensure immediate MAIT activation in response to any infectious stimuli that induce the production of innate cytokine, irrespective of the expression of microbial antigens, thus allowing MAIT cells to overcome their restricted TCR specificity. Accordingly, in line with previous findings, our data suggest that innate cytokine rather than MR1-TCR dominates MAIT cells activation and possibly effector function in control of bacterial infection.

Collectively, our results show that natural mouse MAIT cells preferentially reside in peripheral non-lymphoid tissues. They exhibit an effector-memory phenotype and coexpress transcription factors PLZF and RORγt. They have high expression of cytokine receptors, respond to both TCR and innate cytokine stimulation, and are able to produce IFN-γ and IL-17. Altogether, our results demonstrate that mouse MAIT cells resemble human MAIT cells more closely than previously thought. Accordingly, the generation of a relevant mouse model allows further understanding of MAIT cell biology in health and disease.

Perspectives

MAIT cells are now emerging as an important cell population at mucosal surface, potentially bridging innate and adaptive immunity. However, much of the current knowledge on MAIT cells stems from *in vitro* analyses and still requires experimental models for a better understanding of this innate lymphocyte population.

The mouse model described in this thesis is a promising tool for advancing our knowledge on MAIT cells. Although we succeeded in identifying mouse MAIT cells and studying their features using surrogate marker RORγ-GFP, several other challenges lie ahead. One such issue concerns how reliable the surrogate marker RORγ-GFP is. Downregulation of *Rorc* (RORγt) and reciprocal upregulation of T_H1 factor *Tbx21* (T-bet) has been reported in committed T_H17 cells stimulated by IL-12[118]. This correlated with corresponding downregulation of *Il17a*, and upregulation of *Ifng*[118]. Although others and we observed IFN-γ producing MAIT cells preserved RORγt expression[62], we cannot rule out that MAIT cells may downregulate RORγt under certain conditions. For such reason, RORγ-GFP may not be ideal to label activated MAIT cells. Thus, MR1 tetramers are indeed required for a more reliable identification of MAIT cells in the future work.

Although we have a growing understanding of MAIT cells, a number of important questions are still unsolved. By providing a physiologically relevant mouse model, we hope to facilitate MAIT research.

The development of MAIT cells has been poorly investigated. Microbiota has been implicated in MAIT cells development[11,18,20]. However, the finding of mature MAIT cells from fetus suggests that MAIT cells may undergo developmental maturation prior to the colonization of commensal microbes[54]. What definitive role microbiota plays during MAIT development is still an open question. Like NKT cells, MAIT cells are selected by DP thymocytes and require PLZF during development[64,65]. The endogenous ligand for thymic MAIT selection and to what extent NKT and MAIT cells share developmental program are not known.

MAIT cells have been suggested having the potential to enhance immune responses, whether they play an immunoregulatory role remains to be addressed.

Several studies suggested that MAIT cells might selectively expand and discriminate specific microbial antigens in the context of bacterial infections[76,85]. On the other hand, they respond to innate cytokine stimulation, regardless of the presence of microbial ligands[19,62,80,81,84]. Understanding how MAIT cells are regulated and what features selective antigens have will open up the potential for the designing of MAIT-targeted adjuvant and vaccine.

Given that MAIT cells react to BCG-infected cells *in vitro* and are able to recruit to the infected bladder during urinary tract infection, they may possibly participate in immune responses to intravesical BCG instillation for treating bladder cancer. Understanding whether MAIT cells contribute to BCG immunotherapy will provide a unique opportunity for novel therapeutic intervention.

Acknowledgements

I would like to express my sincere gratitude to the following people who helped me accomplish this study.

My supervisor **Olivier Lantz**, thanks for your guidance and support over the past four years. Thanks for your enthusiasm and valuable discussions on science; being open-minded and encouraging me to develop my own ideas on research.

For our group members, I would like to thank **Katarzyna Franciszkiewicz** for your great company at work and lunch. You are a working partner, a mentor, and a friend. You remind me of my master supervisor. **Ruby Alonso** for sharing all those exciting and disappointing moments during our PhD. Thanks for growing up with me in the scientific world. Bon courage for the last year. **Stanislas Mondot** for teaching me gut microbiology and R though I'm too dumb to understand programming. Thanks for always encouraging me and sharing wonderful stories of Australia. **Yvonne Mburu** for your encouragement and optimistic attitude. Thanks for introducing me to the best French course in Paris. Very good luck in the future. I'll miss your warm smiles. **Aurelie Darbois Delahousse** for always being cheerful. Thanks for your help in processing tissues and of course genotyping. I really enjoy teamwork with you and Kat. **Virginie Premel** for technical support and lab management. Thanks for keeping the lab organized and making the best tiramisu. **Qian Zhou** for teaching me scientific terms in Chinese and sharing funny stories of your former lab. **Marion Salou** for continuation of the project. I hope you will enjoy working on mice.

Our former lab members, I would like to thank **Lionel Le Bourhis** for sharing your enormous knowledge and brilliant ideas. Thanks for your guidance during early years of my PhD. **Natalie Seach** for being a role model as scientist, being knowledgeable, creative, hard-working, and having excellent communication skills. **Claire Soudais** for your help with mouse work. I'm impressed by your exquisite techniques. Thank you for your advices on this project and sharing your sporting spirit with us. **Stephanie Bessoles** for always being warm-hearted and sharing your knowledge of NK cells and baking. **Héloïse Flament** for your support and all the funny talks about cats. **Lucia Guerri** and **Mathilde Dusseaux** for being my first teachers in the lab and

introducing me to the fancy multicolor FACS. **Daphné Laubreton** for your great contribution to the initial work of this project. **Hélène Duret** for your technical assistance and dedication to the automated screening. **Manal Sarkis** for synthesizing all the compounds and always being supportive. We don't see each other very often, but I really like to talk with you. **Christine Sedlik**, **Jordan Denizeau**, and **Philippe De La Rochere** for helpful discussions and technical support on ELISPOT, ELISA, Labchip, and many others. **Clara Young**, **Lucile Fressigne**, **Fatoumata Samassa**, and **Alexandra Kachaner** for all the laughter we shared. Good luck with your MD or PhD studies.

I would like to thank flow cytometry platform staff **Zosia Maciorowski, Annick Viguier,** and **Sophie Grondin** for your valuable advice and assistance in FACS and cell sorting. And **animal facility staff** for taking good care of mice.

I would like to thank my PhD committee tutors, **Nicolas Manel and Kamel Benlagha** for your advices and suggestions on my PhD project. And also to our **collaborators**, especially **Jean-Pierre de Villartay** for your help with TCR sequencing.

I would also like to thank **all the colleagues from unit 932** for your critical comments during labmeeting and all the moments we shared in Institut Curie.

Special thanks to my master supervisor **Jenny Hallgren** for your guidance and encouragement over those memorable years. Thanks for seeing my potential and inspiring me to pursue a career in immunology.

I would also like to thank all the friends and colleagues from Uppsala University. Special thanks to **Joakim Dahlin** for teaching me flow cytometry and other techniques and finishing the project I couldn't complete. Thanks for the "mast" years we shared in Uppsala. Tack så mycket! **Zhoujie Ding** for editing my thesis, being the best (lab+room)mate, and taking good care of Flora.

Finally, I would like to thank **Xiaodong Yang** for IT technical help and being supportive for all these years.

最后，感谢爸爸妈妈一直以来的信任与支持。

References

1. Lanier, L. L. Shades of grey — the blurring view of innate and adaptive immunity. *Nat. Rev. Immunol.* **13,** 73–74 (2013).

2. Magombedze, G., Reddy, P. B. J., Eda, S. & Ganusov, V. V. Cellular and population plasticity of helper CD4+ T cell responses. *Frontiers in Physiology* **4 AUG,** (2013).

3. Walker, J. a, Barlow, J. L. & McKenzie, A. N. J. Innate lymphoid cells - how did we miss them? *Nat. Rev. Immunol.* **13,** 75–87 (2013).

4. Wencker, M. *et al.* Innate-like T cells straddle innate and adaptive immunity by altering antigen-receptor responsiveness. *Nat. Immunol.* **15,** 80–87 (2014).

5. Porcelli, S., Yockey, C. E., Brenner, M. B. & Balk, S. P. Analysis of T cell antigen receptor (TCR) expression by human peripheral blood CD4-8- alpha/beta T cells demonstrates preferential use of several V beta genes and an invariant TCR alpha chain. *J. Exp. Med.* **178,** 1–16 (1993).

6. Lantz, O. & Bendelac, A. An invariant T cell receptor alpha chain is used by a unique subset of major histocompatibility complex class I-specific CD4+ and CD4-8- T cells in mice and humans. *J. Exp. Med.* **180,** 1097–1106 (1994).

7. Tilloy, F. *et al.* An Invariant T Cell Receptor a Chain Defines a Novel TAP-independent Major Histocompatibility Complex Class Ib–restricted a/b T Cell Subpopulation in Mammals. *J. Exp. Med.* **189,** (1999).

8. Dellabona, P., Padovan, E., Casorati, G., Brockhaus, M. & Lanzavecchia, A. An invariant V alpha 24-J alpha Q/V beta 11 T cell receptor is expressed in all individuals by clonally expanded CD4-8- T cells. *J. Exp. Med.* **180,** 1171–1176 (1994).

9. Riegert, P., Wanner, V. & Bahram, S. Genomics, isoforms, expression, and phylogeny of the MHC class I-related MR1 gene. *J. Immunol.* **161,** 4066–4077 (1998).

10. Bendelac, A. *et al.* CD1 recognition by mouse NK1+ T lymphocytes. *Science* **268,** 863–865 (1995).

11. Treiner, E. *et al.* Selection of evolutionarily conserved mucosal-associated invariant T cells by MR1. *Nature* **422,** 164–169 (2003).

12. Gapin, L., Godfrey, D. I. & Rossjohn, J. Natural Killer T cell obsession with self-antigens. *Curr. Opin. Immunol.* **25,** 168–173 (2013).

13. Kinjo, Y., Kitano, N. & Kronenberg, M. The role of invariant natural killer T cells in microbial immunity. *Journal of Infection and Chemotherapy* **19,** 560–570 (2013).

14. Kjer-Nielsen, L. *et al.* MR1 presents microbial vitamin B metabolites to MAIT cells. *Nature* **491,** 717–23 (2012).

15. Corbett, A. J. *et al.* T-cell activation by transitory neo-antigens derived from distinct microbial pathways. *Nature* **509,** 361–5 (2014).

16. Crowe, N. Y. *et al.* Glycolipid antigen drives rapid expansion and sustained cytokine production by NK T cells. *J. Immunol.* **171,** 4020–4027 (2003).

17. Brigl, M. *et al.* Innate and cytokine-driven signals, rather than microbial antigens, dominate in natural killer T cell activation during microbial infection. *J. Exp. Med.* **208,** 1163–77 (2011).

18. Dusseaux, M. *et al.* Human MAIT cells are xenobiotic-resistant, tissue-targeted, CD161hi IL-17-secreting T cells. *Blood* **117,** 1250–9 (2011).

19. Ussher, J. E. *et al.* CD161(++) CD8(+) T cells, including the MAIT cell subset, are specifically activated by IL-12+IL-18 in a TCR-independent manner. *Eur. J. Immunol.* 1–9 (2013). doi:10.1002/eji.201343509

20. Le Bourhis, L. *et al.* Antimicrobial activity of mucosal-associated invariant T cells. *Nat. Immunol.* **11,** 969 (2010).

21. Gold, M. C. *et al.* Human mucosal associated invariant T cells detect bacterially infected cells. *PLoS Biol.* **8,** e1000407 (2010).

22. Kita, H. *et al.* Quantitation and phenotypic analysis of natural killer T cells in primary biliary cirrhosis using a human CD1d tetramer. *Gastroenterology* **123,** 1031–1043 (2002).

23. Chandra, S. & Kronenberg, M. *Activation and Function of iNKT and MAIT Cells*. *Advances in Immunology* **127,** (Elsevier Inc., 2015).

24. Das, R., Sant'Angelo, D. B. & Nichols, K. E. Transcriptional control of invariant NKT cell development. *Immunol. Rev.* **238,** 195–215 (2010).

25. Prodger, J. L. *et al.* Foreskin T-cell subsets differ substantially from blood with respect to HIV co-receptor expression, inflammatory profile, and memory status. *Mucosal Immunology* **5,** 121–128 (2012).

26. Constantinides, M. G. & Bendelac, a. Transcriptional regulation of the NKT cell lineage. *Curr Opin Immunol* **25,** 161–167 (2013).

27. Lee, Y. J., Holzapfel, K. L., Zhu, J., Jameson, S. C. & Hogquist, K. a. Steady-state production of IL-4 modulates immunity in mouse strains and is determined by lineage diversity of iNKT cells. *Nat. Immunol.* **14,** 1146–1154 (2013).

28. Savage, A. K. *et al.* The transcription factor PLZF directs the effector program of the NKT cell lineage. *Immunity* **29,** 391–403 (2008).

29. Watarai, H. *et al.* Development and Function of Invariant Natural Killer T Cells Producing TH2- and TH17-Cytokines. *PLoS Biology* **10,** e1001255 (2012).

30. Doisne, J.-M. *et al.* Skin and peripheral lymph node invariant NKT cells are mainly retinoic acid receptor-related orphan receptor (gamma)t+ and respond preferentially under inflammatory conditions. *J. Immunol.* **183,** 2142–2149 (2009).

31. Cerundolo, V., Silk, J. D., Masri, S. H. & Salio, Mariolina1. Cerundolo V, Silk JD, Masri SH, S. M. H. invariant N. cells in vaccination strategies. N. R. I. (2009) 9:28–38. doi:10. 1038/nri245. Harnessing invariant NKT cells in vaccination strategies. *Nat. Rev. Immunol.* **9,** 28–38 (2009).

32. Holzapfel, K. L., Tyznik, A. J., Kronenberg, M. & Hogquist, K. a. Antigen-dependent versus -independent activation of invariant NKT cells during infection. *J. Immunol.* **192,** 5490–8 (2014).

33. Kawano, T. *et al.* CD1d-restricted and TCR-mediated activation of valpha14 NKT cells by glycosylceramides. *Science* **278,** 1626–1629 (1997).

34. Kinjo, Y. *et al.* Recognition of bacterial glycosphingolipids by natural killer T cells. *Nature* **434,** 520–525 (2005).

35. Sriram, V., Du, W., Gervay-Hague, J. & Brutkiewicz, R. R. Cell wall glycosphingolipids of Sphingomonas paucimobilis are CD1d-specific ligands for NKT cells. *Eur. J. Immunol.* **35,** 1692–1701 (2005).

36. Mattner, J. *et al.* Exogenous and endogenous glycolipid antigens activate NKT cells during microbial infections. *Nature* **434,** 525–529 (2005).

37. Kinjo, Y. *et al.* Natural killer T cells recognize diacylglycerol antigens from pathogenic bacteria. *Nat. Immunol.* **7,** 978–986 (2006).

38. Kinjo, Y. *et al.* Invariant natural killer T cells recognize glycolipids from pathogenic Gram-positive bacteria. **12,** (2011).

39. Fischer, K. *et al.* Mycobacterial phosphatidylinositol mannoside is a natural antigen for CD1d-restricted T cells. *Proc. Natl. Acad. Sci. U. S. A.* **101,** 10685–10690 (2004).

40. Chang, Y. J. *et al.* Influenza infection in suckling mice expands an NKT cell subset that protects against airway hyperreactivity. *J. Clin. Invest.* **121,** 57–69 (2011).

41. Brigl, M., Bry, L., Kent, S. C., Gumperz, J. E. & Brenner, M. B. Mechanism of CD1d-restricted natural killer T cell activation during microbial infection. *Nat. Immunol.* **4,** 1230–1237 (2003).

42. Godfrey, D. I. & Rossjohn, J. New ways to turn on NKT cells. *J. Exp. Med.* **208,** 1121–5 (2011).

43. Kain, L. *et al.* The Identification of the Endogenous Ligands of Natural Killer T Cells Reveals the Presence of Mammalian α-Linked Glycosylceramides. *Immunity* **41,** 543–554 (2014).

44. Leite-De-Moraes, M. C. *et al.* A distinct IL-18-induced pathway to fully activate NK T lymphocytes independently from TCR engagement. *J. Immunol.* **163,** 5871–5876 (1999).

45. Nagarajan, N. A. & Kronenberg, M. Invariant NKT cells amplify the innate immune response to lipopolysaccharide. *J. Immunol.* **178,** 2706–2713 (2007).

46. Smithgall, M. D. *et al.* IL-33 amplifies both Th1- and Th2-type responses through its activity on human basophils, allergen-reactive Th 2 cells, iNKT and NK Cells. *Int. Immunol.* **20,** 1019–1030 (2008).

47. Vahl, J. C. *et al.* NKT Cell-TCR Expression Activates Conventional T Cells in Vivo, but Is Largely Dispensable for Mature NKT Cell Biology. *PLoS Biol.* **11,** (2013).

48. Lepore, M. *et al.* Parallel T-cell cloning and deep sequencing of human MAIT cells reveal stable oligoclonal TCRβ repertoire. *Nat. Commun.* **5,** 3866 (2014).

49. Martin, E. *et al.* Stepwise development of MAIT cells in mouse and human. *PLoS Biol.* **7,** e54 (2009).

50. Reantragoon, R. *et al.* Antigen-loaded MR1 tetramers define T cell receptor heterogeneity in mucosal-associated invariant T cells. **210,** 2305–2320 (2013).

51. Billerbeck, E. *et al.* Analysis of CD161 expression on human CD8+ T cells defines a distinct functional subset with tissue-homing properties. *Proc. Natl. Acad. Sci. U. S. A.* **107,** 3006–11 (2010).

52. Gold, M. C. *et al.* Human thymic MR1-restricted MAIT cells are innate pathogen-reactive effectors that adapt following thymic egress. *Mucosal Immunol.* **6,** 35–44 (2013).

53. Walker, L. J. *et al.* Human MAIT and CD8αα cells develop from a pool of type-17 precommitted CD8+ T cells. *Blood* **119,** 422–33 (2012).

54. Leeansyah, E., Loh, L., Nixon, D. F. & Sandberg, J. K. Acquisition of innate-like microbial reactivity in mucosal tissues during human fetal MAIT-cell development. *Nat. Commun.* **5,** 3143 (2014).

55. Fergusson, J. R. *et al.* CD161 Defines a Transcriptional and Functional Phenotype across Distinct Human T Cell Lineages. *Cell Rep.* **9,** 1075–1088 (2014).

56. Lanier, L. L., Chang, C. & Phillips, J. H. Human NKR-P1A. A disulfide-linked homodimer of the C-type lectin superfamily expressed by a subset of NK and T lymphocytes. *J. Immunol.* **153,** 2417–2428 (1994).

57. Fergusson, J. R., Fleming, V. M. & Klenerman, P. CD161-Expressing Human T Cells. *Front. Immunol.* **2,** 1–7 (2011).

58. Le Bourhis, L. *et al.* MAIT cells detect and efficiently lyse bacterially-infected epithelial cells. *PLoS Pathog.* **9,** e1003681 (2013).

59. Kurioka, a *et al.* MAIT cells are licensed through granzyme exchange to kill bacterially sensitized targets. *Mucosal Immunol.* 1–12 (2014). doi:10.1038/mi.2014.81

60. Sharma, P. K. *et al.* High Expression of CD26 Accurately Identifies Human Bacterial-Reactive MR1-restricted MAIT cells. *Immunology* n/a–n/a (2015). doi:10.1111/imm.12461

61. Tang, X.-Z. *et al.* IL-7 licenses activation of human liver intrasinusoidal mucosal-associated invariant T cells. *J. Immunol.* **190,** 3142–52 (2013).

62. Turtle, C. J. *et al.* Innate signals overcome acquired TCR signaling pathway regulation and govern the fate of human CD161(hi) CD8α^{+} semi-invariant T cells. *Blood* **118,** 2752–62 (2011).

63. Savage, A. K., Constantinides, M. G. & Bendelac, A. Promyelocytic leukemia zinc finger turns on the effector T cell program without requirement for agonist TCR signaling. *J. Immunol.* **186,** 5801–5806 (2011).

64. Seach, N. *et al.* Double positive thymocytes select mucosal-associated invariant T cells. *J. Immunol.* **191,** 6002–9 (2013).

65. Rahimpour, a. *et al.* Identification of phenotypically and functionally heterogeneous mouse mucosal-associated invariant T cells using MR1 tetramers. *J. Exp. Med.* **212,** 1095–1108 (2015).

66. Thomas, S. Y. *et al.* PLZF induces an intravascular surveillance program mediated by long-lived LFA-1-ICAM-1 interactions. *J. Exp. Med.* **208,** 1179–1188 (2011).

67. Ivanov, I. I. *et al.* The orphan nuclear receptor RORgammat directs the differentiation program of proinflammatory IL-17+ T helper cells. *Cell* **126,** 1121–1133 (2006).

68. Sawa, S. *et al.* RORγt+ innate lymphoid cells regulate intestinal homeostasis by integrating negative signals from the symbiotic microbiota. *Nat. Immunol.* **12,** 320–326 (2011).

69. Coquet, J. M. *et al.* Diverse cytokine production by NKT cell subsets and identification of an IL-17–producing CD4−NK1.1− NKT cell population. *Proc. Natl. Acad. Sci. U. S. A.* **105,** 11287–11292 (2008).

70. Narayan, K. *et al.* Intrathymic programming of effector fates in three molecularly distinct γδ T cell subtypes. *Nature Immunology* **13,** 511–518 (2012).

71. Huang, S. *et al.* Evidence for MR1 antigen presentation to mucosal-associated invariant T cells. *J. Biol. Chem.* **280,** 21183–93 (2005).

72. Huang, S. *et al.* MR1 antigen presentation to mucosal-associated invariant T cells was highly conserved in evolution. *Proc. Natl. Acad. Sci. U. S. A.* **106,** 8290–8295 (2009).

73. Reantragoon, R. *et al.* Structural insight into MR1-mediated recognition of the mucosal associated invariant T cell receptor. *J. Exp. Med.* **209,** 761–74 (2012).

74. Soudais, C. *et al.* In Vitro and In Vivo Analysis of the Gram-Negative Bacteria-Derived Riboflavin Precursor Derivatives Activating Mouse MAIT Cells. *J. Immunol.* (2015). doi:10.4049/jimmunol.1403224

75. Eckle, S. B. G. *et al.* A molecular basis underpinning the T cell receptor heterogeneity of mucosal-associated invariant T cells. *J. Exp. Med.* **211,** 1585–1600 (2014).

76. Gold, M. C. *et al.* MR1-restricted MAIT cells display ligand discrimination and pathogen selectivity through distinct T cell receptor usage. *J. Exp. Med.* **211,** 1601–1610 (2014).

77. Kawachi, I., Maldonado, J., Strader, C. & Gilfillan, S. MR1-restricted V alpha 19i mucosal-associated invariant T cells are innate T cells in the gut lamina propria that provide a rapid and diverse cytokine response. *J. Immunol.* **176,** 1618–1627 (2006).

78. Serriari, N. E. *et al.* Innate mucosal-associated invariant T (MAIT) cells are activated in inflammatory bowel diseases. *Clin. Exp. Immunol.* **176,** 266–274 (2014).

79. Georgel, P., Radosavljevic, M., Macquin, C. & Bahram, S. The non-conventional MHC class I MR1 molecule controls infection by Klebsiella pneumoniae in mice. *Mol. Immunol.* **48,** 769–775 (2011).

80. Chua, W.-J. *et al.* Polyclonal MAIT Cells Have Unique Innate Functions in Bacterial Infection. *Infect. Immun.* **80,** 3256–67 (2012).

81. Meierovics, A., Yankelevich, W. C. & Cowley, S. C. MAIT cells are critical for optimal mucosal immune responses during in vivo pulmonary bacterial infection. (2013). doi:10.1073/pnas.1302799110

82. Ussher, J. E., Klenerman, P. & Willberg, C. B. Mucosal-associated invariant T-cells: new players in anti-bacterial immunity. *Front. Immunol.* **5,** 450 (2014).

83. Howson, L. J., Salio, M. & Cerundolo, V. MR1-Restricted Mucosal-Associated Invariant T Cells and Their Activation during Infectious Diseases. *Front. Immunol.* **6,** (2015).

84. Jo, J. *et al.* Toll-Like Receptor 8 Agonist and Bacteria Trigger Potent Activation of Innate Immune Cells in Human Liver. **10,** 1–13 (2014).

85. Jiang, J. *et al.* Mucosal-associated Invariant T-Cell Function Is Modulated by Programmed Death-1 Signaling in Patients with Active Tuberculosis. *Am. J. Respir. Crit. Care Med.* **190,** 329–39 (2014).

86. Smith, D. J., Hill, G. R., Bell, S. C. & Reid, D. W. Reduced Mucosal Associated Invariant T-Cells Are Associated with Increased Disease Severity and Pseudomonas aeruginosa Infection in Cystic Fibrosis. *PLoS One* **9,** e109891 (2014).

87. Leung, D. T. *et al.* Circulating Mucosal Associated Invariant T Cells Are Activated in Vibrio cholerae O1 Infection and Associated with Lipopolysaccharide Antibody Responses. *PLoS Negl. Trop. Dis.* **8,** e3076 (2014).

88. Grimaldi, D. *et al.* Specific MAIT cell behaviour among innate-like T lymphocytes in critically ill patients with severe infections. *Intensive Care Med.* **40,** 192–201 (2014).

89. Cosgrove, C. *et al.* Early and nonreversible decrease of CD161++ /MAIT cells in HIV infection. *Blood* **121,** 951–61 (2013).

90. Leeansyah, E. *et al.* Activation , exhaustion , and persistent decline of the antimicrobial MR1-restricted MAIT-cell population in chronic HIV-1 infection. **121,** 1124–1136 (2015).

91. Fernandez, C. S. *et al.* MAIT cells are depleted early but retain functional cytokine expression in HIV infection. *Immunol. Cell Biol.* 1–12 (2014). doi:10.1038/icb.2014.91

92. Brenchley, J. M. *et al.* Microbial translocation is a cause of systemic immune activation in chronic HIV infection. *Nat. Med.* **12,** 1365–1371 (2006).

93. Illés, Z., Shimamura, M., Newcombe, J., Oka, N. & Yamamura, T. Accumulation of Valpha7.2-Jalpha33 invariant T cells in human autoimmune inflammatory lesions in the nervous system. *Int. Immunol.* **16,** 223–230 (2004).

94. Annibali, V. *et al.* CD161highCD8+T cells bear pathogenetic potential in multiple sclerosis. *Brain* **134,** 542–554 (2011).

95. Miyazaki, Y., Miyake, S., Chiba, A., Lantz, O. & Yamamura, T. Mucosal-associated invariant T cells regulate Th1 response in multiple sclerosis. *Int. Immunol.* **23,** 529–535 (2011).

96. Teunissen, M. B. M. *et al.* The IL-17A-Producing CD8(+) T Cell Population in Psoriatic Lesional Skin Comprises Mucosa-Associated Invariant T cells and Conventional T Cells. *J. Invest. Dermatol.* **00,** 1–10 (2014).

97. Hinks, T. S. C. *et al.* Innate and adaptive T cells in asthmatic patients: Relationship to severity and disease mechanisms. *J. Allergy Clin. Immunol.* 323–333 (2015). doi:10.1016/j.jaci.2015.01.014

98. Harms, R. Z., Lorenzo, K. M., Corley, K. P., Cabrera, M. S. & Sarvetnick, N. E. Altered CD161bright CD8+ Mucosal Associated Invariant T (MAIT)-Like Cell Dynamics and Increased Differentiation States among Juvenile Type 1 Diabetics. *PLoS One* **10,** e0117335 (2015).

99. Magalhaes, I. *et al.* Mucosal-associated invariant T cell alterations in obese and type 2 diabetic patients. **125,** 1–11 (2015).

100. Cho, Y.-N. *et al.* Mucosal-Associated Invariant T Cell Deficiency in Systemic Lupus Erythematosus. *J. Immunol.* **193,** 3891–3901 (2014).

101. Peterfalvi, A. *et al.* Invariant Vα7.2-Jα33 TCR is expressed in human kidney and brain tumors indicating infiltration by mucosal-associated invariant T (MAIT) cells. *Int. Immunol.* **20,** 1517–1525 (2008).

102. Gunter, C. & Dhand, R. Human biology by proxy. *Nature* **420,** 509–509 (2002).

103. Assessing the status of human immunology. *Nat. Immunol.* **9,** 569 (2008).

104. Mestas, J. & Hughes, C. C. W. Of Mice and Not Men: Differences between Mouse and Human Immunology. *J. Immunol.* **172,** 2731–2738 (2004).

105. Frazer, K. a *et al.* A sequence-based variation map of 8.27 million SNPs in inbred mouse strains. *Nature* **448,** 1050–1053 (2007).

106. Croxford, J. L., Miyake, S., Huang, Y.-Y., Shimamura, M. & Yamamura, T. Invariant V(alpha)19i T cells regulate autoimmune inflammation. *Nat. Immunol.* **7,** 987–994 (2006).

107. Chiba, A. *et al.* Mucosal-associated invariant T cells promote inflammation and exacerbate disease in murine models of arthritis. *Arthritis Rheum.* **64,** 153–161 (2012).

108. Davis, R. C. *et al.* A genome-wide set of congenic mouse strains derived from CAST/Ei on a C57BL/6 background. *Genomics* **90,** 306–313 (2007).

109. Estrada-Smith, D. *et al.* Impact of chromosome 2 obesity loci on cardiovascular complications of insulin resistance in LDL receptor-deficient C57BL/6 mice. *Diabetes* **55,** 2265–2271 (2006).

110. Hoag, K. A. *et al.* A quantitative-trait locus controlling peripheral B-cell deficiency maps to mouse chromosome 15. *Immunogenetics* **51,** 924–929 (2000).

111. Ikeda, A. *et al.* Microtubule-associated protein 1A is a modifier of tubby hearing (moth1). *Nat. Genet.* **30,** 401–405 (2002).

112. Omura, T. *et al.* Robust Axonal Regeneration Occurs in the Injured CAST/Ei Mouse CNS. *Neuron* 1215–1227 (2015). doi:10.1016/j.neuron.2015.05.005

113. Kile, B. T. & Hilton, D. J. The art and design of genetic screens: mouse. *Nat. Rev. Genet.* **6,** 557–567 (2005).

114. Lochner, M. *et al.* In vivo equilibrium of proinflammatory IL-17+ and regulatory IL-10+ Foxp3+ RORγt+ T cells. *J. Exp. Med.* **205,** 1381–1393 (2008).

115. Terrence, K., Pavlovich, C. P., Matechak, E. O. & Fowlkes, B. J. Premature expression of T cell receptor (TCR)alphabeta suppresses TCRgammadelta gene rearrangement but permits development of gammadelta lineage T cells. *J. Exp. Med.* **192,** 537–548 (2000).

116. Hooper, L. V., Littman, D. R. & Macpherson, a. J. Interactions Between the Microbiota and the Immune System. *Science (80-.).* **336,** 1268–1273 (2012).

117. Germanov, E. *et al.* Critical role for the chemokine receptor CXCR6 in homeostasis and activation of CD1d-restricted NKT cells. *J. Immunol.* **181,** 81–91 (2008).

118. Lee, Y. K. *et al.* Late Developmental Plasticity in the T Helper 17 Lineage. *Immunity* **30,** 92–107 (2009).

Appendix

Double Positive Thymocytes Select Mucosal-Associated Invariant T Cells

Natalie Seach,*[,1,2] Lucia Guerri,*[,2,3] Lionel Le Bourhis,* Yvonne Mburu,* Yue Cui,* Stéphanie Bessoles,* Claire Soudais,* and Olivier Lantz*,[†]

**INSERM U932, Institut Curie, Paris 75005, France*
†Laboratoire d'Immunologie Clinique, Centre d'Investigation Clinique Biothérapie 507, Institut Gustave- Roussy/Institut Curie, 75005 Paris, France
[1]Current address: Department of Anatomy and Developmental Biology, Monash University, Melbourne, VIC, Australia.
[2]N.S. and L.G. contributed equally to this work.
[3]Current address: Department of Developmental Immunology, Max Planck Institute of Immunobiology and Epigenetics, Freiburg, Germany.

Address correspondence and reprint requests to
Dr. Olivier Lantz,
Laboratoire d'Immunologie Clinique and INSERM U932,
Institut Curie, 26 Rue d'Ulm, 75005 Paris, France.
E-mail address: olivier.lantz@curie.fr

J Immunol 2013; 191:6002-6009; Prepublished online 15 November 2013; doi: 10.4049/jimmunol.1301212

Double Positive Thymocytes Select Mucosal-Associated Invariant T Cells

Natalie Seach,*[,1,2] Lucia Guerri,*[,2,3] Lionel Le Bourhis,* Yvonne Mburu,* Yue Cui,* Stéphanie Bessoles,* Claire Soudais,* and Olivier Lantz*[,†]

NKT and mucosal-associated invariant T (MAIT) cells express semi-invariant TCR and restriction by nonclassical MHC class Ib molecules. Despite common features, the respective development of NKT and MAIT subsets is distinct. NKTs proliferate extensively and acquire effector properties prior to thymic export. MAIT cells exit the thymus as naive cells and acquire an effector/memory phenotype in a process requiring both commensal flora and B cells. During thymic development, NKTs are selected by CD1d-expressing cortical thymocytes; however, the hematopoietic cell type responsible for MAIT cell selection remains unresolved. Using reaggregated thymic organ culture and bone marrow chimeras, we demonstrate that positive selection of mouse iVα19 transgenic and Vβ6 transgenic MAIT cell progenitors requires MHC-related 1–expressing $CD4^+CD8^+$ double positive thymocytes, whereas thymic B cells, macrophages, and dendritic cell subsets are dispensable. Preincubation of double positive thymocytes with exogenous bacterial ligand increases MHC-related 1 surface expression and enhances mature MAIT cell activation in the in vitro cocultures. The revelation of a common cell type for the selection of both NKT and MAIT subsets raises questions about the mechanisms underlying acquisition of their specific features. ***The Journal of Immunology*****, 2013, 191: 6002–6009.**

Lymphocytes restricted by nonclassical MHC class Ib (MHC-Ib) molecules exhibit unique features of both innate and adaptive immunity (1). Only two subpopulations of innate-like T lymphocytes display conservation between species of both TCR and their respective MHC-Ib–restricting element: the CD1d-restricted NKT and the more recently defined MHC-related 1 (MR1)–restricted mucosal-associated invariant T cell (MAIT) (2, 3).

MAIT cells are defined by expression of a semi-invariant TCR consisting of a canonical iVα7.2-Jα33 iTCRα-chain in humans (iVα19-Jα33 in mice) associated with a limited set of Vβ segments (Vβ2, 13, 22 in humans and Vβ6, 8 in mice) (4). Indicative of strong selective pressure, both the MAIT iTCR and its restriction partner, MR1, are highly conserved between species (4, 5)

MAIT are double negative (DN) and $CD8\alpha\beta^{int}$ or CD8αα in humans and are abundant in the human blood (1–8% of T cells) and liver (20–50%) but are rare (0.03–0.1%) in conventional mouse strains (4, 6, 7). In contrast, NKTs are abundant in laboratory mice but constitute less than 1% of human blood T cells (3). NKT cells recognize glycolipids presented by CD1d (8), whereas human MAIT cells were recently shown to react against metabolites of the riboflavin (vitamin B2) biosynthetic pathway (9). These riboflavin metabolites represent a novel class of Ag, whose distribution among microorganisms is consistent with the broad anti-microbial reactivity of MAIT cells to bacteria and yeast, but not virus (10, 11). MAIT cells may regulate intestinal microbiota or protect against specific bacterial infection (12).

Both NKT and MAIT cells require a functional thymus for selection (4, 13). However, although similarities exist, their developmental pathways are distinct. NKT cells are selected, and expand and acquire their effector/memory phenotype in the thymus, whereas MAIT cells exhibit minimal intrathymic proliferation and display a naive phenotype in both human thymus and cord blood (6, 7, 14).

Human MAIT cells express high levels of the C-type lectin CD161 as well as the IL-18R in cord blood, indicative that their specific differentiation program is already set in the thymus (6, 7, 15). Following thymic egress, MAIT cells undergo extensive clonal expansion and acquire their effector/memory phenotype in a process dependent upon both B cells and the commensal flora (2, 7, 15). In addition to IFN-γ, human MAIT cells secrete IL-17, consistent with their uniform expression of the retinoic acid–related orphan receptor γt isoform (6). Interestingly, both human NKT and MAIT cells express the transcription factor ZBTB16 early in ontogeny, indicating at least a partial overlap in their initial developmental programming (15, 16).

The nature of the thymic selecting cell plays an important role in determining conventional T, NKT, or MAIT cell differentiation

*INSERM U932, Institut Curie, Paris 75005, France; and †Laboratoire d'Immunologie Clinique, Centre d'Investigation Clinique Biothérapie 507, Institut Gustave-Roussy/Institut Curie, 75005 Paris, France

[1]Current address: Department of Anatomy and Developmental Biology, Monash University, Melbourne, VIC, Australia.

[2]N.S. and L.G. contributed equally to this work.

[3]Current address: Department of Developmental Immunology, Max Planck Institute of Immunobiology and Epigenetics, Freiburg, Germany.

Received for publication May 7, 2013. Accepted for publication October 16, 2013.

This work was supported by INSERM, Institut Curie, Agence Nationale de la Recherche (Blanc and Labex Project Biologie des Cellules Dendritique) and Fondation Aupetit. O.L.'s group was funded through the label "Equipe Labellisée de la Ligue Contre le Cancer." L.G. was funded by the Fondation Association pour la Recherche sur le Cancer and the Fondation pour la Recherche Médicale. L.L.B. received a fellowship from the European Molecular Biology Organization. Y.M. is supported by the Cancer Research Institute/Irvington Lloyd J. Old Fellowship in Tumor Immunology. S.B. is supported by the Fondation de la Recherche Médicale.

Address correspondence and reprint requests to Dr. Olivier Lantz, Laboratoire d'Immunologie Clinique and INSERM U932, Institut Curie, 26 Rue d'Ulm, 75005 Paris, France. E-mail address: olivier.lantz@curie.fr

The online version of this article contains supplemental material.

Abbreviations used in this article: BM, bone marrow; BMT, BM transplantation; DC, dendritic cell; DN, double negative; DP, double positive; HC, hematopoietic cell; hTSC, hematopoietic thymic stromal cell; Macs, macrophage; MAIT, mucosal-associated invariant T cell; MHC-Ib, MHC class Ib; MLN, mesenteric lymph node; MR1, MHC-related 1; RTOC, reaggregated thymic organ culture; SAP, signaling lymphocyte activation molecule–associated protein; SLAM, signaling lymphocyte activation molecule; SP, single positive; Tg, transgenic; TN, triple negative; TSC, thymic stromal cell; wt, wild-type.

www.jimmunol.org/cgi/doi/10.4049/jimmunol.1301212

programs. Indeed, conventional αβT cell development stems from interactions with classical MHC/peptide complexes presented by thymic epithelium, whereas the expression of MHC-Ib molecules by hematopoietic elements likely leads to the intrinsic effector function of "innate-like" T cell subsets (1, 17, 18). Indeed, hematopoietic cells (HCs) select the majority of T cells restricted by MHC-Ib molecules: H2-M3–restricted (19), NKT (13), and MAIT cells (2). NKTs are selected exclusively by $CD4^+CD8^+$ double positive (DP) thymocytes (20). H2-M3–restricted T cells can be selected upon both epithelium and HCs; however, the latter imparts enhanced effector functions dependent upon signaling lymphocyte activation molecule (SLAM)–associated protein (SAP) transduction (18).

The identity of the HC type responsible for MAIT cell selection remains unresolved (2, 20). Initial bone marrow (BM) chimera studies found normal levels of Vα19-Jα33 transcript in the mesenteric lymph nodes (MLNs) of mice when MHC-I expression was confined to $CD3\varepsilon^{-/-}$ donor BM. These findings suggested that MR1 expression by T cells, in contrast to NKT cells, was not required for intrathymic MAIT cell selection and that other thymic HCs were likely involved. Aside from the abundant epithelial and mesenchymal components, the thymic stroma consists of rare HC types, including dendritic cells (DCs), macrophages (Macs), and B cells (21). Subsequent studies have demonstrated that MAIT cells develop normally in fetal thymic organ cultures in the absence of B cells and exogenous microbial ligand, indicating a nonrequirement for these components (7).

The virtual absence of detectable MR1 surface expression on primary cells has hampered efforts to identify the cell type(s) involved in the intrathymic selection of MAIT cells. Recently, increased intracellular expression of MR1 has been reported for DP thymocytes, which, alongside Macs and DC, could stimulate MAIT cell hybridomas in the presence of a stabilizing MR1 Ab (22). Despite these potential candidates, the cell type(s) responsible for MAIT cell selection remains elusive. This issue is important, as the array of secreted and surface molecules available for cell–cell interaction differs across the cell lineages and likely imparts unique signals in the specification of T cell phenotype and function. To identify the HC type(s) implicated in MAIT cell development, we used reaggregated thymic organ culture (RTOC) and bone marrow transplantation (BMT) assays to assess the requirement of specific thymic components in the selection process.

Materials and Methods

Mice

C57BL/6 mice were obtained from Charles River Laboratories animal facility, Labresles France. $TAP^{-/-}$ $Ii^{-/-}$ Vβ6 transgenic (Tg) $MR1^{+/-}$ (and $MR1^{-/-}$), iVα19 Tg $Ca^{-/-}$ $MR1^{+/-}$ (and $MR1^{-/-}$), $RAG2^{-/-}MR1^{+/-}$ (and $MR1^{-/-}$), and $CD3\varepsilon^{-/-}$ mice have been previously described elsewhere (7) and were maintained under specific pathogen–free conditions at the central animal facility, Institut Curie, Paris, France. BM from $TCR\alpha^{-/-}$ mice was kindly provided by A. Lehuen (INSERM U986, Paris). All animal experiments were performed in accordance with the guidelines of the French Veterinary Department in an accredited mouse facility.

Time matings

Overnight matings for 2 consecutive days were set up between $TAP^{-/-}Ii^{-/-}$ Vβ6 Tg $MR1^{-/-}$ mating pairs. Pregnant females were sacrificed between days E14and E16 to harvest embryos. Approximately 6–10 pregnant mice were used per RTOC experiment.

Anti-CD3 Ab treatment of $RAG^{-/-}$ mice

Adult $RAG^{-/-}MR1^{+/-}$ (and $MR1^{-/-}$) mice were injected i.p. with 200 μg anti-mouse CD3 (145-2C11) (eBioscience) to induce DP thymocytes (23). Mice were sacrificed at day 8 post injection, and the thymus was analyzed for development of DP thymocytes and subsequent use in the RTOC assay.

RTOC

E14-E16 $TAP^{-/-}Ii^{-/-}$ Vβ6 Tg $MR1^{-/-}$ thymic lobes were isolated as previously described (24). Pooled lobes were digested in 1 ml RPMI 1640 containing 0.5 (Wünsch) units/ml Liberase (Roche) and 0.02% (w/v) DNase I at 37°C for 30 min. Embryonic digest was incubated with anti-CD45 microbeads and separated using the AutoMACS Separator (Miltenyi Biotec) to enrich for stromal cells, which were resuspended in RTOC media: DMEM GlutaMAX 10% FCS, 100 U/ml penicillin, 100 mg/ml streptomycin, 50 mM 2-ME, 10 mM HEPES, 1 mM nonessential amino acids, and 1 mM sodium pyruvate (all from Life Technologies).

The iVα19 Tg thymocyte progenitors were prepared from pools of day 3–5 neonatal thymus from $CD45.2^+$ iVα19 Tg $Ca^{-/-}MR1^{-/-}$ mice. Vβ6 Tg fetal thymocytes were obtained from $CD45.2^+$ $TAP^{-/-}Ii^{-/-}$ Vβ6 Tg $MR1^{-/-}$ E14–E16 embryos. A total of 5×10^5 iVα19 or Vβ6 Tg thymocytes were mixed with 4×10^5 supporting thymic stromal cells (TSCs) from $TAP^{-/-}$ $Ii^{-/-}MR1^{-/-}$ embryos. RTOCs were complemented with 2.5×10^5 purified $CD45.1^+$ thymocytes or candidate $CD45.1^+$ hematopoietic TSC (hTSC) subsets (Supplemental Fig. 1). Total cell mixture was delivered with a 10-μl pipette tip as a standing drop onto a Millipore filter (0.8-mm pore size, 13-mm diameter) resting on the surface of 2.5 ml RTOC media in 60-mm petri dishes and incubated at 37°C with 5% CO_2. A culture period of 6 and 9 d, respectively, was required for optimal maturation of iVα19 Tg and Vβ6 Tg thymocytes in the RTOC system (data not shown). Following incubation, RTOCs were digested with Col/DNAse to release thymocytes and were stained with surface Abs to assess Tg MAIT cell development.

Immunostaining and flow cytometric analysis

All cell samples were incubated with anti-FcR supernatant (clone 2.4G2) prior to Ab staining. The following anti-mouse fluorochrome or biotin-conjugated Abs were purchased from eBioscience, BD Pharmingen, and BioLegend unless otherwise stated: CD11b (clone M1/70), CD11c (N418), CD19 (1D3), CD25 (PC61.5) CD4 (LT34), CD44 (IM-7) CD45.2 (104), CD8α (Ly-2), CD90.1 (HIS51), CD90.2 (30-H12), EpCAM (G8.8), F4/80 (BM8), HSA (M1/69), TCRb (H57-597), Vb6 (RR4-7), Vb8 (F23.1), CD69 (clone [^{1}H].2F3), CD44 (IM7). Cells were acquired with an LSR2 cytometer (Becton-Dickinson), using DAPI to exclude dead cells, and were analyzed using FlowJo software v9.4.11 (TreeStar).

Cell preparation and separation of adult thymus subsets

The hTSC subsets (DCs, B cells, and Macs) and thymocyte subsets were purified from adult $CD45.1^+$ B6 ($MR1^{wt/wt}$) mice. For hTSC subsets, pools of four to five thymuses were enzymatically digested, as previously described (21). To enrich for hTSC subsets, cells were incubated with anti-CD5 microbeads to deplete thymocytes and run through an AutoMACS Separator. Enriched hTSC subsets were immunolabeled and separated according to defined antigenic surface expression [(25), Supplemental Fig. 1] using a FACSAria III cell sorter (BD Biosciences). Whole thymocytes were purified based on positive expression of CD90. DN, DP, and single positive (SP) thymocyte subsets were purified using anti-CD4 and anti-CD8 Abs. DN cells were further gated negative for lineage expression (CD19, F4/80, CD11c, CD11b) to avoid contamination with non–T cells. Thymic epithelium was purified from digested tissue on the basis of negative CD45 and positive EpCAM expression (21). Thymic subsets were collected in 50% FBS in RPMI 1640. Following the sort, subsets were resuspended in RTOC media, enumerated, and stored on ice until further use.

BM transplantation

Groups of four to five adult $RAG^{-/-}MR1^{-/-}$ hosts were irradiated (900 cGy) and reconstituted with 10×10^6 donor BM cells prepared from $CD45.2^+$ Vα19 Tg $MR1^{-/-}$ mice either alone or in combination with BM from B6 $CD45.1^+$, $RAG^{-/-}$, $TCR\alpha^{-/-}$, or $CD3\varepsilon^{-/-}$ mice [all $MR1^{wt/wt}$ (wt, wild type)]. The thymus and MLNs from transplanted mice were harvested at 8 wk post BMT and assessed for iVα19 Tg T cell development.

Bacterial ligand preparation and stimulation assay

The preparation of the bacterial supernatant will be described elsewhere (C. Soudais and O. Lantz, manuscript in preparation). Briefly, *Escherichia coli* were grown to saturation. Supernatant was collected, filtered, biochemically processed before being aliquoted, and lyophilized for further use. One arbitrary unit corresponds to 25 μl bacterial supernatant. Whole splenocytes from iVα19 Tg $Ca^{-/-}$ $MR1^{+/-}$ or BM chimeric mice were depleted of APCs and $CD4^+$ T cells. A total of 2.5×10^5 purified DN, DP, and SP thymocyte subsets from $MR1^{+/+}$ and $MR1^{-/-}$ mice or 2.5×10^5 purified splenic APCs from $MR1^{+/+}$ mice were preincubated with serial dilutions of semipurified bacterial ligand for 30 min before adding 2.5 ×

10^5 iVα19 Tg responder cells. After an 18-h coculture, cell activation was monitored by cytometry analysis.

MR1 surface staining

Purified DP thymocytes from $MR1^{+/+}$ and $MR1^{-/-}$ mice were incubated for 4 h in RTOC medium ± 4 arbitrary units of purified bacterial ligand (*E. coli*). Following incubation, $MR1^+$ and $MR1^-$ cells were stained with anti-MR1 Ab (clone 26.5) (26). Primary Abs were detected with $F(ab')_2$ fragment goat anti-mouse IgG–PE conjugate (Jackson ImmunoResearch Laboratories).

Quantitative PCR for MR1 expression

RNA isolation was performed on purified adult thymocyte (DN, DP, and SP) subsets and total thymic epithelium, using the RNAqueous-Micro Kit. After reverse transcription, quantitation of MR1 and GAPDH cDNA was performed using Assays-on-Demand primers provided by Applied Biosystems. MR1 expression was normalized to GAPDH content, using the ΔΔct method.

Statistical analysis

Statistical analysis was performed using the nonparametric Mann–Whitney *U* test. In Figs. 1E, 1F, 2D, and 2E, fold expansion refers to the number of mature Vβ6 T cells in each RTOC of the experimental groups, compared with the average of the ones measured in the control group.

Results

Thymocytes mediate selection of MAIT cells in RTOC

To determine the cell type responsible for intrathymic MAIT cell selection, we employed RTOC techniques, which enable the in vitro differentiation of T cell progenitors in the presence of defined stromal and hematopoietic elements (27). As MAIT cells are rare in laboratory mice, reliable detection in the thymus is difficult. We took advantage of two well-characterized Tg mouse models expressing an invariant Vα19-Jα33 TCRα-chain (iVα19 Tg) or Vβ6 Tg TCRβ-chain from a MAIT hybridoma (4, 7). Vβ6 and Vβ8 segments are overexpressed in iVα19 Tg $C\alpha^{-/-}$ mice (hereafter iVα19 Tg) in an MR1-dependent manner, whereas an MR1-dependent increase in iVα19-Jα33 chain use is found in Vβ6 Tg mice and reflects MAIT cell selection (7). RTOC relies on embryonic TSCs, which reorganize to form a three-dimensional microenvironment capable of supporting T cell development and maturation in vitro (27). To further increase MAIT cell frequency, we used stroma from $TAP^{-/-}Ii^{-/-}$ mice, as the absence of classical MHC molecules decreases mainstream T cell selection (7).

To assess selection of iVα19 Tg T cell progenitors, whole thymocytes were isolated from neonatal $CD45.2^+$ iVα19 Tg $C\alpha^{-/-}$ $MR1^{-/-}$ mice and mixed with supporting TSCs from $TAP^{-/-}Ii^{-/-}$ $MR1^{-/-}$ embryos. Candidate $CD45.1^+MR1^+$-selecting cells were isolated from adult thymus tissue, as outlined in Supplemental Fig. 1. Purified $CD45.1^+$ $Thy1^+$ adult thymocytes were added to RTOC at a ratio of 1:1 with iVa19 Tg progenitors. The hTSC subsets, including DCs, Macs, and B cells, were seeded into RTOCs according to their original representation within adult thymus, and adjusted for cell death and potential loss during preparation (Supplemental Fig. 1). As a positive control, whole $CD45.1^+$ $MR1^+$ thymus suspension was added to RTOC in which all potential thymus-selecting cell types are present.

Following incubation, RTOCs were analyzed by flow cytometry for Tg T cell development, as described in Fig. 1A: Significant maturation of iVα19 Tg T cells was consistently observed, as indicated by the development of a prominent $TCR\beta^{high}HSA^{low}$ subset (panel Aiii). Mature Tg thymocytes were mostly DN or $CD8^+$ (panel Aiv) with little $CD4^+$ T cell development as observed in iVα19 Tg mice (7). The proportion of $V\beta8^+$ cells (Fig. 1B) in both mature DN and CD8 subsets was determined for control (panel Bi) and test RTOCs (panel Bii) as a readout for MAIT cell selection.

The baseline use of Vβ8 segments by iVα19 Tg thymocytes was ~ 23% for both DN (Fig. 1C) and CD8 (Fig. 1D) subsets in control RTOCs, which did not contain any MR1-sufficient cells. In contrast, addition of $MR1^+$ whole adult thymus suspension increased the Vβ8 proportion within both mature DN and CD8 Tg subsets, indicating the presence of a selecting cell type within adult thymic tissue. In line with previous data, the addition of $MR1^+$ B cells did not affect MAIT cell development (7). However, purified $MR1^+$ thymocytes readily induced Vβ8 bias, at a level similar to that seen with whole thymus cells. In contrast, purified $MR1^+$ DCs and Macs did not induce a Vβ8 bias in either DN (Fig. 1C) or CD8 (Fig. 1D) iVα19 Tg thymocyte subsets.

To verify that iVα19 Tg MAIT progenitors had undergone proper thymic selection, as opposed to aberrant activation/expansion of mature thymocyte subsets, iVα19 Tg RTOCs were complemented with $CD45.1^+$ $MR1^+$ adult thymocytes, as previously described and analyzed for phenotypic markers of thymocyte development. In line with positive selection (28), upregulation of the early activation marker CD69 was observed on a fraction of $TCR\beta^{hi}$ $CD4^+$ $CD8^+$ DP thymocytes and mature $Vb8^+$ iVα19 Tg thymocytes following 6 d of RTOC culture (Supplemental Fig. 2A). Analysis of the activation/memory markers CD25/CD44 on mature $DN/CD8^+$ iVα19 Tg thymocytes revealed that a small proportion of $Vb8^+$ thymocytes expressed CD44 but did not express CD25 (Supplemental. Fig. 2C, 2D). Importantly, the proportion of $Vb8^+CD44^+$ or $Vb8^+CD25^+$ iVα19 Tg thymocytes did not increase following complementation with $MR1^+$ thymocytes, arguing against confounding activation/expansion (Supplemental Fig. 2D). Taken together, our data demonstrate that $MR1^+$ thymocytes, but not other HC cell types, can mediate the efficient selection and maturation of iVα19 Tg MAIT cells in our in vitro RTOC system.

Forced expression of Tg TCRα-chains can modify T cell ontogeny (29) We therefore assessed the selection of Vβ6 Tg MAIT cell progenitors in the RTOC system. Whole Vβ6 Tg thymocytes from E15 Vβ6 Tg $TAP^{-/-}Ii^{-/-}MR1^{-/-}$ fetal thymus were reaggregated with supporting stroma plus or minus candidate $CD45.1^+$ $MR1^+$–selecting cells. MAIT cell development was assessed as in Fig. 1A. In the absence of MR1, we observed little maturation of Vβ6 Tg fetal thymocyte progenitors, as demonstrated by the small number of $V\beta6^+$ events in mature Tg thymocyte subsets from control RTOCs (Fig. 1B*iii*). However, a clear expansion of mature $V\beta6^+$ thymocytes was observed in both DN and CD8 subsets (Fig. 1B*iv*), upon the addition of whole $MR1^+$ thymus as well as purified $MR1^+$ thymocytes (Fig. 1E, 1F). In line with the development of iVα19 Tg thymocytes, Vβ6 Tg thymocytes upregulated CD69 and retained a predominantly naive phenotype upon maturation in RTOC, indicative of proper thymic selection (Supplemental Fig. 2). Notably, $MR1^+$ thymic B cells, DCs, or Macs did not induce $V\beta6^+$ Tg thymocyte development above that of control levels, indicating a specific role for $MR1^+$ thymocytes in MAIT cell selection (Fig. 1E, 1F).

DP thymocytes govern MAIT cell development

αβT cell development occurs in an ordered fashion. $CD3^-CD4^-$ $CD8^-$ triple negative (TN) immature thymocytes develop into $CD4^+CD8^+$ (DP) before positive selection and maturation into $CD4^+$ or $CD8^+$ SP subsets. Whole $MR1^+$ thymocytes were shown to mediate selection of both iVα19 and Vβ6 Tg progenitors. To assess the capacity of discrete thymocyte subsets to select MAIT cells, we used RAG-deficient mice in which thymocyte development is arrested at the early TN3 stage. Injection of anti-CD3 Abs into these mice induces differentiation into DP, but not SP, thymocyte subsets [Fig. 2A, (23)]. Cells from the $RAG^{-/-}$ thymus were incapable of mediating MAIT cell selection, as shown by the absence of Vβ8 bias (Fig 2B, 2C) or Vβ6 T cell expansion (Fig.

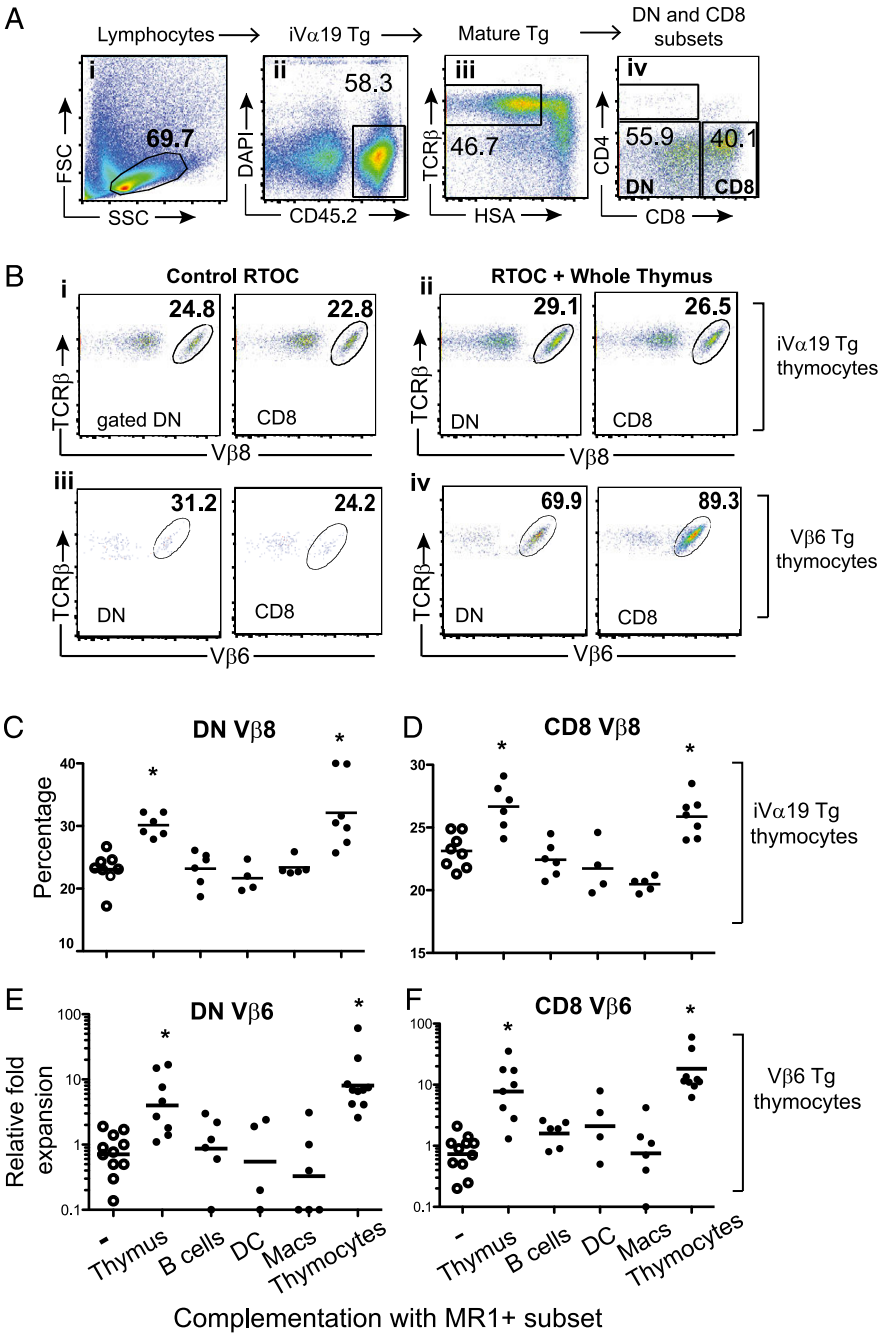

FIGURE 1. Thymocytes mediate MAIT cell selection in RTOC. iVα19 or Vβ6 Tg MR1$^-$ thymocytes were re-aggregated with TAP$^-$Ii$^-$MR1$^-$ thymic stroma without (control RTOC) or with the indicated MR1$^+$ cells and analyzed 6 and 9 d later for iVα19 or Vβ6 inocula, respectively. (**A**) Gating strategy: (**Ai**) Lymphocytes gated on forward/side scatters, (**Aii**) Live CD45.2$^+$ iVα19 Tg thymocytes, (**Aiii**) TCRβ^{hi}HSA^{lo} mature thymocytes, and (**Aiv**) Mature, DN and CD8 subsets. (**B**) Representative dot plots of DN and CD8 subsets from iVα19 (**Bi**, **Bii**) and Vβ6 Tg thymocytes (**Biii**, **Biv**). Vβ8 use (**C**, **D**) and Vβ6 fold expansion (**E**, **F**) in RTOCs without (−) or with complementation by the indicated MR1$^+$ subset (see *Materials and Methods* for the computation). FACS plots are representative, n = 8–10. Each dot represents an individual RTOC pooled from > 10 individual experiments. *$p < 0.05$ compared with control RTOCs.

2D, 2E) in DN and CD8$^+$ subsets from respective iVα19 and Vβ6 Tg RTOCs. Importantly, in addition to early thymocyte subsets, the RAG$^{-/-}$ thymus contains significant numbers of DCs and Macs, further supporting the idea that these hTSC subsets do not participate in early MAIT cell selection events. In contrast, the addition of thymocytes from RAG$^{-/-}$ MR1$^{+/-}$ mice, in which DPs had been induced via anti-CD3 stimulation, robustly induced MAIT cell selection in both iVα19 Tg (Fig. 2B, 2C) and Vβ6 Tg (Fig. 2D, 2E) RTOC systems. Importantly, the ability of DP to select MAIT cells was strictly dependent upon the presence of MR1, as thymocytes from anti-CD3–treated RAG$^{-/-}$ MR1$^{-/-}$ mice were incapable of inducing MAIT cell selection (Fig. 2). Notably, the capacity of DP thymocytes to select MAIT cells appeared to be strictly temporally regulated, as the addition of purified mature MR1$^+$ SP thymocytes did not allow for MAIT cell selection (Fig. 2B–E).

The singular ability of DP thymocytes to select MAIT cells is reminiscent of NKT cell development (13, 20). However, in contrast to CD1d, MR1 is undetectable on the surface of DP thymocytes (13, 22). Of interest, MR1 mRNA levels were 25 fold higher in DP thymocytes than in DN, SP, or thymic epithelium (Supplemental Fig. 3). This finding is consistent with previous reports that demonstrated increased intracellular expression of MR1 protein in the DP subset and indicates that DP thymocytes are primed for MAIT cell selection (22). Thus, similar to NKT cells, DP thymocytes appear to play a unique and nonredundant role in the selection of MAIT cells, whereas other hematopoietic elements are dispensable.

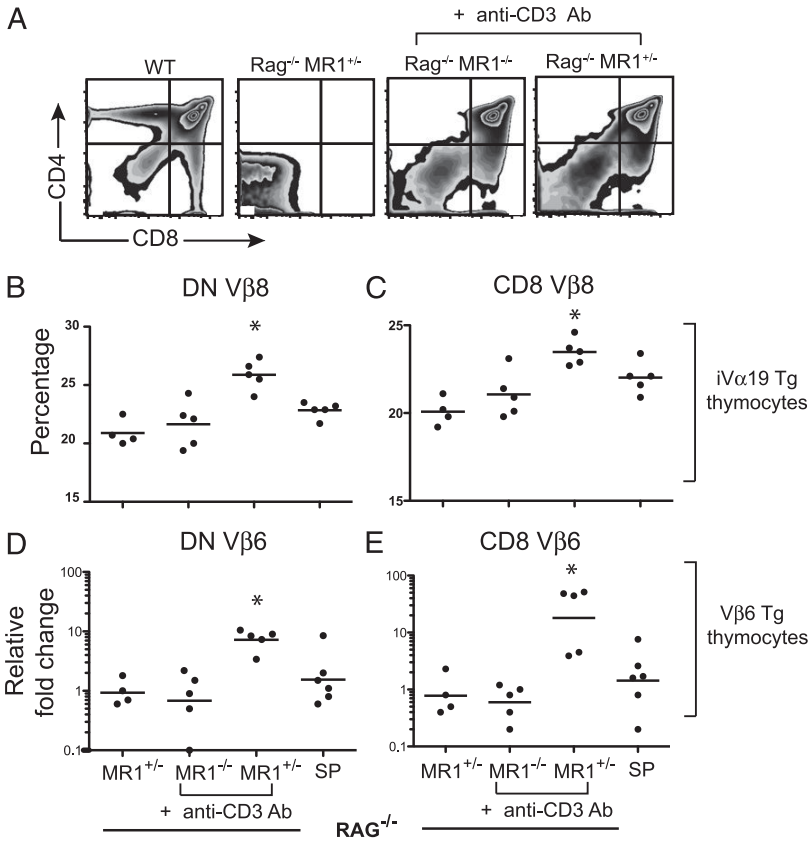

FIGURE 2. DP thymocytes regulate intrathymic MAIT cell development. RTOCs were performed as in Fig. 1 and complemented with whole thymus from the indicated RAG$^{-/-}$ mice or TCRb^{hi} SPs from wt mice. (**A**) Injection of anti-CD3 Ab generates DP thymocytes in RAG$^{-/-}$ mice. Vβ8 use (**B**, **C**) and Vβ6 fold expansion (**D**, **E**) in RTOCs without (−) or with complementation by the indicated cells. FACS plots are representative ($n = 5$). Each dot represents an individual RTOC pooled from two to three separate experiments. *$p < 0.05$ compared with cells from untreated RAG mice.

DP thymocytes regulate in vivo MAIT cell development

To assess the development of MAIT cells in vivo, we generated BM chimeras in which MR1 expression was restricted to defined thymic cell types. Adult RAG$^{-/-}$MR1$^{-/-}$ hosts were irradiated and reconstituted with donor BM from CD45.2$^+$ iVα19 Tg MR1$^{-/-}$ mice, as a source of MAIT cell progenitors, either alone or complemented with BM from MR1$^+$ CD45.1$^+$ wt or T/B cell-deficient mice. In this setting, iVα19 Tg MR1$^{-/-}$ thymic progenitors encounter MR1 expressed by all hematopoietic lineages when administered with wt BM, whereas MR1 expression is restricted to TN and DP thymocyte subsets when administered with CD3$^{-/-}$ and TCRα$^{-/-}$ donor BM, respectively. Complementation with RAG$^{-/-}$ BM will lack expression of MR1 on both T and B cells and confine expression to Mac and DC subsets.

Successful BM reconstitution was determined 8 wk post BMT by the development of mature CD45.2$^+$CD3$^+$ (iVα19 Tg) T cells in the thymus and MLNs, as assessed by flow cytometry. Mice reconstituted with iVα19 Tg MR1$^{-/-}$ BM alone generated mature thymocytes with a baseline expression of Vβ8 segments (~19%) for both DN (Fig. 3A) and CD8 (Fig. 3B) subsets. Addition of wt CD45.1 BM to iVα19 Tg MR1$^{-/-}$ BM rescued MAIT cell development, as demonstrated by the significant increase of Vβ8 segment use in mature DN (~40%) and CD8 (~35%) subsets. Importantly, complementation with TCRα$^{-/-}$, but not RAG$^{-/-}$, donor BM significantly increased Vβ8 bias within both mature DN and CD8 subsets (Fig. 3A, 3B), at a level comparable to that of wt donor BMT (Fig. 3A).

In the MLN, addition of wt and TCRα$^{-/-}$ BM, but not RAG$^{-/-}$ BM, increased Vβ8 use in CD3$^+$ DN (Fig. 3C) and CD8$^+$ (Fig. 3D) iVα19 Tg T cell subsets. The Vβ8 bias in the CD8 subset was less apparent after complementation with wt BM (Fig. 3D) and may be related to low-level peripheral expansion of CD8 T cells on classical MHC-I molecules, as a Vβ8 bias is already observed in the absence of MR1$^+$ BM complementation. B cells are not required for intrathymic MAIT cell selection [Fig. 1A, (7)] but are critical for expansion of peripheral MAIT cells (2). Thus, it is possible that some MAIT cell selection is occurring in the thymus of mixed iVα19 Tg MR1$^{-/-}$/RAG$^{-/-}$ chimeras but is undetectable in peripheral organs owing to a lack of MR1$^+$ B cell–mediated expansion. iVα19 Tg MR1$^{-/-}$ BM was therefore complemented with CD3ε$^{-/-}$ BM in which MR1$^+$ B cells, but not T cells, are present. Even in the presence of MR1$^+$ B cells, no increase in Vβ8 use was observed in either the thymus (Fig. 3A, 3B) or the MLN (Fig. 3C, 3D) of mixed iVα19 Tg MR1$^{-/-}$/CD3ε$^{-/-}$ chimeric mice.

To assess the functional capacity of MAIT cells selected in BM chimeras, APC-depleted splenocytes from chimeric BMT mice were cocultured with purified MR1$^+$ splenic APCs preincubated with exogenous bacterial ligand purified from *E. coli*. Following overnight incubation, iVα19 Tg T cells (gated DN/CD8$^+$ Vβ8$^+$) were analyzed for expression of activation markers CD25/CD69 by flow cytometry (Fig. 3E). Notably, only T cells from iVα19 Tg/TCRα$^{-/-}$ chimeric mice, but not iVα19 Tg or iVα19 Tg/RAG$^{-/-}$ chimeric mice, upregulated CD25/CD69 in cocultures indicative of functional MAIT cell selection (Fig. 3F).

Together, these data indicate that selection of functional, MR1-reactive iVα19 Tg MAIT cells requires MR1 expression exclusively by DP thymocytes and that early thymocytes as well as MR1-sufficient resident thymic DC and Mac populations cannot induce functional MAIT cell development.

The finding that DP thymocytes are required exclusively for MAIT selection is surprising, given our earlier studies showing significant iVα19-Jα33 transcript in the MLNs of wt chimeric mice, in which MHC I expression was confined to CD3ε$^{-/-}$ BM

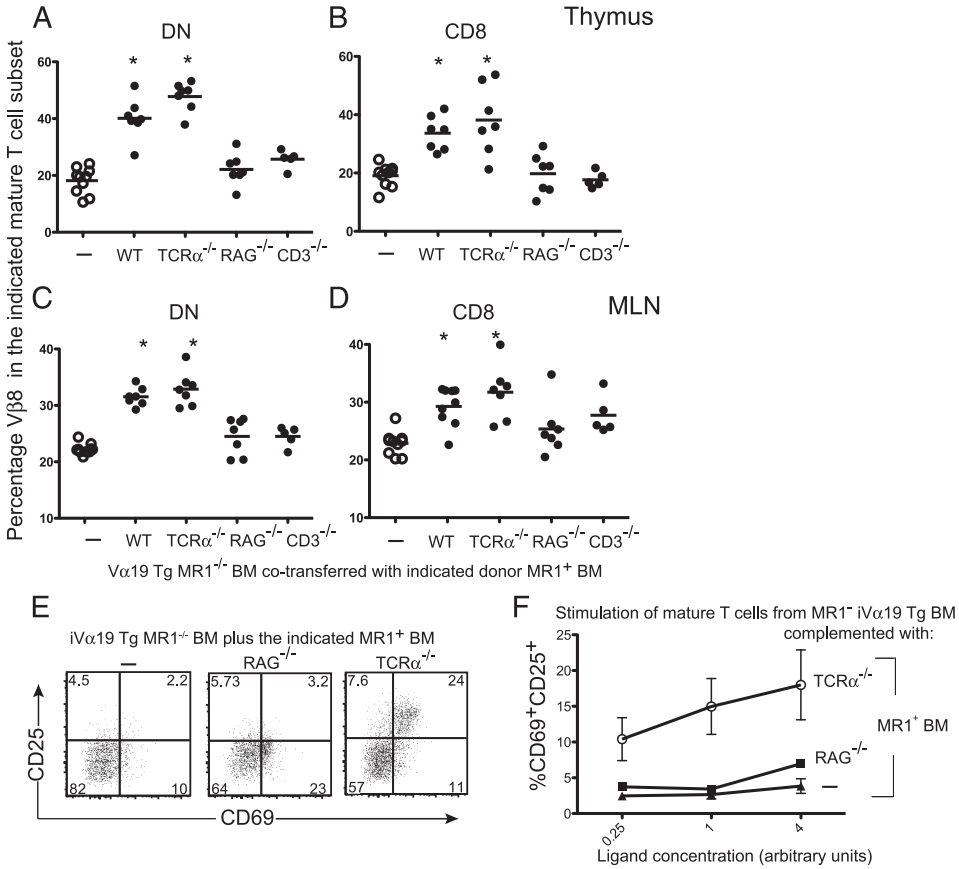

FIGURE 3. DP thymocytes regulate MAIT cell development in vivo. iVα19 Tg MR1$^{-/-}$ BM was administered to RAG$^{-/}$ MR1$^{-/-}$ recipient hosts either alone (−) or in combination with BM derived from the indicated MR1^{+} wt or T/B cell–deficient mouse strain. Percentage Vβ8 use was measured for Vα19 Tg mature thymocyte subsets (**A**, **B**) and MLN (**C**, **D**). Each dot represents an individual mouse pooled from two separate experiments. (**E** and **F**) Purified iVα19 Tg splenic cells isolated from the indicated BMT group were cocultured with MR1^{+} APCs plus bacterial ligand and assessed for surface expression of CD25/CD69 by flow cytometry (E). (F) Graph shows percentage activation of iVα19 Tg T cells (gated DN/CD8^{+} Vb8^{+}) following overnight incubation with indicated ligand concentration. *$p < 0.05$ compared with control groups.

(2). Although we cannot rule out the possibility of a very small amount of intrathymic MAIT cell selection, in the absence of MR1^{+} T cells, followed by B cell–mediated peripheral expansion in our former experiments, the current data from both RTOC and BM chimeras in this article strongly suggest that the overwhelming majority of MAIT cell selection occurs upon reciprocal interaction between MR1-expressing DP thymocytes.

DP thymocytes can present exogenous ligand to MAIT cells in vitro

At steady state, the surface expression of MR1 is undetectable on primary cells (26). To determine the presence of functional MR1 molecules on DP thymocytes, we assessed the capacity of these cells to be loaded with, and present, exogenous ligand to peripheral MAIT cells. Importantly, riboflavin and folate derivatives, present in most culture media, are unable to activate human MAIT cells (9) and mouse iVα19 Tg T cells (data not shown). Purified wt thymocyte subsets were cocultured with mature iVα19 Tg Ca$^{-/-}$ MR1$^{+/-}$ MAIT cells in the presence or absence of bacterial ligand. In accordance with a previous report (22), DP thymocytes alone did not stimulate Tg MAIT cells, as indicated by the absence of surface CD25/CD69 expression. However, when preincubated with increasing concentrations of exogenous ligand, DP thymocytes activated MAIT cells in a dose- and strictly MR1-dependent manner (Fig. 4A, 4B). Notably, both immature DN and mature SP subsets harbored limited stimulatory capacity, in line with their inability to mediate intrathymic MAIT cell selection within both in vitro and in vivo models.

The ability of DP thymoyctes to stimulate mature MAIT cells following loading with bacterial ligand correlated with a slight, but reproducible, upregulation in MR1 surface expression as assessed by flow cytometry (Fig. 4C). Anti-MR1 staining (clone 26.5) was undetectable on untreated DP from MR1-sufficient mice when compared with control staining on MR1$^{-/-}$ DP thymocytes. Incubation with bacterial ligand, however, resulted in the rapid upregulation of MR1 surface expression after a 4-h coculture (Fig. 4C). The lack of detectable surface MR1 expression on ex vivo DP is reminiscent of H2-M3 molecules, which, in the absence of ligand, remain largely in the endoplasmic reticulum and suggests that endogenous ligand availability may also limit MR1 surface expression at steady state (26). It is likely that provision of the bacterial ligand results in the increased trafficking of intracellular MR1 to the surface and/or stabilized surface expression, thereby enhancing the capacity of DP to activate MAIT cells in vitro. These data strongly support a role for MR1/endogenous ligand complexes in the positive selection of MAIT cell progenitors.

Discussion

In this study we resolve a longstanding question regarding the identity of the thymic cell type responsible for MAIT cell selection. Using

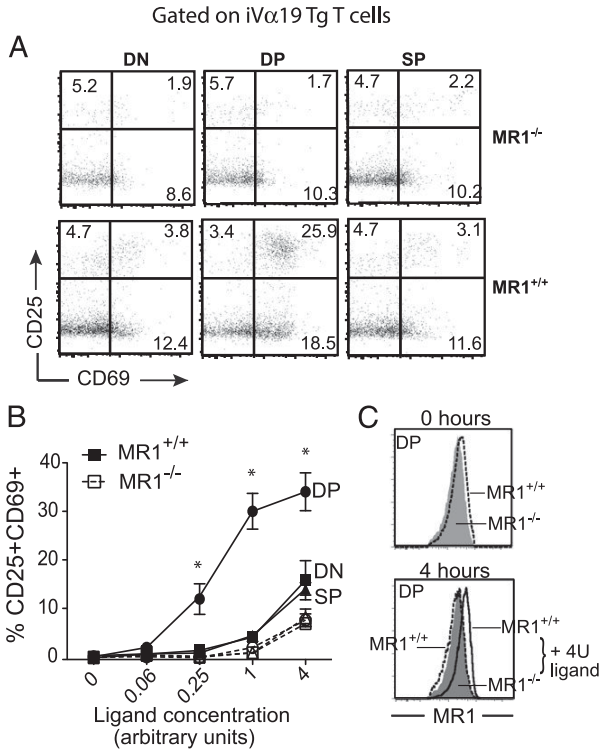

FIGURE 4. DP thymocytes preferentially present bacterial ligand to MAIT cells. (**A**) Activation of iVα19 Tg splenic cells with bacterial ligand (1 U/ml) after overnight incubation with purified thymocyte subset from $MR1^{-/-}$ or $MR1^{+/+}$ mice. (**B**) Dose–response curves of Vα19 Tg activation. (**C**) Incubation of DP thymocytes with bacterial ligand rapidly increases MR1 expression. Fresh DPs were stained with anti-MR1 Ab at 0 or 4 h following incubation with bacterial ligand. FACS plots are representative ($n > 5$) from two to three independent experiments. Activation data are pooled from three independent experiments. $*p < 0.05$, DP activation compared with all other samples.

discrete thymic hematopoietic subsets, we demonstrate a unique and nonredundant role for DP thymocytes in the selection of MAIT cell precursors, whereas all other thymic subsets were dispensable.

Surface MR1 protein is undetectable on primary cell lines, and it is highly probable that MR1 is not stable at the cell membrane in the absence of endogenous or exogenous ligand (9, 26, 30). Indeed, we show that exposure to cognate bacterial ligand resulted in the rapid upregulation of MR1 membrane expression by DP thymocytes and the activation of peripheral MAIT cells. Although the identity of the endogenous MAIT ligand remains unresolved, as DP thymocytes per se do not activate mature MAIT cells, it is likely that DP cells present self-ligand/MR1 complexes to developing thymocytes during intrathymic selection events. In line with this, mutagenesis studies of both MR1 and iTCR indicate that binding of exogenous versus endogenous ligands leads to different MR1/ligand conformations (30).

Thymic and splenic B cells, DCs, and, to a greater extent, Macs can stimulate MAIT cells in the presence of exogenous ligand, supporting a role for these cell types in regulating MAIT cell function (10, 11). However, in contrast to DP thymocytes, thymic APCs, as well as conventional thymic epithelium, could not select intrathymic MAIT cell progenitors in either our RTOC or BM chimera systems, indicating a specialized role for DP in this process. In the absence of detectable surface MR1, it is unclear whether this disparity is due to a physiological lack of MR1 presentation by epithelium and other HC types and/or additional coreceptor signaling required for complete MAIT selection. However, although undetectable at steady state, increased MR1 transcript and intracellular protein expression by DP likely correlates with increased surface MR1 expression levels (26). Conversely, DP may present a specialized set of endogenous ligand to developing T cells favoring MAIT cell selection, compared with other cell types.

The finding that DP thymocytes play a unique and nonredundant role in the selection of both MAIT and NKT subsets raises questions about the mechanisms underlying their respective developmental programs. Given the sequential rearrangement of V-J genes, the availability of NKT and MAIT TCR α-chain segments likely occurs late in DP development, indicating a similar temporal window of selection (12). However, although both subsets share common features, such as the expression of the ZBTB16 transcription factor and a DN/CD8αα subset in humans, NKT cells display a clear TH2 potentiality and CD4 bias, whereas MAIT cells have a predominant TH1/17 phenotype, CD8 bias, and differential homing pattern (2, 31).

The strict temporal regulation of MR1 transcript and intracellular protein, as well as surface CD1d expression on DP thymocytes, indicates DP thymocytes are primed to mediate selection of both NKT and MAIT cell progenitors. DP thymocytes express detectable CD1d surface protein, and NKT cell development is likely mediated by presentation of agonist self-ligand (8). In contrast, DP thymocytes lack detectable MR1 surface expression, and although microbial-derived riboflavin metabolites are capable of activating mature MAIT cells, the identity of the endogenous ligand(s) remains unknown. Thus, it is possible that early differences in avidity/affinity of the NKT/MAIT TCR with their respective CD1d/MR1 ligand complex may govern the initiation of distinct developmental programs.

Cosignaling through SLAM/SAP/Fyn pathways is further required for complete NKT cell differentiation and may be temporally and physically linked to the CD1d-TCR triggering (32, 33). In contrast, MAIT cell development appears to be SAP independent, as MAIT cells are present at quasinormal levels in SAP-deficient patients in whom NKT cells are virtually absent (7). Because DP thymocytes express high levels of SLAM receptors (33), the revelation of a common thymic selecting element indicates that both NKT and MAIT progenitors likely encounter SLAM proteins on their DP counterparts during development. One possibility is that low-level surface MR1 on DP thymocytes, as well as the constant shuttling of MR1 molecules between the intracellular and membrane compartments, may lead to differential SLAM receptor recruitment and/or SAP signal transduction in comparison with the NKT cell development. This possibility would result in the regulation of a specific developmental program during MAIT cell selection.

Acknowledgments

We thank the technical staff at the Curie Animal Facility (in particular Colin Jouhanneau), the staff at the Evry Animal facility, as well as Zofia Maciorowski, Annick Viguier, and Sophie Grondin from the Curie Cytometry Platform for expert cell sorting, and A. Lehuen (INSERM) for the gift of TCRα knockout bone marrow.

Disclosures

The authors have no financial conflicts of interest.

References

1. Rodgers, J. R., and R. G. Cook. 2005. MHC class Ib molecules bridge innate and acquired immunity. *Nat. Rev. Immunol.* 5: 459–471.
2. Treiner, E., L. Duban, S. Bahram, M. Radosavljevic, V. Wanner, F. Tilloy, P. Affaticati, S. Gilfillan, and O. Lantz. 2003. Selection of evolutionarily conserved mucosal-associated invariant T cells by MR1. *Nature* 422: 164–169.

3. Bendelac, A., P. B. Savage, and L. Teyton. 2007. The biology of NKT cells. *Annu. Rev. Immunol.* 25: 297–336.
4. Tilloy, F., E. Treiner, S. H. Park, C. Garcia, F. Lemonnier, H. de la Salle, A. Bendelac, M. Bonneville, and O. Lantz. 1999. An invariant T cell receptor alpha chain defines a novel TAP-independent major histocompatibility complex class Ib-restricted alpha/beta T cell subpopulation in mammals. *J. Exp. Med.* 189: 1907–1921.
5. Tsukamoto, K., J. E. Deakin, J. A. Graves, and K. Hashimoto. 2013. Exceptionally high conservation of the MHC class I-related gene, MR1, among mammals. *Immunogenetics* 65: 115–124.
6. Dusseaux, M., E. Martin, N. Serriari, I. Péguillet, V. Premel, D. Louis, M. Milder, L. Le Bourhis, C. Soudais, E. Treiner, and O. Lantz. 2011. Human MAIT cells are xenobiotic-resistant, tissue-targeted, CD161hi IL-17-secreting T cells. *Blood* 117: 1250–1259.
7. Martin, E., E. Treiner, L. Duban, L. Guerri, H. Laude, C. Toly, V. Premel, A. Devys, I. C. Moura, F. Tilloy, et al. 2009. Stepwise development of MAIT cells in mouse and human. *PLoS Biol.* 7: e54.
8. Rossjohn, J., D. G. Pellicci, O. Patel, L. Gapin, and D. I. Godfrey. 2012. Recognition of CD1d-restricted antigens by natural killer T cells. *Nat. Rev. Immunol.* 12: 845–857.
9. Kjer-Nielsen, L., O. Patel, A. J. Corbett, J. Le Nours, B. Meehan, L. Liu, M. Bhati, Z. Chen, L. Kostenko, R. Reantragoon, et al. 2012. MR1 presents microbial vitamin B metabolites to MAIT cells. *Nature* 491: 717–723.
10. Le Bourhis, L., E. Martin, I. Péguillet, A. Guihot, N. Froux, M. Coré, E. Lévy, M. Dusseaux, V. Meyssonnier, V. Premel, et al. 2010. Antimicrobial activity of mucosal-associated invariant T cells. *Nat. Immunol.* 11: 701–708.
11. Gold, M. C., S. Cerri, S. Smyk-Pearson, M. E. Cansler, T. M. Vogt, J. Delepine, E. Winata, G. M. Swarbrick, W. J. Chua, Y. Y. Yu, et al. 2010. Human mucosal associated invariant T cells detect bacterially infected cells. *PLoS Biol.* 8: e1000407.
12. Le Bourhis, L., L. Guerri, M. Dusseaux, E. Martin, C. Soudais, and O. Lantz. 2011. Mucosal-associated invariant T cells: unconventional development and function. *Trends Immunol.* 32: 212–218.
13. Bendelac, A. 1995. Positive selection of mouse NK1+ T cells by CD1-expressing cortical thymocytes. *J. Exp. Med.* 182: 2091–2096.
14. Gold, M. C., T. Eid, S. Smyk-Pearson, Y. Eberling, G. M. Swarbrick, S. M. Langley, P. R. Streeter, D. A. Lewinsohn, and D. M. Lewinsohn. 2013. Human thymic MR1-restricted MAIT cells are innate pathogen-reactive effectors that adapt following thymic egress. *Mucosal Immunol.* 6: 35–44.
15. Walker, L. J., Y. H. Kang, M. O. Smith, H. Tharmalingham, N. Ramamurthy, V. M. Fleming, N. Sahgal, A. Leslie, Y. Oo, A. Geremia, et al. 2012. Human MAIT and CD8αα cells develop from a pool of type-17 precommitted CD8+ T cells. *Blood* 119: 422–433.
16. Savage, A. K., M. G. Constantinides, J. Han, D. Picard, E. Martin, B. Li, O. Lantz, and A. Bendelac. 2008. The transcription factor PLZF directs the effector program of the NKT cell lineage. *Immunity* 29: 391–403.
17. Urdahl, K. B., J. C. Sun, and M. J. Bevan. 2002. Positive selection of MHC class Ib-restricted CD8(+) T cells on hematopoietic cells. *Nat. Immunol.* 3: 772–779.
18. Bediako, Y., Y. Bian, H. Zhang, H. Cho, P. L. Stein, and C. R. Wang. 2012. SAP is required for the development of innate phenotype in H2-M3—restricted Cd8 (+) T cells. *J. Immunol.* 189: 4787–4796.
19. Cho, H., Y. Bediako, H. Xu, H. J. Choi, and C. R. Wang. 2011. Positive selecting cell type determines the phenotype of MHC class Ib-restricted CD8+ T cells. *Proc. Natl. Acad. Sci. USA* 108: 13241–13246.
20. Wei, D. G., H. Lee, S. H. Park, L. Beaudoin, L. Teyton, A. Lehuen, and A. Bendelac. 2005. Expansion and long-range differentiation of the NKT cell lineage in mice expressing CD1d exclusively on cortical thymocytes. *J. Exp. Med.* 202: 239–248.
21. Gray, D. H., A. P. Chidgey, and R. L. Boyd. 2002. Analysis of thymic stromal cell populations using flow cytometry. *J. Immunol. Methods* 260: 15–28.
22. Chua, W. J., S. Kim, N. Myers, S. Huang, L. Yu, D. H. Fremont, M. S. Diamond, and T. H. Hansen. 2011. Endogenous MHC-related protein 1 is transiently expressed on the plasma membrane in a conformation that activates mucosal-associated invariant T cells. *J. Immunol.* 186: 4744–4750.
23. Shinkai, Y., and F. W. Alt. 1994. CD3 epsilon-mediated signals rescue the development of CD4+CD8+ thymocytes in RAG-2$^{-/-}$ mice in the absence of TCR beta chain expression. *Int. Immunol.* 6: 995–1001.
24. Seach, N., M. Hammett, and A. Chidgey. 2013. Isolation, characterization, and reaggregate culture of thymic epithelial cells. *Methods Mol. Biol.* 945: 251–272.
25. Guerri, L., I. Peguillet, Y. Geraldo, S. Nabti, V. Premel, and O. Lantz. 2013. Analysis of APC types involved in CD4 tolerance and regulatory T cell generation using reaggregated thymic organ cultures. *J. Immunol.* 190: 2102–2110.
26. Huang, S., S. Gilfillan, M. Cella, M. J. Miley, O. Lantz, L. Lybarger, D. H. Fremont, and T. H. Hansen. 2005. Evidence for MR1 antigen presentation to mucosal-associated invariant T cells. *J. Biol. Chem.* 280: 21183–21193.
27. Jenkinson, E. J., G. Anderson, and J. J. Owen. 1992. Studies on T cell maturation on defined thymic stromal cell populations in vitro. *J. Exp. Med.* 176: 845–853.
28. Bendelac, A., P. Matzinger, R. A. Seder, W. E. Paul, and R. H. Schwartz. 1992. Activation events during thymic selection. *J. Exp. Med.* 175: 731–742.
29. Erman, B., L. Feigenbaum, J. E. Coligan, and A. Singer. 2002. Early TCRalpha expression generates TCRalphagamma complexes that signal the DN-to-DP transition and impair development. *Nat. Immunol.* 3: 564–569.
30. Young, M. H., L. U'Ren, S. Huang, T. Mallevaey, J. Scott-Browne, F. Crawford, O. Lantz, T. H. Hansen, J. Kappler, P. Marrack, and L. Gapin. 2013. MAIT cell recognition of MR1 on bacterially infected and uninfected cells. *PLoS ONE* 8: e53789.
31. Treiner, E., L. Duban, I. C. Moura, T. Hansen, S. Gilfillan, and O. Lantz. 2005. Mucosal-associated invariant T (MAIT) cells: an evolutionarily conserved T cell subset. *Microbes Infect.* 7: 552–559.
32. Nichols, K. E., J. Hom, S. Y. Gong, A. Ganguly, C. S. Ma, J. L. Cannons, S. G. Tangye, P. L. Schwartzberg, G. A. Koretzky, and P. L. Stein. 2005. Regulation of NKT cell development by SAP, the protein defective in XLP. *Nat. Med.* 11: 340–345.
33. Griewank, K., C. Borowski, S. Rietdijk, N. Wang, A. Julien, D. G. Wei, A. A. Mamchak, C. Terhorst, and A. Bendelac. 2007. Homotypic interactions mediated by Slamf1 and Slamf6 receptors control NKT cell lineage development. *Immunity* 27: 751–762.